ADAPTIVE CONTROL OF POWER AMPLIFIER LINEARIZATION TECHNIQUES BY USING HYBRID ANALOG AND DIGITAL APPROACHES

A THESIS SUBMITTED TO
THE BOARD OF GRADUATE PROGRAMS
OF
MIDDLE EAST TECHNICAL UNIVERSITY, NORTHERN CYPRUS CAMPUS

BY

BASSAM ABDULWAHAB

IN PARTIAL FULFILLMENT OF THE REQUIREMENTS
FOR
THE DEGREE OF MASTER OF SCIENCE
IN ELECTRICAL AND ELECTRONICS ENGINEERING PROGRAM

SEPTEMBER 2021

Approval of the Board of Graduate Programs

PROF. DR. CUMALİ SABAH
Chairperson

I certify that this thesis satisfies all the requirements as a thesis for the degree of Master of Science

ASSOC.PROF.DR. MURAT FAHRİOĞLU
Program Coordinator

This is to certify that we have read this thesis and that in our opinion it is fully adequate, in scope and quality, as a thesis for the degree of Master of Science.

ASSOC.PROF.DR.
TAYFUN NESİMOĞLU
Supervisor

Examining Committee Members

ASSOC. PROF. DR. SOYDAN REDIF	EUL/ EEE	
ASSOC. PROF. DR. TAYFUN NESIMOGLU	METU NCC/ EEE	
ASST. PROF. DR. CANRAS BATUNLU	METU NCC/ EEE	

I hereby declare that all information in this document has been obtained and presented in accordance with academic rules and ethical conduct. I also declare that, as required by these rules and conduct, I have fully cited and referenced all material and results that are not original to this work.

Name, Last name :

Signature :

ABSTRACT

ADAPTIVE CONTROL OF POWER AMPLIFIER LINEARIZATION TECHNIQUES BY USING HYBRID ANALOG AND DIGITAL APPROACHES

Abdulwahab, Bassam
Master of Science, Electrical and Electronics Engineering Program
Supervisor: Assoc. Prof. Dr. Tayfun Nesimoglu

September 2021, 134 pages

Power Amplifiers (PA) are widely used in mobile communication systems, yet power amplifiers have a non-linear region which is the major problem in all communication and radar systems. Moreover, PAs show a low power efficiency when operating in their linear region and are highly non-linear when operating in their high-efficiency region. To overcome such issues, there are different methods to linearize PAs and other methods to enhance their power efficiency. These linearization methods are built to meet a certain linearity level for a specific application. However, the linearization techniques are not built to cope with the changes that might occur to the system. In this thesis an adaptive control mechanism for linearization techniques is studied, the goal is to achieve a linearization system for the PA that can maintain the desired linearity level without compromising the efficiency. The idea of the system is to find an intelligent way that can be added to any linearization technique to detect and measure any changes in the system and the effect of this change on the system, then adapt the system to overcome this change and achieve linearity. A digitally programmable feedback control system will be added to the PA linearization technique, having a microcontroller in a feedback

circuitry that will work as an efficient detector to detect any changes on the sampled signal with accuracy as to control an adaptive network. Accordingly, the microcontroller will decide the voltage control changes required to maintain the required linearity.

Keywords: Power Amplifiers, Linearization Techniques, Adaptive Control

ÖZ

YÜKSELTEÇ DOĞRUSALLAŞTIRMA TEKNIKLERINDE UYARLANABILIR HIBRID ANALOG VE DIJITAL KONTROL MEKANIZMALARININ UYGULANMASI

Abdulwahab, Bassam
Yüksek Lisans, Elektrik ve Elektronik Mühendisliği
Tez Yöneticisi: Doç. Dr. Tayfun Nesimoglu

Eylül 2021, 134 Sayfa

Güç Yükselteçleri (GY), mobil iletişim sistemlerinde yaygın olarak kullanılmaktadır, ancak tüm iletişim ve radar sistemlerinde en büyük sorun olan doğrusal olmayan bir bölgeye sahiptir. Ayrıca, GY, doğrusal bölgede çalışırken düşük güç verimliliği gösterir ve yüksek verimlilik bölgelerinde çalışırken de yüksek oranda doğrusal değildir. Bu tür sorunların üstesinden gelmek ve doğrusallaştırma ile güç verimliliklerini artırmak için çeşitli yöntemler vardır. Bu doğrusallaştırma yöntemleri genellikle spesifik bir uygulama için önceden belirlenmiş bir doğrusallık düzeyini karşılamak üzere oluşturulur. Ancak doğrusallaştırma teknikleri, sistemde meydana gelebilecek anlık değişikliklere adapte olamamaktadır. Bu tezde verimden ödün vermeden istenen doğrusallık seviyesini koruyabilen bir doğrusallaştırma sistemi elde etmek için uyarlamalı doğrusallaştırma tekniğine yönelik uyarlamalı bir kontrol yöntemi önerilerek, incelenip test edilmiştir. Sistemin amacı, sistemdeki herhangi bir değişikliği ve bu değişikliğin sistem üzerindeki etkisini tespit etmek ve ölçmek için herhangi bir doğrusallaştırma tekniğine eklenebilecek akıllı bir yol bulmak olup, ardından bu değişikliği çözerek doğrusallığı sağlamak için sistemi uyarlamaktır. GY doğrusallaştırma tekniğine dijital olarak programlanabilen bir geri besleme kontrol sistemi eklenmiştir ve bu devre, adaptif ağı korumak için içerisinde

yer alan mikro işlemci ile daha efektif ve kesin bir şekilde örneklenmiş sinyallerdeki değişiklikleri tespit edilebilmektedir. Buna göre, mikrodenetleyici, doğrusallığı korumak için gerekli voltaj kontrol değişikliklerine karar vermektedir.

Anahtar Kelimeler: Güç Yükselteci, Doğrusallaştırma Teknikleri, Uyarlamalı Kontrol.

DEDICATED TO MY BELOVED FAMILY

ACKNOWLEDGMENTS

Firstly, all thanks and praises are due to ALLAH. Secondly:

I would like to thank Assoc. Prof. Dr. Tayfun Nesimoglu for his supervision, guidance, advice, criticism, encouragements, and insight throughout the research.

I would also like to thank Prof. Dr. Ali Muhtaroglu for his suggestions and comments.

I would also like to thank Abhilash Patel for providing, helping with the FFT algorithm.

I would like to express my gratitude to my friends Abdulrahman Zkert and Besher Homsi for their help with programing the Arduino.

I would like to express my gratitude to my friends Wasim Ramadan and Mohammed Al-Saleh for their help with writing the thesis.

Last but not least, I am filled with gratitude to my beloved father Mohammed Soltan, mother Reda Tawfik, brothers Assem and Ali, sisters Sondos and Toka for their love, support, motivation, understanding and always being by my side during this study.

TABLE OF CONTENTS

LIST OF TABLES

TABLES

LIST OF FIGURES

FIGURES

LIST OF ABBREVIATIONS

ABBREVIATIONS

RF	:	Radio Frequency
PA	:	Power Amplifier
ISM	:	Industrial, Scientific, and Medical
ETSI	:	European Telecommunication Standards Institute
HD	:	Harmonic Distortions
SHF	:	Second Harmonic Frequency
SHZ	:	Second Harmonic Zone
IMD	:	Intermodulation Distortion
THD	:	Total Harmonic Distortion
IM3/IMD3	:	3^{rd} Order Intermodulation Distortion
IM5/IMD5	:	5^{th} Order Intermodulation Distortion
kHz	:	Kilo Hertz (10^3)
MHz	:	Mega Hertz (10^6)
GHz	:	Giga Hertz (10^9)
BW	:	Bandwidth
IF	:	Intermediate Frequency
MCU	:	Microcontroller Unit
DC	:	Direct Current
RMS	:	Root Mean Square
AM	:	Amplitude Modulation
PM	:	Phase Modulation
PAE	:	Power Added Efficiency
ACPR	:	Adjacent Channel Power Ratio
ACLR	:	Adjacent Channel Leakage Ratio
BJT	:	Bipolar Junction Transistor
MOSFET	:	Metal-Oxide-Semiconductor Field-Effect Transistor
Q-point	:	Quiescent Point

PWM	:	Pulse Width Modulation
BPF	:	Band-Pass Filter
P_{1dB}	:	1dB Gain Compression Point
TOI/P_{3dB}	:	3^{rd} Order Intercept Point
ADC	:	Analog to Digital Conversion
DAC	:	Digital to Analog Conversion
DSP	:	Digital Signal Processing
DPA	:	Doherty Power Amplifier
APD	:	Analog Predistorter
DPD	:	Digital Predistorter
PD	:	Predistorter
LUT	:	Look-Up-Table
LSM	:	Least Square Method
CFR	:	Crest Factor Reductio
DBHM	:	Double-Balanced Harmonic Mixer
LO	:	Local Oscillator
HB	:	Harmonic Balance
ADS	:	Advanced Design Systems
CF	:	Carrier Frequency

CHAPTER 1

INTRODUCTION

This introduction chapter summarizes the motive behind this research and gives brief information on the importance, use, and fields of use of radio frequency power amplifiers (RF PA). It also explains the challenges and problems faced when working with RF PA which leads to the objective of this study. Finally, it gives an outline of this thesis.

1.1 Motivation

The radio frequency (RF) field covers a very wide range of frequencies which is between 100 MHz and 1000 GHz [1]. This huge range covers almost all of today's applications. These applications are responsible for human's basic daily uses, interactions, and needs, from mobile phones, personal computers, cars, factories to medical devices in either of which power amplifiers (PA) are the main building block in one form or another.

With the importance of the application, the behavior of the devices used is required to be as perfect as possible not to have any negative effects on the application. One of the most important applications that fall into the RF field is medicine, which falls into the industrial, scientific, and medical (ISM) band which is at 2.4 GHz with a 1 MHz bandwidth for its applications according to the ETSI EN 300 440,324 [2-3]. Medical applications are the most crucial to human life, hence it is required to have the most accurate equipment operation. Diathermy is one of the medical applications that use the ISM that applies heating to the body for relaxation and healing, another

more recent and more important application is the hyperthermia therapy that uses microwaves to heat tissues and kills cancer cells [4-5].

The presence of an RF PA in the machines used in the medical applications mentioned above is vital. With such an important task, the performance of the PA must be on point otherwise it might lead to a life-threatening situation. Unfortunately, PAs exhibit some nonlinearities because of the distortions that are added by the PA itself to the main signal. Those distortions, not only do they affect the signal or the data going through the PA, but also the efficiency of the PA. The challenge is to get rid of these distortions, which are called harmonic distortions (HD) and intermodulation distortion (IMD), to achieve a linear PA and maintain this linearity.

To show the effect of the distortions on the signal, a simulation was done using MATLAB to show such effects. Figure 1.1 shows (a) a normal 2-tone (a signal with 2 frequencies), (b) the same signal after adding the distortions (c) the spectrum of the corrupted signal. The main 2-tone signal can be seen at 9 kHz and 11 kHz, while the IMD is seen on the left and right sides of each of the main 2 frequencies in (c).

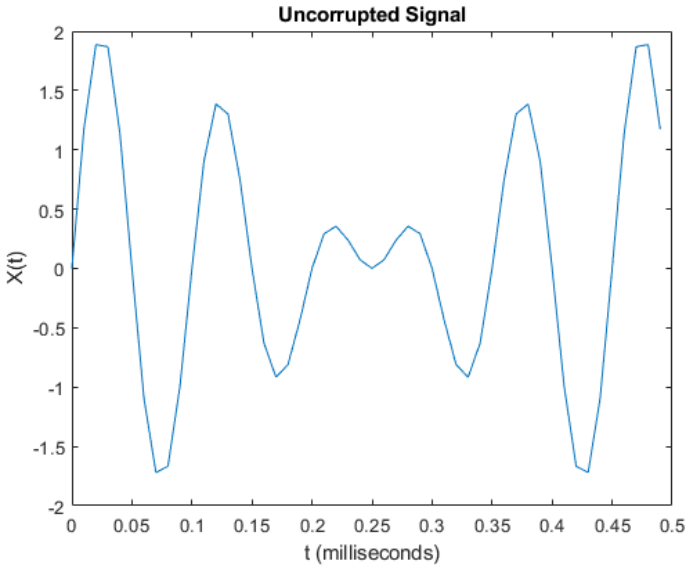

(a)

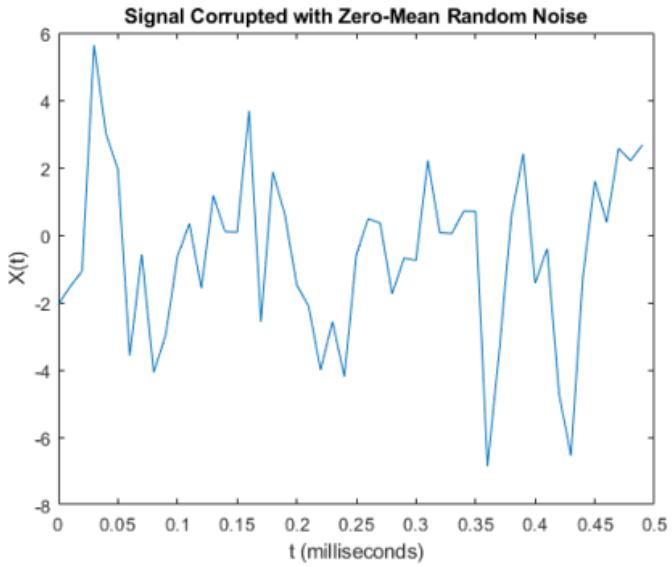

(b)

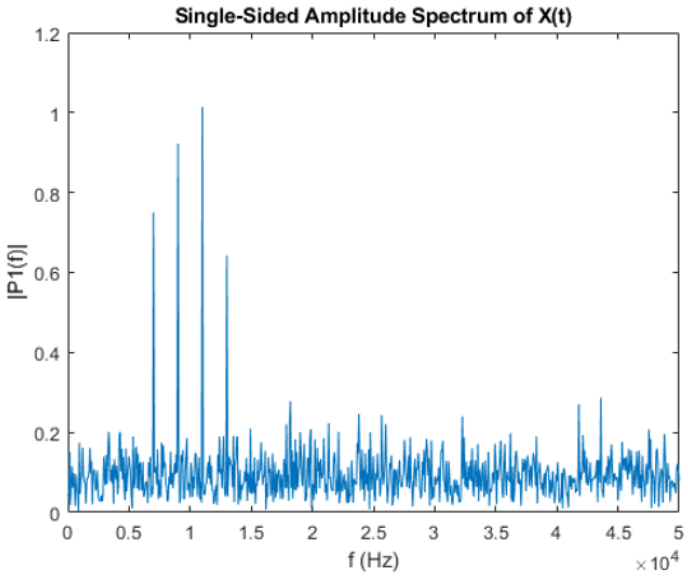

(c)

Figure 1.1 (a) Uncorrupted 2-tone signal (b) Signal corrupted with noise and IMD (c) The spectrum of the corrupted signal

1.2 Research Objectives

This research has two main objectives as proposed by the title of the thesis as well. The first objective is to achieve adaptability in power amplifier linearization that has a fast response to any change that might occur in the system. For that aim, a microcontroller unit (MCU) is used as a smart controller and decision-maker, so that it can detect the change almost simultaneously and accordingly adjust the system to adapt to that change. The decision-making is dependent on measurements that the MCU samples from the system and according to predefined criteria the MCU makes the decision.

The second objective is that the ability of the adaptive system to be implemented on almost any linearization technique. To achieve this aim, the MCU is to control the DC control of the variables available in the system. Most of the linearization techniques are dependent on an analog circuit that is responsible for linearizing the PA, and these circuits require voltage tuning to achieve linearity, here lies the main idea of the adaptable system, which is the control of tuning voltage of the analog circuitry available in the linearization technique.

1.3 Achievements

This study has led to the following achievements.

It is shown that using an MCU as smart control of any linearization technique is feasible. With a capable MCU, a downconverted signal can be detected by using the MCU's ADC to sample that signal, the sampled signal can then be processed by using the FFT algorithm which results in a spectrum that has the wanted and unwanted signals clearly shown and distinguished.

An MCU also can use a different approach for detection that is by detecting the power of the signal, and depending on the MCU's coding, this measured power is distinguished to be dominated by either of the fundamentals or the IMD3.

1.4 Thesis Outline

This thesis consists of seven chapters including this chapter. Chapter 2, Chapter 3, and Chapter 4 are the review chapters. The chapters' focus is organized as follows:

Chapter 2 discusses power amplifiers and their nonlinear behavior. The chapter starts with discussing the characteristics of an ideal power amplifier and how it should operate under ideal conditions, then the different types of power amplifiers and the specialty of each type. Lastly, the chapter explains the nonlinearity of the power amplifiers and their causes and effects on the signal and its types.

Chapter 3 discusses the power amplifier linearization techniques. Starting with feedback, feedforward, and then predistortion. It also explains the working principle and the idea behind each of the linearization techniques, and the correction range of each technique, and their complexity too with various examples from the literature. Finally, it gives a comparison between all these techniques considering correction, complexity, and price.

Chapter 4 presents the adaptive linearization of power amplifiers. The chapter explains the two types of adaptive linearization, which are digital and analog, and the pros and cons of each of the approaches. Finally, the previous research that was done in the literature.

Chapter 5 presents the theory and simulation behind this research. It starts with explaining the linearization technique that was chosen to implement this study. Then the proposed adaptive linearization control system and how it works in detail, with the different visual representations of the system. Then the methodology was

followed to investigate this system and to further support the working principle of the system. Finally, it includes all the simulations that were done to simulate the working of the proposed adaptive control system.

Chapter 6 discusses the experiments and results. In this chapter the implementation of the proposed adaptive control system is presented, the experiments that were done to prove the concept explained in chapter 5, and the results of these experiments.

Chapter 7 summarizes and concludes this study and discusses the future work that this research may promote.

CHAPTER 2

RF POWER AMPLIFIERS AND NON-LINEARITY

2.1 Introduction

A power amplifier (PA), is an electronic device whose main purpose is to convert a low-power input signal into a high-power output signal. Ideally, the output signal is a good clone of the original input signal, meaning that there should not be any added distortion to the signal or any phase change. Amplifiers are fundamental building blocks of almost all electronic devices and equipment. The ideal functionality of a PA requires the amplifier to have two main characteristics, linearity and power efficiency, which will be discussed later in this chapter.

With the technological advances that are increasing by the day, the role of PAs in communication systems has never been more essential, high efficient and linear PAs are the key component in mobile and communication systems. A PA is generally located before the antenna and determines the transmitting power level in a communication system.

Although PAs are widely used and a very critical component in any communication system, their characteristics, considering linearity and efficiency are the topic of most of today's research in communication systems. Since they show a non-linear behavior when they are at a high efficient region of operation, as well as a low efficiency when operating at their linear region. Hence, a compromise is made according to the application between efficiency and linearity. PAs are classified according to their characteristics, each class has its linearity and efficiency characteristics such as Class-A, Class-B ...etc. These classifications of PAs will be discussed in this chapter.

2.2 Characteristics of Ideal Amplifiers and Efficiency

An ideal amplifier has 100% efficiency. It has a linear output response to the input, which means, with the increase of the input signal's amplitude the output signal's amplitude increases linearly, while the phase remains constant as shown in Figure 2.1. This increment in the output signal is represented by the amplifier's gain, which should be independent of the input signal's level [6].

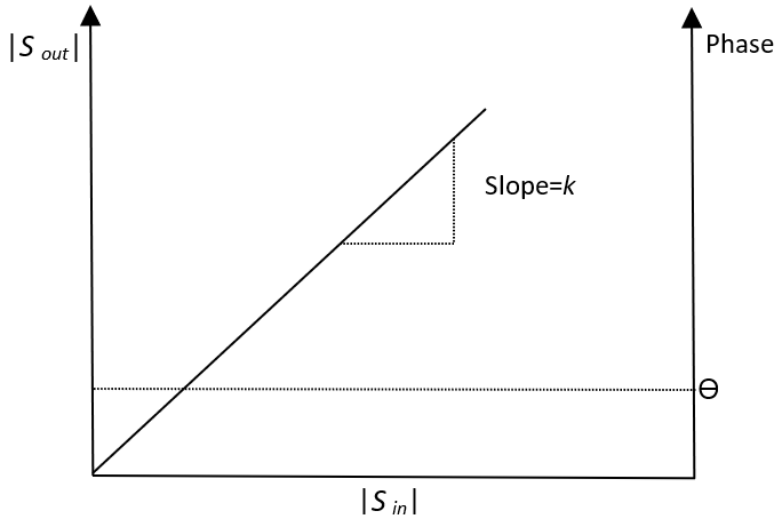

Figure 2.1 Amplitude (AM/AM) and phase (AM/PM) characteristics of an ideal amplifier [6]

This linear relation between the input and the output of an amplifier can be represented by the following equations.

$$S_{in}(t) = A\cos(\omega_c t) \qquad \text{Eq. 2-1}$$

$$S_{out}(t) = k\,A\cos(\omega_c t + \theta) \qquad \text{Eq. 2-2}$$

Where A is the amplitude of the input signal, k is the amplifier's gain, ω_c is the angular frequency and θ is the phase shift. As it can be seen from Eq. 2-1, 2-2 that neither the gain nor the phase shift of the amplifier is a function of time, which represents the ideality of the amplifier.

The power efficiency of an amplifier is a measure that represents how much of the power fed into the amplifier has been converted into useful output power. The efficiency is also dependent on the DC supply as well in real-life measurements. There are different approaches to measuring an amplifier's power efficiency. One measure is the ratio between the amplifier's output power to the input DC power, Eq. 2-3.

$$\eta = \frac{P_{out}}{P_{Dc}} \qquad \text{Eq. 2-3}$$

This measure is known as the *drain efficiency*, the problem with this measure is that it doesn't consider the RF input power to the amplifier. Hence, a better measure of the efficiency is the *power added efficiency* (PAE), Eq. 2-4 [1][6].

$$\eta_{PAE} = PAE = \frac{P_{out} - P_{in}}{P_{DC}} = \left(1 - \frac{1}{G}\right)\frac{P_{out}}{P_{DC}} = \left(1 - \frac{1}{G}\right)\eta \qquad \text{Eq. 2-4}$$

Where *G* is the amplifier's gain. Another useful measure is the *total power*, Eq. 2-5. For instance, silicon bipolar junction amplifiers or BJTs in the cellular communication band of 800-900 MHz have PAE on the order of 80%, but efficiency drops with the increasing frequency [1].

$$\eta_t = \frac{P_{out}}{(P_{in} - P_{DC})} \qquad \text{Eq. 2-5}$$

Power amplifier's main building component is the semiconductor switches, Bipolar Junction Transistors (BJTs), and Metal-Oxide-Semiconductor Field-Effect Transistors (MOSFETs). Both transistors have their characteristics in building a PA. In a comparison made between MOS and Bipolar power amplifiers, using the same fabrication process with the same DC supply (same class). The general results showed the superiority of Bipolar PA over the MOS with 8.2 dB vs 5.5 dB gain, and a PAE of 16% vs 12%, respectively [8].

2.3 Classification of Power Amplifiers

Amplifier's design and DC biasing (Q-point) leads to different characteristics of the amplifier. Those characteristics are mainly linearity, power efficiency, output power, and gain. One way of distinguishing between each amplifier's characteristics is to categorize them or class them according to their characteristics. Considering that the amplifier is excited by a single cycle sinusoidal input signal, classification shows the duration of conduction of the power amplifier relative to the complete input cycle, i.e., Full cycle 360° conduction [6].

There are two main groups of classes. First, are the conduction angle-controlled amplifiers which represent class A, B, AB, and C amplifiers. Second, are the "switching" amplifiers which represent classes E, F, and J. which are controlled by digital circuits and pulse width modulation (PWM). The class efficiencies range between 50% that of class A, to 100% for class F at the cost of its linearity [9].

2.3.1 Class-A Power Amplifier

Class A amplifiers are one of the classifications which are most linear but less efficient amongst the RF power amplifiers. Where the amplifier is biased to conduct over the entire input signal's cycle, Figure 2.2, which affects its efficiency to be 50% as a maximum [1]. This class of amplifiers mostly uses a BJT in its design, and practically the device is not perfectly linear, hence the output is connected to a bandpass filter (BPF) to filter out the harmonics of the input signal generated by the non-linearity of the amplifier [6].

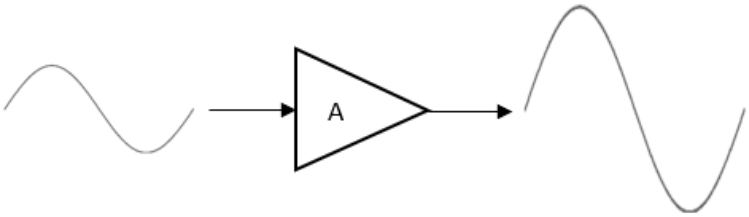

Figure 2.2 Input and output current flow of class-A amplifier [6]

Hence, class A amplifiers are used in applications requiring low power, high linearity, and high gain broad band operation [9].

2.3.2 Class-B Power Amplifier

Class B amplifier, Figure 2.3, provides higher efficiency than that of class-A amplifiers at the cost of lower linearity. The amplifiers of that class are biased to conduct for a half cycle, i.e. 180°. Typically, class-B amplifiers have inductive loading which prevents any DC voltage drop across it, unlike the resistive loading. The efficiency of a class-B amplifier can reach 78.5% and that is the maximum achievable efficiency for this class [6] [10].

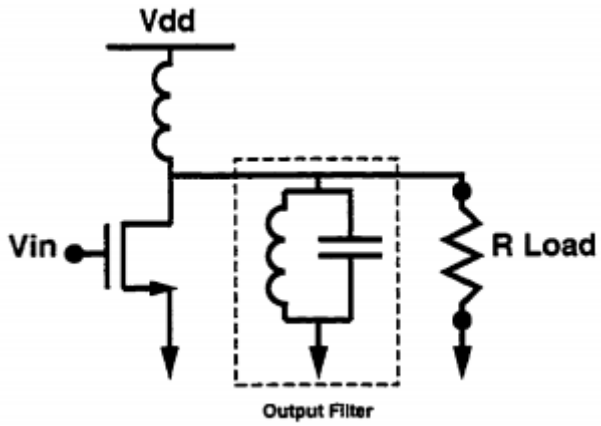

Figure 2.3 Generic configuration for class-B and class-C amplifiers [10]

Normally, two class-B amplifiers are connected forming a push-pull configuration. In this configuration, the active devices are biased 180° out of phase so that each of the devices will be conducting for a half cycle. The addition of their outputs results in complete cycle conduction. Class-B amplifiers are used in high power applications where efficiency is necessary [6] [10].

2.3.3 Class-AB Power Amplifier

As the name implies class AB amplifiers are one way to represent an amplifier with the high linearity of a class A amplifier, alongside the high efficiency of that of class B. In class-AB amplifiers, both active devices are allowed to conduct at the same time. In another word, the conduction angle of the class-AB power amplifier varies between 180° and 360° [11].

2.3.4 Class-C Power Amplifier

Class-C amplifiers are more efficient than both, class-A and class-B. The amplifier in this class is biased below the threshold point so that the amplifier is active for even less than a half-cycle. As the conduction angle of the amplifier decreases the efficiency increases, when the conduction period is 0 the efficiency is 100% [6].

This of course causes the output power to reach 0. To avoid that reduction in the output power, a compromise is made where the conduction angle is 150° with an 85% efficiency. Class-C amplifiers are used for broadband high-power applications, i.e. transmitters in radio stations [9] [10].

2.3.5 Switching Mode Power Amplifiers

The second type of class, switching mode type is controlled via a digital circuit or PWM signals. This means that these classes do not have a conduction angle it is always 0. This type of power amplifier is either in the 'ON' state or 'OFF' state which improves the efficiency of the amplifier [9]. Table 2.1 below shows some of the state-of-art switching mode amplifiers and their development over the past years [12].

Table 2.1 Switching mode power amplifiers development [12]

	Year	BW (GHz)	Gain (dB)	Efficiency (%)
Class-E	2006 [13]	1.8-2.3	9-10	57-62
	2009 [14]	2-2.5	10-13	74-77
	2011 [15]	0.9-2.2	10-13	63-89
	2017 [12]	0.9-2.3	7.5-13	57-88
Class-F	2012 [16]	1.45-2.45	9-12	70-80
	2013 [17]	1.35-2	8.2-16.9	65-76
Class-J	2009 [18]	1.4-2.6	11-12	57-72

2.4 Amplifiers Non-linearity

Any electronic device has losses, as long as they are not ideal, and in practice, there is no ideal device. The losses occur in the devices due to thermal effects because of the biasing, and these losses, in turn, develop a non-linear behavior device at a low

power level. Additionally, active devices, like transistors (amplifiers), are becoming non-linear at a high power level due to the device's non-linearity, which generates a negative effect such as gain compression and the generation of pseudo-frequency components. This is known as the *dynamic range* of the device, meaning, the minimum and maximum power ranges at which the device would operate as desired [1].

Amplifier's non-linearity doesn't only depend on high power levels, other parameters affect the linearity of an amplifier, such as frequency and operating voltage. Although, these parameters also affect the linearity of an amplifier at a low power level the non-linearity is not an issue, hence, non-linearity becomes a considerable factor when the input level is high enough to drive the amplifier to behave non-linearly. The saturation point is the point at which the input power level is high enough so that the amplifier behaves non-linearly [6].

Non-linearity doesn't only happen in the suppression of the output signal's level, but also in the phase of the signal. The output signal's phase may shift depending on the input signal's level, and the operating point of the amplifier. This effect is known as AM/PM conversion, which later on becomes a cause of intermodulation distortion (IMD).

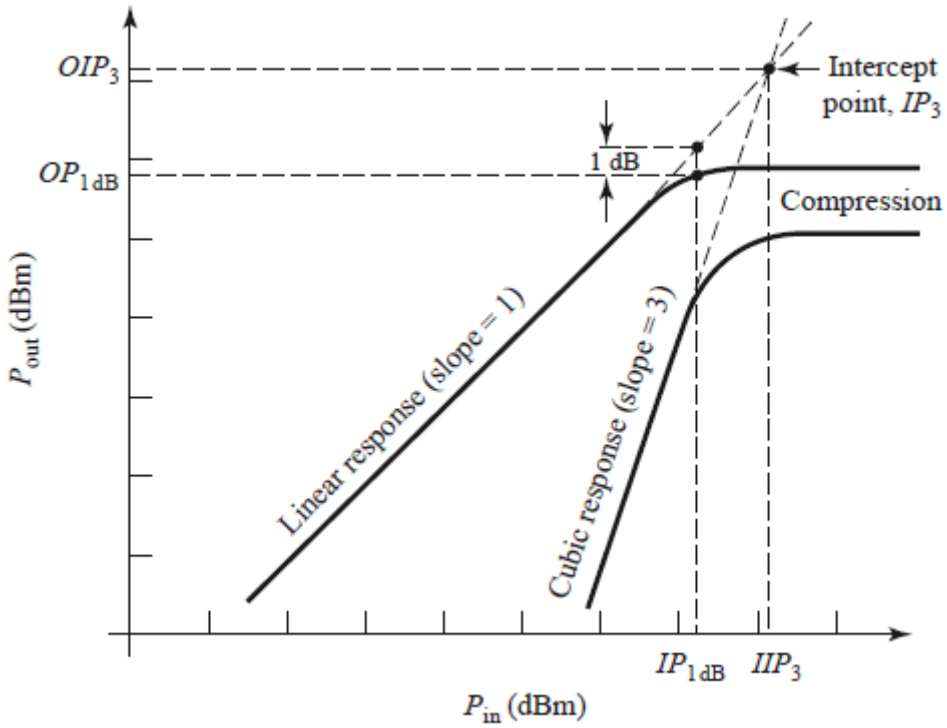

Figure 2.4 A non-linear amplifier input vs output response [1]

Figure 2.4 shows the response of a typical non-linear amplifier. There are a few important points on the graph that needs to be defined. The 1 dB *gain-compression point* (P_{1dB}), which is the point at which the gain is dropped by 1 dB lower than the linear gain response of the amplifier. The 1 dB compression point can be shown in terms of the output power OP_{1dB} or the input power IP_{1dB} as shown in the figure. The third-order intercept point (TOI or P_{3dB}) is the point at which the linear response of the amplifier and the third-order IMD would be equal, TOI is typically 10-12 dB above the P_{1dB} compression point [6]. It can also be stated in terms of the output power OIP_{3dB} or input power IIP_{3dB}.

The non-linear characteristics of devices like amplifiers are desirable for some functions like signal amplification, frequency conversion. However, these characteristics also lead to undesirable effects such as the P_{1dB} and the generation of pseudo frequencies, these effects increase losses, signal distortion, and signal

interference with other channel signals [19]. Listed below are two important non-linearity effects in RF and microwave systems [1]:

- Harmonic generation (multiples of the fundamental signal)
- Intermodulation distortion (IMD, products, and difference of two-tone signal)

2.4.1 Harmonic distortion

Harmonic distortion (HD) is one of the effects of non-linear amplifiers. It is the multiples of the input signal's frequency, i.e. $n\omega_0$, for n = 1,2,3,...., ω_0 is a single input frequency (tone). Often, these harmonics lie outside of the passband of the amplifier, so they can be filtered out using a bandpass filter at the output of the amplifier. The graphical representation of HD can be seen in Figure 2.5, below.

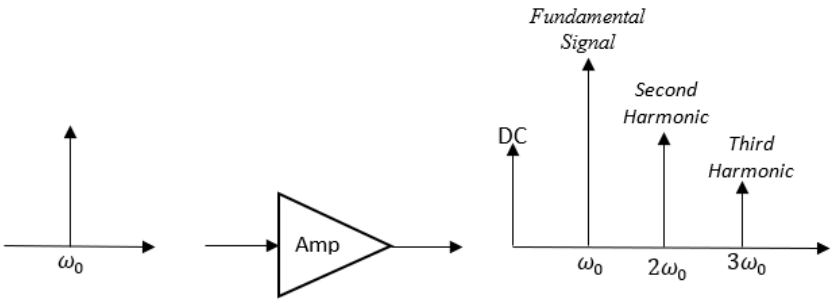

Figure 2.5 Single-tone input with the HD at the output

2.4.2 Intermodulation Distortion (IMD)

When the input signal of an amplifier is no longer a single frequency, but two closely spaced frequencies the situation differs. consider a two-tone input signal at frequencies ω_1, ω_2 with a bandwidth of $\Delta\omega = \omega_2 - \omega_1$, these two signals' power level is chosen to be equal and high enough for the amplifier to produce IMD. The

resultant output signal consists of many different copies of the fundamental signals, these copies are either HD or the products of the fundamentals. Figure 2-6 shows the spectrum of an amplifier with a two-tone input signal. The order of the IMD is defined by $|m|+|n|$, i.e.The third-order IMD is given by $2\omega_2$-ω_1,where m=2,n=1 [1].

As it can be seen from Figure 2.6, the output consists of many intermodulation products of the fundamentals. The second-order products are undesired in an amplifier but they are the basis of mixers, yet they are located far from fundamentals so they can be easily filtered. On the other hand, six third-order products can be seen on the spectrum, two of which are located very close to the fundamentals which are very hard to separate from the fundamental signals, these are known as *third-order intermodulation distortion* (IMD3). IMD3 is one of the main causes of the amplifier's non-linearity. Which led to another approach of separating them which is linearization techniques.

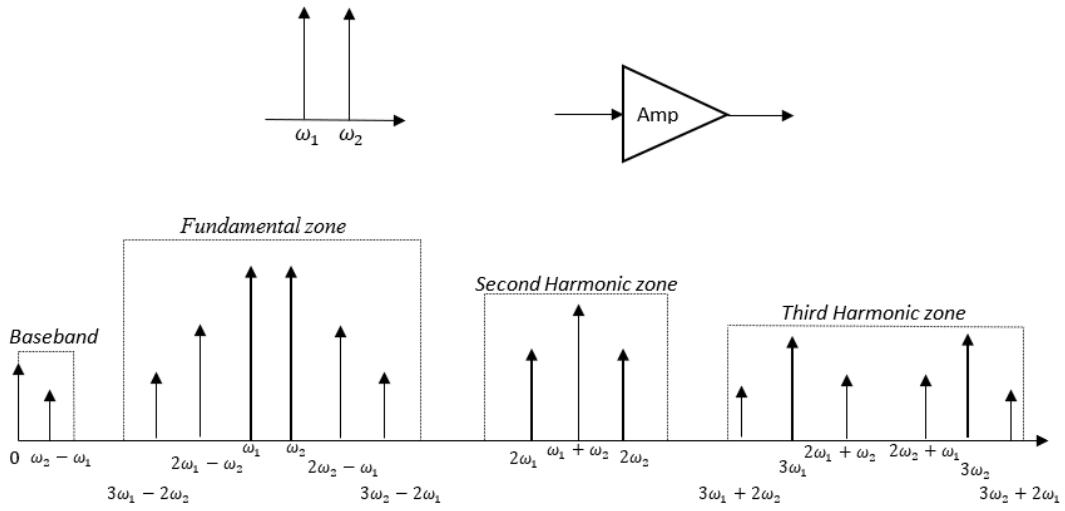

Figure 2.6 Output spectrum with a two-tone input signal [6]

2.5 Summary

The power amplifier's function and classes were discussed in this chapter alongside its characteristics. The non-linear behavior shown by amplifiers characteristics is caused by different reasons, whether it’s because of the losses that occur because of the thermal effects of the DC bias, or the generation of the harmonic and intermodulation distortions.

A single-tone test can be used to investigate the amplifier's generation of harmonic distortion, while a two-tone test is used for intermodulation distortion. The results of these two tests showed a high level of different frequencies generation which leads to non-linearity. Which indicates the need for a linearized amplifier.

CHAPTER 3

LINEARIZATION TECHNIQUES

3.1 Introduction

The use of power amplifiers has become essential in nearly all the surrounding devices and machines. Most of today's application requires a power amplifier in their circuitry in one way or another, these applications vary from scientific, medical, communication to space programs. The non-linearity of power amplifiers causes problems whether with the loss of information or suppression in signals power. These problems in some applications cannot be tolerated and must be fixed. Hence, the work on linearization techniques started and has become one of the major research areas in the past couple of decades.

Linearization techniques are introduced as a solution for the amplifier's non-linearity. The working idea behind these techniques is quite simple, which is, building a circuit that can compensate for the amplifier's non-linear behavior and working on minimizing or even canceling it. In this chapter three main linearization techniques will be discussed, feedback, feedforward, and predistortion.

3.2 Feedback Technique

One of the main techniques used in linearization is Feedback [20]. Figure 3.1, this technique linearizes transmitters of single power amplifiers by forcing the output to follow the input via a continuous comparison between them. There are different types of feedback techniques, RF using direct feedback, Envelope feedback, and Polar and Cartesian loop feedback.

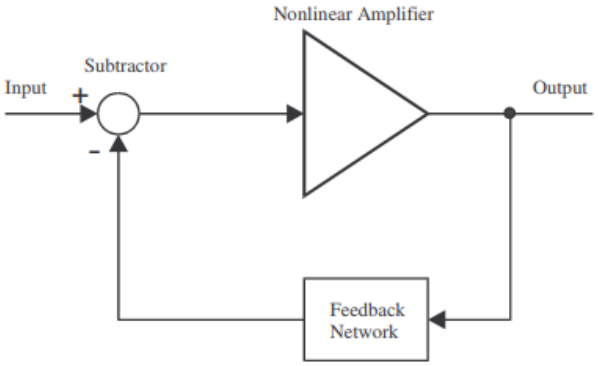

Figure 3.1 Feedback block diagram

In the literature, there are many examples of using feedback techniques for linearization. In 1998 an error-feedback was used which uses the difference between a linearly scaled input signal and the output signal in the feedback loop to minimize non-linearities, unlike the other feedback topologies, this study used an additional amplifier in the feedback loop not to trade off the main-amplifiers gain for linearity. The tests were done at 1 GHz which resulted in a reduction in THD from 0.62% to 0.20% [21]. Later, another type of feedback was used which is power feedback, also known as *multiplicative feedback* which is based on detecting the power of both input and weighted output signals and then compared with an error signal, this type works to compensate only for amplitude modulation to amplitude modulation (AM-to-AM) distortion, which means that the input power to the PA is either enlarged or dropped to compensate for the amplitude nonlinearity, and hence distortion is suppressed. The system was tested over a 100 kHz BW and resulted in a 10 dB reduction in adjacent channel interference [22].

Another study that combined two feedback techniques, active feedback and second harmonic feedback (SHF), has used the second-order harmonics zone power with an active element in the feedback loop as a source of nonlinearity. Sampling the

amplifier's output then amplifying SHZ and canceling out the fundamentals at the feedback loop showed a 10 dB reduction in IMP_5 and 23 dB reduction in IMP_3 with no reduction in the amplifier's gain [23].

Cartesian feedback, which is another feedback type that uses cartesian coordinates, hence the name. Unlike the polar feedback which treats the signal as amplitude and phase, cartesian feedback separates the signal into two symmetrical components *I* and *Q*, therefore two identical feedback loops. The loops must be decoupled from each other otherwise the system becomes compromised. In the case of coupling the system is then said to have phase misalignment. A study that worked on solving the phase alignment problem of the cartesian feedback technique achieved a $\pm 90°$ tolerance in the phase [24]. A second study using cartesian feedback, in which the output signal is attenuated and downconverted then the IMP related to *IQ* demodulation are removed using Butterworth LPF. After that, the *I* and *Q* components are phase adjusted and then subtracted from the input signal achieving I_{Error} and Q_{Error} signals which then are fed to the amplifier. This approach achieved a 22 dB improvement in ACPR at 5 MHz [25].

3.3 Feedforward Technique

The second major technique used is Feedforward, Figure 3.2, this technique is mainly based on subtracting the input signal from the output signal which results in an error signal containing only the distortion products, which is further amplified, and phase adjusted to be subtracted from the distorted output signal to cancel out the IMD [6]. As it can be seen from the figure, feedforward has two main loops. The first is for generating the error signal by canceling out fundamentals, and the second is for amplification and phase adjustment of the error signal.

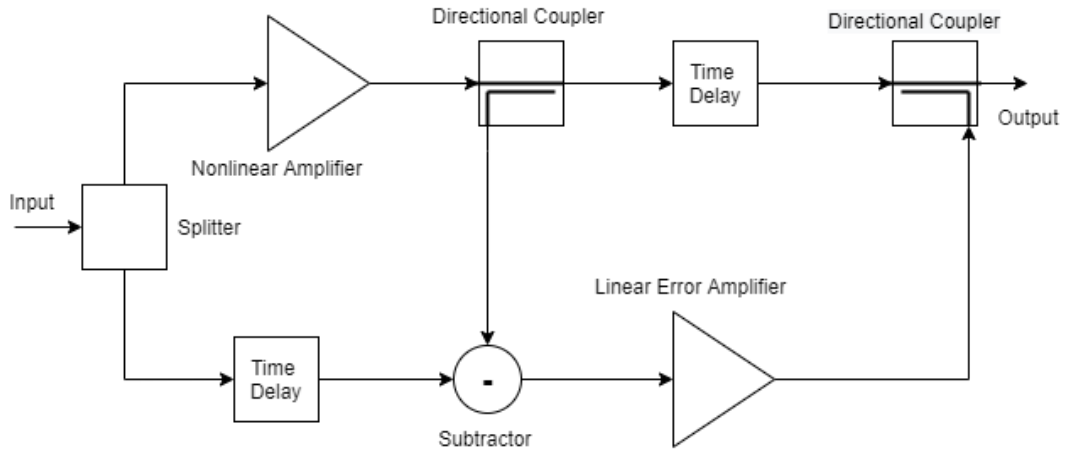

Figure 3.2 Basic Feedforward system block diagram

Feedforward has been used frequently in linearizing PAs, for instance, in 1997 and by using a 32 dB directional coupler for the first loop to achieve the cancellation of fundamentals and 11 dB coupler for the second loop since there is an error amplifier before the coupler, and a 200° phase shifter located before the error amplifier to adjust the error signal to be out of phase to minimize distortions, S-G. Kang, II-K. Lee and K-S. Yoo, achieved a 35 dB IMD cancellation over a 30 MHz bandwidth [26]. Another study, which achieved a feedforward amplifier with better characteristics by changing the main PA into Doherty PA or DPA. The structure of the proposed DPA has two drive amplifiers before the peaking amplifier and the carrier amplifier to allow low power capability phase shifter and attenuators to be used. Which adds more control over the input power for the carrier amplifier and more phase balance. Also the choice of the error PA such that the efficiency of the system is 27.2% and an IMD3 level below -62.5 dBc, which is much higher efficiency than regular feedforward amplifiers [27]. More recently, in 2012, a study implemented a digital-signal processing feedforward amplifier technique, based on Bussgang theorem, using ADC and DAC with modulators to extract the IMD and use that signal in signal cancellation and error cancellation, achieving a 10 dB improvement in the adjacent channel leakage ratio (ACLR) [28].

3.4 Predistortion Technique

The third major technique used is predistortion, Figure 3.3, predistortion is one of the most obvious techniques to linearize amplifiers, as well as one of the most used techniques. A predistorter precedes the amplifier to be linearized. It has characteristics that approximate the inverse of those of the PA so that the overall characteristics approach that of a linear amplifier [6].

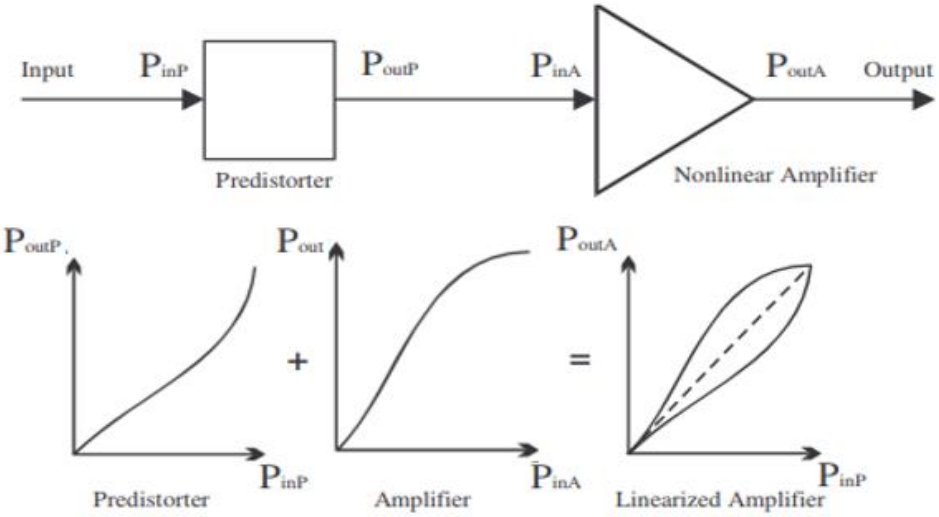

Figure 3.3 Predistortion linearization block diagram

In the previous techniques as well as this one, there are two ways of circuitry to perform the design of the linearization circuitry, digital or analog, since predistortion is more widely used these two types are identified as analog predistortion or APD and digital predistortion or DPD. The literature on predistortion linearization is rich with many studies and different ideas. Predistortion technique mechanism is quite simple, normally the input signal is divided into two paths, linear path, and nonlinear path, the linear path has time delay equal to the time the signal takes in the nonlinear path as well as a phase shifter to be opposite to the signal resulting from the nonlinear path. In the nonlinear path, a component or more that is introducing the nonlinearity is used with phase shifters.

The nonlinear device used in the nonlinear path can be a diode, an amplifier…etc. In other words, any device that can produce IMDs similar to that of the PA. There are many studies on using different types of nonlinearity sources in the nonlinear path. For instance, using mixers can achieve linearity whether its single balanced mixer to generate the down-converted difference frequency signal and a single-ended mixer to produce the desired IM3 products [29]-[31], or two double-balanced harmonic mixers with phase shifters and attenuators to suppress the fundamentals and amplify the IM3 products in the nonlinear path [32]. The nonlinearity can also be achieved via diodes, but since diodes have a narrow band dynamic range over which they perform linearization, more than a single diode is used with a technique called curve fitting, hence a number of diodes N is used to 'fit' the inverse of the PA nonlinear characteristics [33]. A combination between different diodes can also be used like Schottky diodes and pin diodes [34], in fact, a combination between any nonlinear source component and another can be used in the linearization process.

The linearity of the amplifier can also be achieved with the involvement of digital circuitry. Digital predistortion is the use of signal processing alongside analog components to generate nonlinear products. Analog to digital converters (ADC) is used to convert the down-converted signal to a digital signal that can be processed and analyzed [35]. DPD has proven better linearity for amplifiers with memory effects, with different memory-effects algorithms [36].

Another interesting approach was the use of transmission lines transformers to achieve the linearity of high-power amplifiers since they are superior matching networks for high-power amplifiers [37].

Table 3.1 Linearization techniques comparison [6][38][39]

Technique	Bandwidth	% age efficiency	Complexity	Cost	Correction	Advantages	Disadvantages
Analog Predistortion	Narrow 15-20 MHz	5-8 %	High	Low	3-5 dB	• Cost • Low power consumption	• Complex • Moderate linearization
Digital Predistortion	Narrow 15-20 MHz	12-15 %	High	High	15-20 dB	• Cost • Stability	• Moderate linearization • Specific
Feedback	Narrow 15-20 MHz	5-7 %	Low	Low	4-5 dB	• Simplicity	• BW • Gain
Feedforward	Wide 25-65 MHz	6-10 %	Medium	High	30 dB	• Linearity • BW	• Complex • Loss in delay • Large physical size • Cost

3.5 Summary

The linearization of power amplifiers was investigated in this chapter. There are three main techniques to achieve linear PA Feedback, Feedforward, and Predistortion. Each of the previous techniques has its architecture and design, and different circuitry designs within the main techniques approach's scheme.

All the three different linearization techniques have their advantages and disadvantages, Table 3.1 shows the comparison between the techniques. The linearity achieved by either of the techniques differs and depends on the application and which type of amplifier is used to test this technique. Although, these techniques have different designs and different working principles, yet the main idea to achieve the linearity is the same, which is generating a nonlinear product similar to that of the PA and adjust those nonlinearities such that it cancels out those of the PA.

CHAPTER 4

LITERATURE REVIEW ON ADAPTIVE LINEARIZATION

4.1 Introduction

A power amplifier's linearization plays an important role in any system in order to obtain a clear non-distorted signal. Linearization techniques were introduced to ensure the reduction of the distortion products, whether it is intermodulation distortion or harmonics, caused by the amplifier's nonlinearity. Although, linearization techniques were successful in reducing the distortion products and achieving rather linear amplifiers, yet they are not immune to any change that might occur to the system, hence adaptability is required.

The adaptability concept is relying on the ability of a system to maintain its function regardless of any sudden changes or slowly changing parameters on the system, in this case, the ability of a linearization technique on maintaining a linear PA under changes in the system. In general, adaptability is required to compensate for the amplifier's characteristics drifts. These drifts are caused by one of many different reasons such as a change in temperature, supply voltage variations, and aging of the device. These factors may not only affect the amplifier's characteristics but also if the amplifier is linearized the components used in the linearization technique might also get affected which leads to remarkable degradation in the performance.

Hence, adaptive linearization techniques are used to adjust to the changes in the characteristics caused by the previous reasons. These adaptive techniques are added to the linearization techniques to provide a learning mechanism that learns the change in the system and then adjusts to it. There are two different approaches to achieving adaptability, digital and analog.

4.2 Digital Adaptive Linearization

Digital adaptability in linearization is based on modeling the PA's nonlinear characteristics and then identifying the unwanted signals, i.e., IMD and HD. Then sampling the output of the power amplifier and compare these values with the predefined values in the model of the PA, finally optimizing the linearization technique to minimize the undesired distortions.

The sampling process is normally done using analog to digital converters (ADC) and the processing is done digitally then again using digital to analog converters (DAC) and modulators. The analog signal resulted from the signal processing is fed to the amplifier or the linearization technique controlled by the digital system to achieve adaptability.

The modeled behavior of the PA is saved in a table, that method which is most of the digital adaptive systems based on is called, look-up-table method (LUT). The tables that are used in this method differ depending on the information kept in the table and how it is used. For instance, in [43] the LUT mainly contained the linear input-output characteristics of the PA. Let S_{in} be the amplitude of the input signal, the desired output amplitude, Y_{od}, is known from the table. This value is compared with the actual output of the PA, if a value match is found in the actual output, Y_{ac}, then this value is used to search for the proper input, $S_{in\text{-}d}$, needed to obtain the desired output, Figure 4.1 illustrates the data saved in the LUT in [43] and how it is used. Another approach for using a LUT is as implemented in [50], where the LUT was used to save the error signal that is then added to the input signal.

The LUT is a crucial component in digital adaptability, and different algorithms can model the PA's behavior. The most used algorithms are based on mathematical methods such as the least-squares and crest factor method.

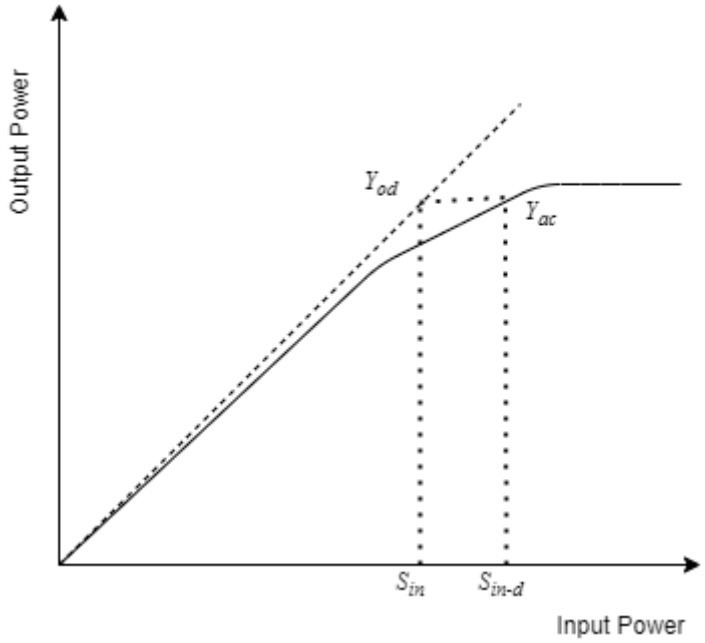

Figure 4.1 LUT usage illustration [43]

4.2.1 Least Squares Method

The method is a procedure that determines the best fit line to data [40]. Which means, with a set of data. Finding the best fit straight line that has a slope that passes through most of the data points. The data points of the set are not necessarily linear functions, all that is required is that the resultant line is a linear combination of these data functions. This method aims to create a line that minimizes the sum of the squares of the errors that are generated by the data functions.

4.2.2 Crest Factor

The crest factor is defined to be a parameter of a waveform that measures the ratio of the peak values to the mean value (RMS value) [41]. In other words, it shows or indicates how dominant the peaks are in a waveform. In PA linearization the crest

factor method is used to identify the peaks, the dominant peaks, part of that are the IMDs, and then working on reducing them, which is called Crest Factor Reduction

(CFR). There are different methods to achieve CFR such as code selection, digital clipping, and pulse injection [42].

For instance, the work done in [42] used a combination of pulse injection and digital clipping to achieve CFR, which shows a 2.2% increase in the PA's efficiency with only the PD stage, but with the inclusion of CFR, it increased to 2.4%, with a combined efficiency increment of 5.6 % with the increase of 1.2 dB in output power.

In general, digital adaptive linearization is composed of two systems, a distortion generator system, and an adaptive control system. The distortion generator system can be any of the linearization techniques discussed before, Feedback, Feedforward, and predistortion. The adaptive control system is a digital system that has a LUT which has a specific parameter that represents the PA nonlinearity which is used for comparison. All LUTs are designed such that there is a constant gain of the distortion system over the PA, desired linear response [43].

A basic adaptive system would include a mixer that is responsible for down-converting the output signal, then an ADC that converts the resultant down-converted signal to the digital domain, using DSP the amplitude is passed through an AM/AM correction LUT, this signal is then used to obtain the phase correction from a second AM/PM LUT, Figure 4.2 [44]-[46].

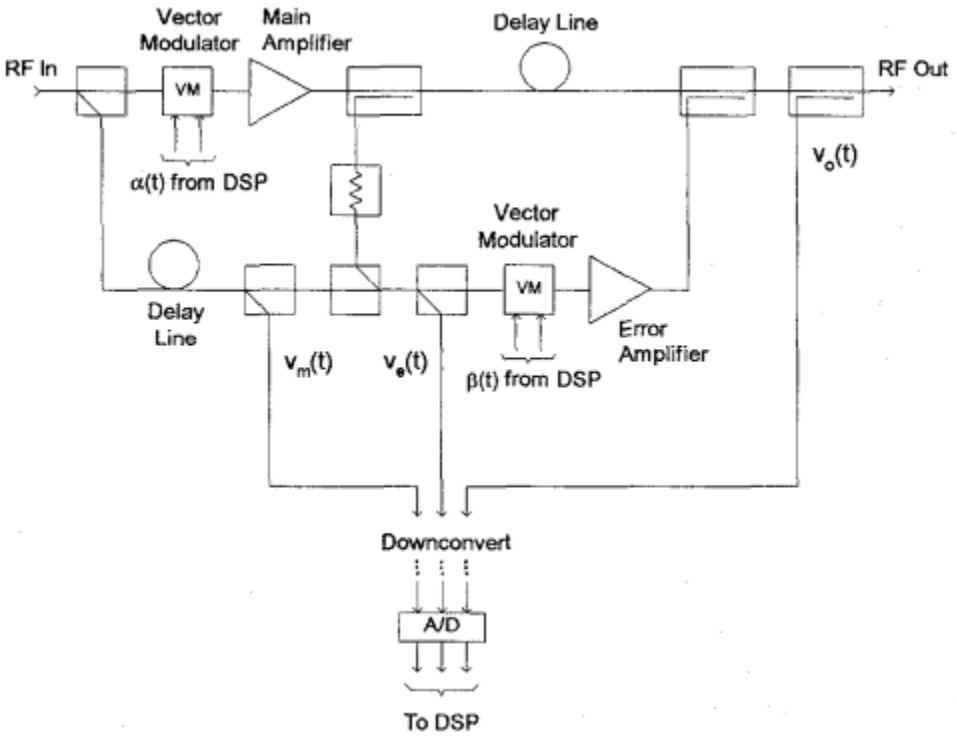

Figure 4.2 An Example Adaptive feedforward amplifier linearizer configuration [44]

As mentioned before, most of the digital adaptability techniques are based on LUT [47]-[53], the differences are between the data saved in that table, might be a model of the amplifier's nonlinear behavior [54] or thermal behavior [55]. Also, the method of obtaining these data might be different, for instance, some work is based on the least square method [56], others are using the Volterra vectors to implement the LSM [57], or even using machine learning to achieve the same goal [58]. The result of using a digital adaptive linearization shows an improvement between 15-40 dB in IMD reduction and an increase in the efficiency between 5-10%.

4.3 Analog Adaptive Linearization

As the name implies, analog adaptation is done without modeling the PA's characteristics to a digital domain and having to perform digital signal processing (DSP) to achieve adaptability. However, the use of a digital component might be applicable for analog adaptation, in which case a microcontroller unit (MCU) is used as a measuring device or a voltage control device, such as in [59]. Which uses an MCU to measure the output of a power detector that detects the out-of-band power at the output of the PA after passing through a bandpass filter, and then accordingly controls two nonlinear second-order functions that represent PA's inverse AM/AM and AM/PM nonlinearities. Another example is DC bias control which is done in [59], which is controlling the DC bias of the gate of the common-source (CS) and the common-gate (CG) stages of a CMOS cascode PA.

Unlike digital adaptive linearization, analog adaptive linearization can be challenging with a complex circuitry design. For instance, Figure 4.3 shows the circuitry of an adaptive feedforward-based linearization. In this work, linearization is achieved using signal cancellation of a feedforward technique [61]. The adaptability is then added to the first loop of the signal cancellation, by adding a synchronous detector which is controlling a signal controller.

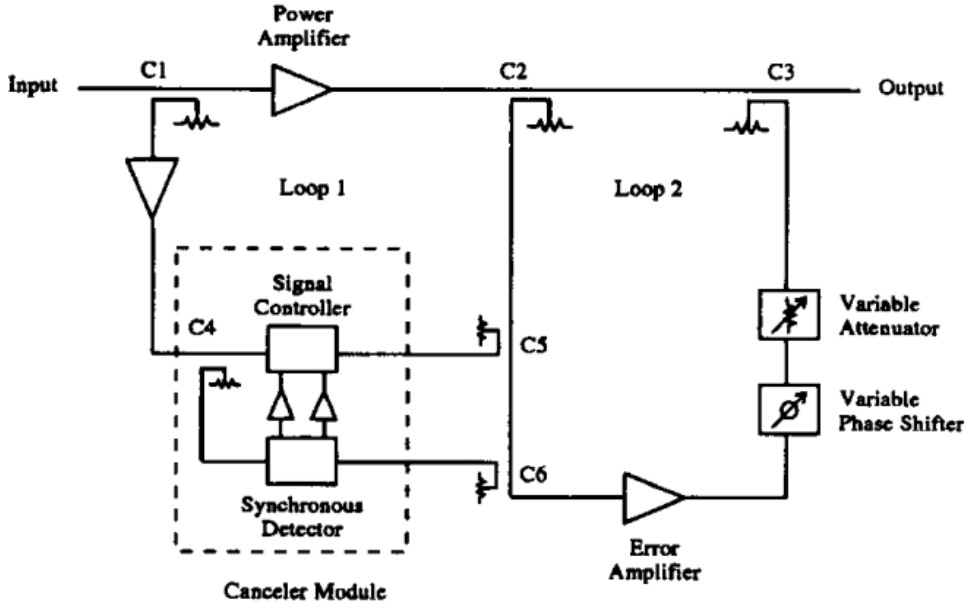

Figure 4.3 Adaptive feedforward linearization [61]

The adaptability is achieved by a comparison that is done by the synchronous detector that compares two samples of power, one from the input, which is sampled by coupler c4, and the output, which is sampled by coupler c6, note that the output sample includes the error of the PA. Then the amplifiers and integrators control the signal controller based on the detector's output, by adjusting the amplitude and phase of the input signal clone injected back to the error loop at coupler c5 [61]. This 'canceler module' loop added to loop 1 achieves adaptability by a continuous comparison between input and output, using this module results in a 25 dB cancellation of the IMD3 products and 13-16 dB cancellation of IMD5 products.

Another study that uses feedforward as a linearization technique to be optimized for adaptability is [62]. The feedforward in this work is adjusted by adding two adaptation controller units to the signal cancellation loop and the error loop as seen in Figure 4.4.

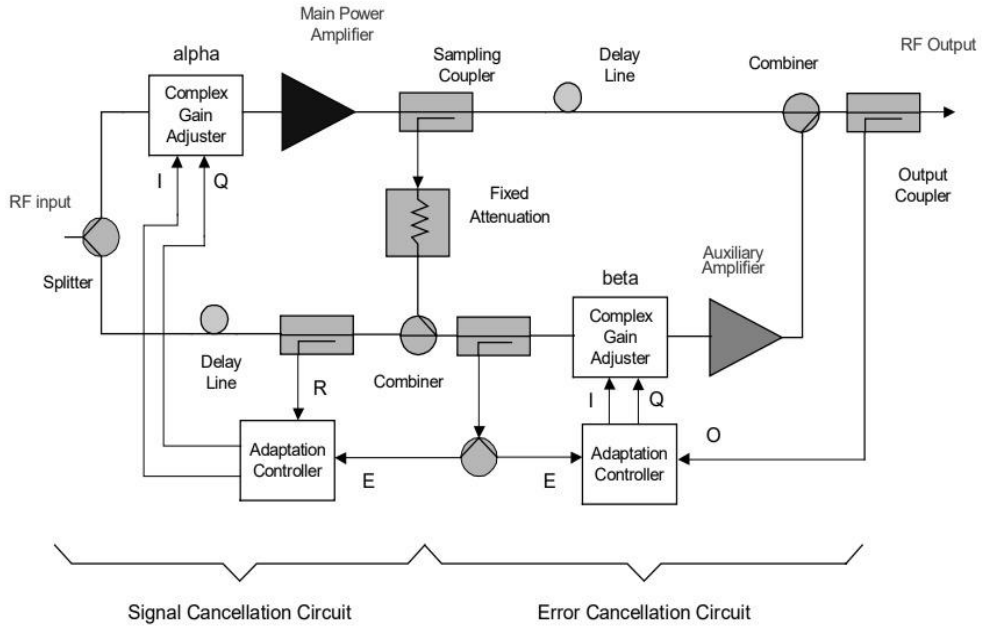

Figure 4.4 Feedforward with adaptation control units [62]

These adaptation control units are responsible for measuring the sample of the linearized output and then adjust the complex gain adjuster (beta) in the error loop. Also by taking a sample from the signal cancellation loop then control the complex gain adjuster (alpha) at the input of the PA accordingly, which achieves an improvement of 40 dBc of IMD3 and 65 dBc of IMD5 [59]-[62].

4.4 Summary

Adaptive linearization is a concept that was adopted by many researchers and has been investigated in many studies. As mentioned before, adaptive linearization techniques can be categorized into two main categories, digital and analog. Digital adaptive techniques have a variety of approaches that uses concepts such as LSM and Crest factor. Analog adaptive techniques are mainly dependent on signal cancellation, which can be achieved with the cost of complex circuitry.

CHAPTER 5

THEORY AND SIMULATIONS OF THE PROPOSED SYSTEM

5.1 Objectives

The adaptability of a linearization technique rests entirely on its ability to respond to the change that might occur in the system. These changes as mentioned before can vary from temperature, variations in supply voltage to aging of components. The response time of the adaptive linearizer is significant in the overall performance and linearity of the power amplifier since the changes that occur in the system can lead to damaging one of the system's components.

The quicker the response time to the change the better is the adaptive linearizer system, the aim is to have an adaptive system that is adapting to the change simultaneously as it is occurring. Which is the purpose of this thesis, to introduce an adaptive control of linearization technique that can detect the change that occurs and adapt the linearizer system to it simultaneously.

In this chapter, the theory and methodology of the adaptive control technique proposed and the linearization system, that was chosen to implement this adaptive control system, will be discussed alongside the components that are used in the system, for both the adaptive system and the linearization system. Then, the simulations that had been done to prove the system's functionality, will be included in this chapter as well.

5.2 The Linearization Technique

The linearization technique that was used to implement the adaptive system is a predistortion technique that was published in 2018 [32]. This work is based on using RF mixers to generate the distortion that is, later on, going to be adjusted to cancel the distortion of the power amplifier. It is very important to note that the linearization technique chosen is not tied to the adaptive control system proposed, rather it is a way to demonstrate the working of the proposed system.

5.2.1 System Overview

Like most of the predistortion techniques, and as the name implies, the system is designed such that it produces a predistorted signal at the input of the PA, the system is mainly divided into two branches, Figure 5.1, these two branches are both fed by the fundamental signals that are the inputs to the system. The first path or branch is the nonlinear path, which is the path where the fundamental signal gets processed using the distortion generator circuitry to produce distortions similar to that of the power amplifier with a suppressed fundamental signal.

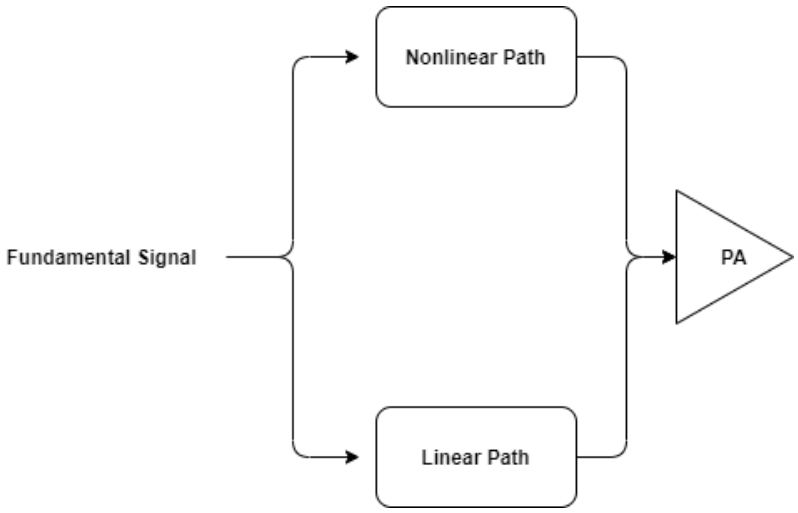

Figure 5.1 General block diagram for predistortion technique

The linear path includes only the fundamental signal which is at the end going to be added to the signal generated from the nonlinear path and then the resultant signal will be fed to the power amplifier.

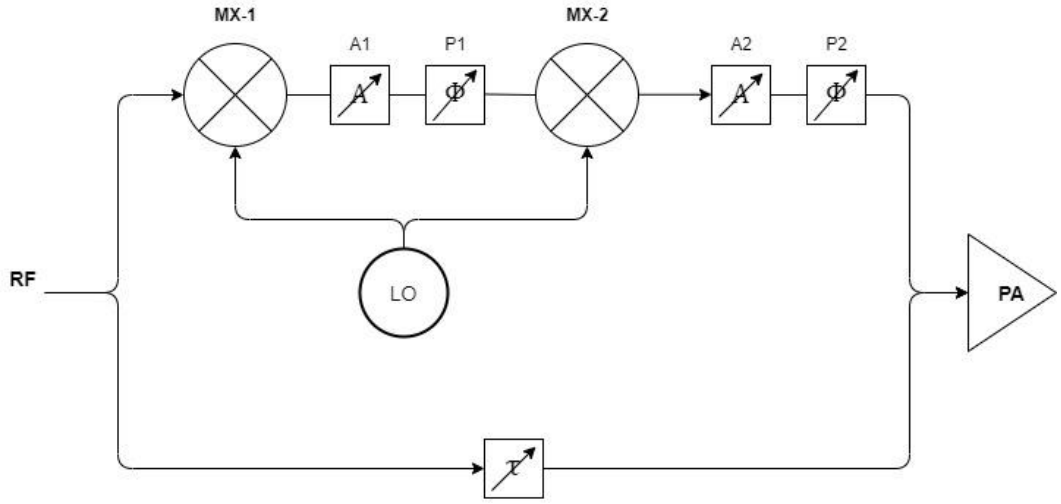

Figure 5.2 Predistortion full system

Figure 5.2 shows the detailed circuitry of the predistortion system used. As it can be seen from the figure the linear path only includes a variable time delay component. This time delay is adjusted to be equal to the time the signal has taken to travel through the nonlinear path so that when the two signals are added together at the input of the PA there will not be any time shift difference.

The nonlinear path is composed of two different functions, first is the distortion generator, which contains the two mixers MX-1 and MX-2, the variable attenuator A1 and the variable phase shifter P1. The second functionality of the nonlinear path lies in the second set of variables, attenuator A2 and phaser shifter P2, these two components' main function is to adjust the magnitude and the phase of the error signal created by the distortion generator circuitry so that it has a magnitude that is high enough to cancel the IMD products of the PA, and to have the optimum phase difference between it and the fundamental signal coming from the linear path that would achieve the highest cancellation of IMD3 and better amplification of fundamental signal at the output of the amplifier.

After the signal has traveled through both paths, they get added at the input of the PA which produces the predistorted signal that has the same characteristics but the opposite phase of that of the PA.

5.2.2 The Distortion Generator

In this work, the distortion generator uses a double-stage double-balanced harmonic mixer (DBHM). Double-Balanced Mixers provide balanced ports for the input RF and LO signals so that it reduces the mixer's unwanted spurs and improves the isolation between the ports [63]. Figure 5.3 shows the distortion generator's block diagram. The RF signal firstly is mixed with a LO frequency which translates it into an intermediate frequency (IF), and the second mixer translates it back into RF since the same LO is used [32]. The advantage of using such a design, other than the generation of the IMD signals required for the linearization, is that the ability to suppress the fundamental signals to a minimum level, which is achieved by controlling the variable attenuator and phase shifter to achieve the optimum level of suppression to fundamentals.

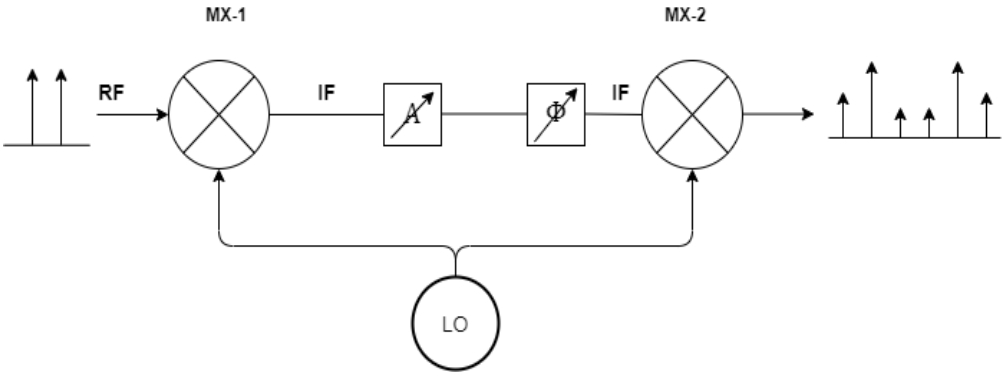

Figure 5.3 Distortion generator block diagram [32]

This advantage allows the production of an error signal which dominantly consists of IMD products. The suppression of the fundamentals is required since the nonlinear path should produce only an error signal that is going to be added with the signal from the linear path. In case the signal from the distortion generator contains a

relatively high level of fundamentals that would cause a problem. Since this error signal is going to be phase shifted and added to the linear signal, assuming a high level of fundamentals, this might lead to fundamental signal cancellation and loss of information.

5.3 Proposed Adaptive Linearization System

This work proposes an adaptive linearization system that is highly adaptable to any of the changes that might occur. Linearization techniques are built to fit specific criteria with a specific power level and application. In practice or in a system that is in operation, maintaining a fixed power level is almost impossible due to the losses that happen in the components themselves and during transmitting and receiving signals.

The adaptable system in this work is mainly composed of a microcontroller unit (MCU) that is controlling other components with different functionality in the system. The proposed system is based on the fact that most of the linearization techniques are using phase and amplitude corrections. These corrections are done using mainly variable attenuators and variable phase shifters, whether these phase and amplitude adjustments are done to the error signal or in a signal cancellation loop. The main idea of this system is the voltage control of the variable attenuators and phase shifters available in the linearization technique.

The originality or what distinguishes the system from the previous work is that the measurements done by the MCU are taken from the output. In other words, the system’s analysis deals with the resultant signals from the error generation circuitry or the cancellation circuitry. This means that the behavior of the components is not necessary for the analysis to be done. For instance, drift in an attenuator's behavior would change the resultant signal that passes through it, and since the analysis is done on that signal, then the system will control the attenuator according to its new behavior. The MCU’s main goal is to achieve low IMD3 levels, assume that the

attenuators available in the system provide attenuation between 0-20 dB, for the sake of argument assume that 20 dB attenuation results in the lowest IMD3 level, if the attenuator had faced any characteristics drift that caused the maximum attenuation value to become 19 dB, then the MCU's control would measure that this is the best value achievable and hence controls the attenuator accordingly.

5.3.1 System's Working Principle

The MCU in the system is connected to the linearization technique in different critical points at which the MCU makes the required measurements and then controls the control voltage of the components mentioned earlier to achieve the required linearization. The connection points are solely dependent on the linearization technique that the proposed system is applied to.

For instance, for the linearization technique chosen in this work to perform experiments and simulations. The proposed system is connected to it at two main points. The first connection point is at the output of the second mixer MX-2 at the distortion generator part of the nonlinear path. Figure 5.4 shows the implementation of the MCU on the distortion generator part of the nonlinear path. As it can be seen the output of the second mixer MX-2 is connected to coupler C1, the coupler's functionality is to take a sample signal without disturbing the flow of the main system. The coupler's coupling is adjusted accordingly to a power level that will not harm the MCU input port. Once the signal is coupled, it goes through a third mixer whose main purpose is to down-convert the signal to a level that is measurable by the MCU. The downconversion happens by mixing the coupled signal with a different frequency desired for the correct downconversion.

Note that the LO frequency connected to MX-1 and MX-2 is different than that of the LO connected to MX-3.

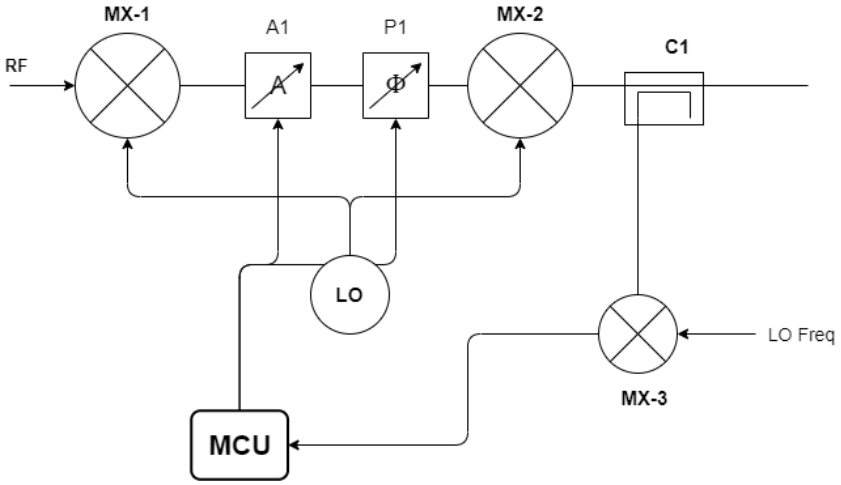

Figure 5.4 Block diagram of the first connection point

The signal received at the MCU port is converted to a digital signal using the MCU's built-in analog to digital converter (ADC), then the signal is sampled and then the samples are saved into an array which is used to perform Fourier Transform. The Fast Fourier Transform (FFT) algorithm, Appendix I, is used to analyze the samples array. Which will result in a frequency spectrum that has the dominant frequencies in the signal.

The dominant frequencies in the signal are the fundamental signals and the IMD3, assuming the input to the system is a two-tone signal. The MCU then identifies the IMD3, and the fundamentals based on a predefined value of both frequencies, and then check the level of each of the IMD3 and fundamentals then the adaptive process starts. The MCU is as mentioned earlier controls the control-voltage of A1-attenuator and P1-phase shifter, the MCU starts to change the voltage and then perform FFT on the signal simultaneously and accordingly controls the voltage to achieve the required objective, the objective here is to have a low fundamental and a high IMD3 in the signal, and that is the aim that is set for the MCU to achieve. Figure 5.5 shows the flow chart of the algorithm that the MCU follows to achieve adaptability in the error signal generation.

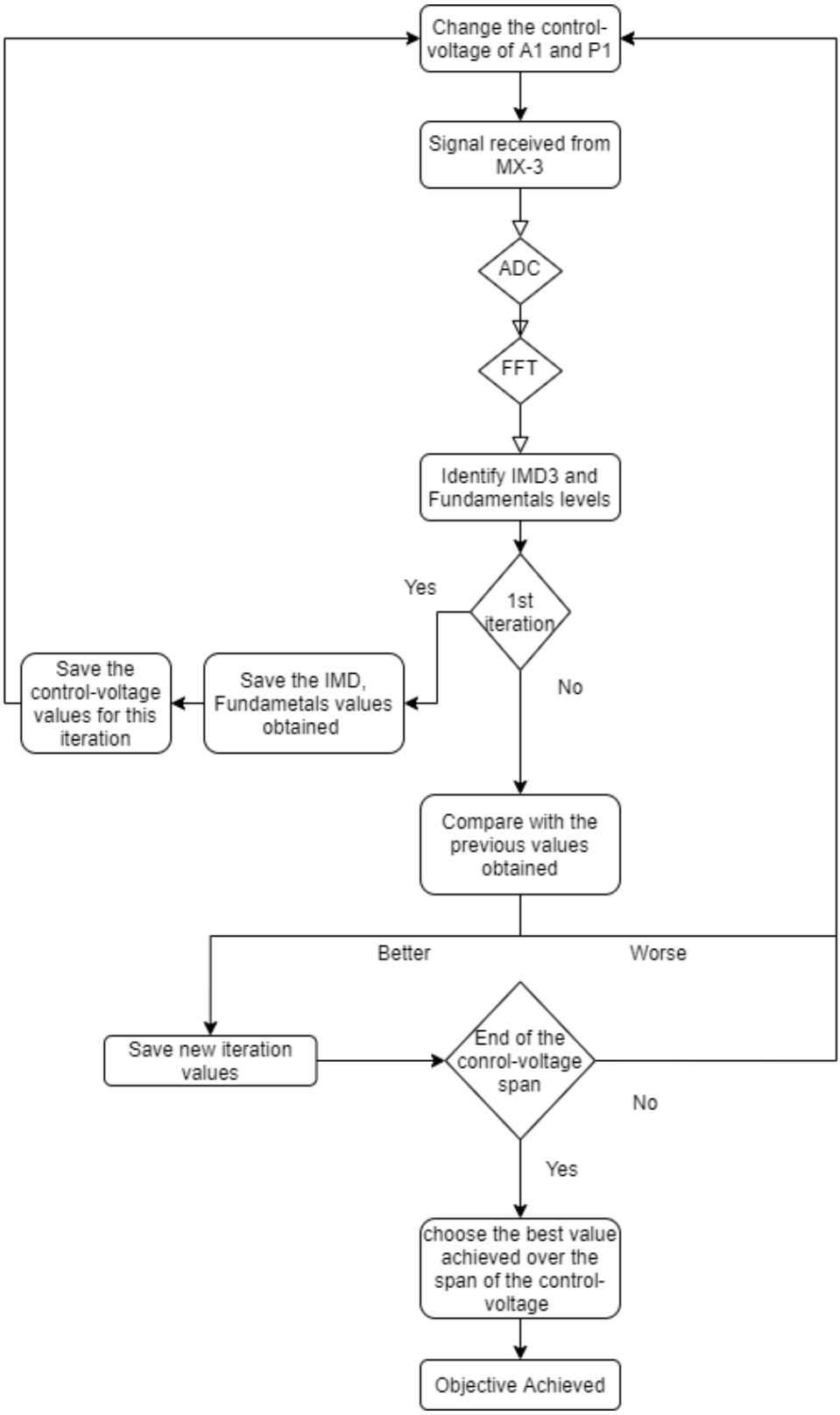

Figure 5.5 Flow chart for error signal algorithm

The second connection point between the system and the MCU is at the output of the power amplifier. Figure 5.6 shows the MCU second connection point with the linearization technique. At this point, as it can be seen the MCU receives one reading and controls 4 DC-control for 2 variable attenuators (A2 and A3) and 2 variable phase shifters (P2 and P3). It can be noticed that the reading approach here is different than the previous approach, the aim is to introduce different approaches to achieve the same goal. Which is reading a sample signal that the MCU will be able to analyze. For this approach, the signal in the linear path was used, which contains only fundamental signals, by adding the adjusted fundamental signals to the output of the PA to achieve fundamental signal cancellation, which leads to a signal dominated by IMD3.

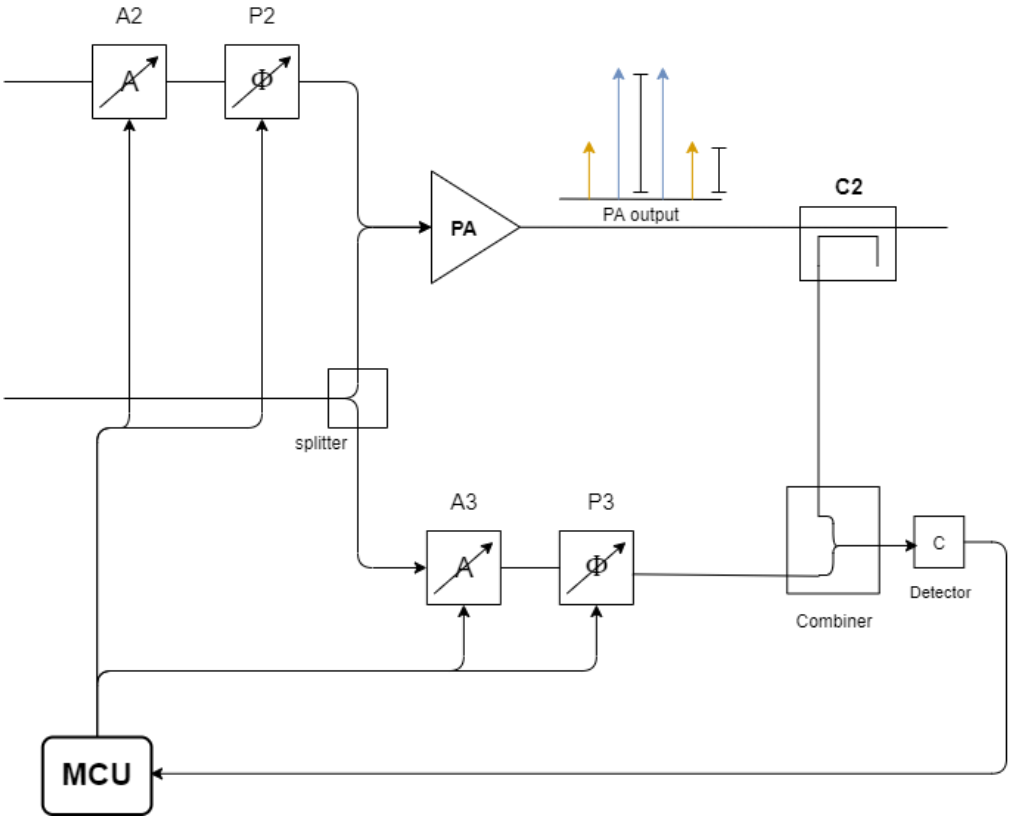

Figure 5.6 Block diagram of the second connection point

The principle of operation of this part of the system can be summarized in a few points that are explained in detail later:

- The coupler C2 takes a sample from the output of the PA.
- The sampled signal is added to the fundamental to achieve signal cancellation.
- The MCU controls A3&P3 to achieve the best fundamental cancellation.
- The remaining signal's power is dominated by the IMD3 power.
- The MCU controls A2&P2 to achieve linearization.

The coupler C2 is used to take a sample from the output signal that is going to be used for analysis. The coupling for the coupler is chosen to match the signal arriving from the linear path. Then these two signals are added using a power combiner that is followed by a crystal detector that measures only the power level of the signal that is delivered to the MCU. Understanding the functionality of each of the 4 (A2, P2, A3, and P3) components that the MCU is controlling at this point is very critical since it is the basis of using this approach. The first set of variables, A2- attenuator and P2- phase shifter are responsible for controlling the level of the output IMD3, controlling the control-voltage of these 2 components means controlling the level of IMD3 in the error signal fed to the PA which means if the IMD3 power available in the error signal is high, then the IMD3 power available in the output of the PA is low, and vice versa.

Similarly, controlling A3-attenuator and P3-phase shifter means controlling the power level of the fundamental signals available in the signal fed to the MCU. So the idea of this approach is simply as follows, the MCU reads the power level that is fed to it by the diode detector, then the MCU controls the voltage of A3 and P3 first which will lead to either a decrease or increase in the overall power, but in order to measure the level of IMD3, the control-voltage needs to achieve the lowest power level read by the MCU, which means the most cancellation of fundamental signals. Meanwhile, the MCU does not change the A2 and P2's control voltage that is to ensure that the drop in power is purely caused by the cancellation of the

fundamentals. After achieving the most cancellation possible, which means that the remaining power in the signal is dominantly the IMD3's power.

The MCU moves to the next step, which is changing the control voltage of A2 and P2 to achieve lower power readings. At this point almost all the power read is from the IMD3 products at the output, the change in the voltage of the two variables would decrease the power of the signal, which confirms that higher linearity is achieved. This approach is using the method of 'polling' which is reading the value of the signal and changing the control voltage of the first two components (A3 and P3), while the other two components (A2 and P2) are on hold. Once the first objective is achieved from controlling the first two components, then the second two components are under the control now and the first two are on hold. Figure 5.7 shows the flow chart of the algorithm to achieve this aim.

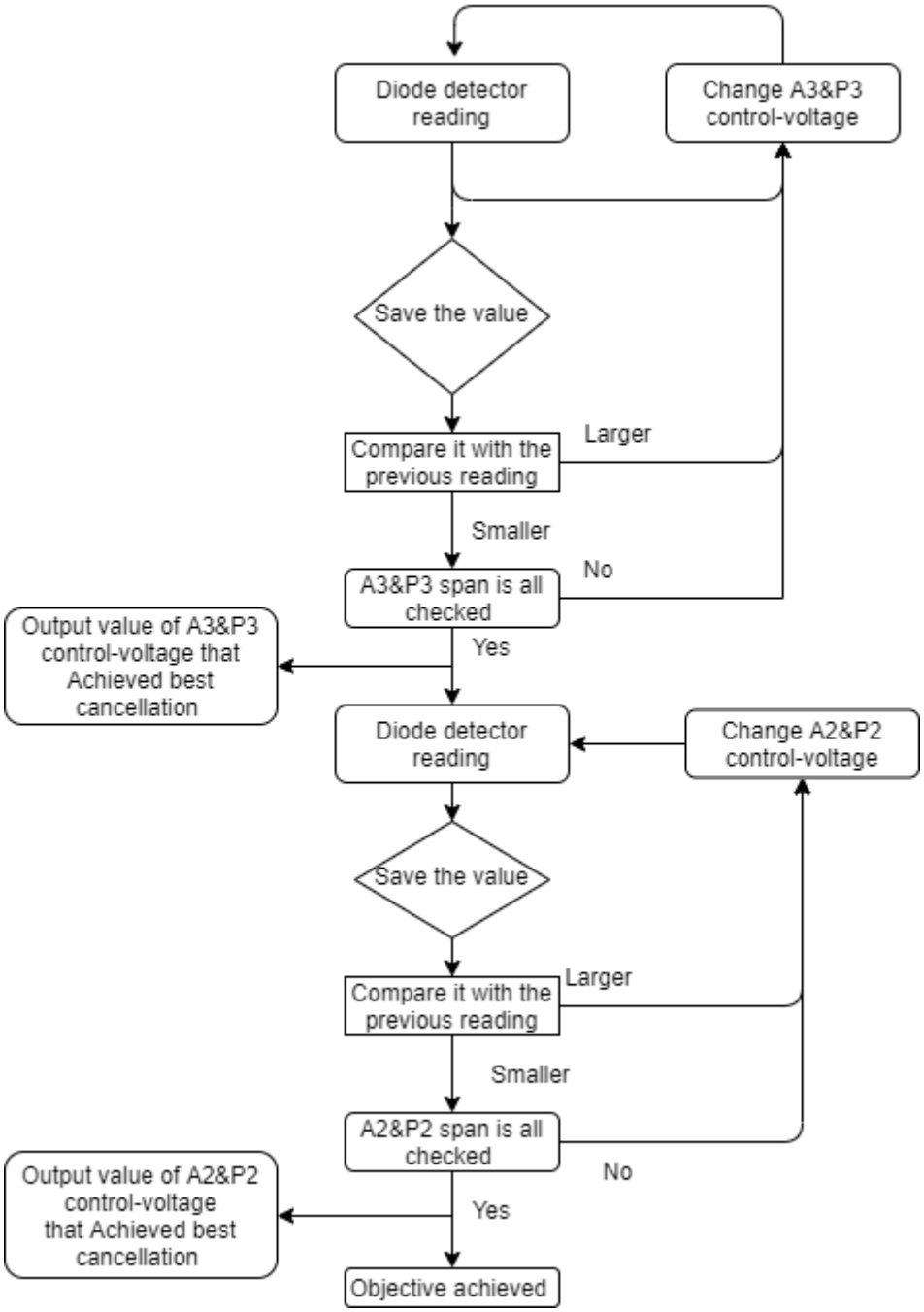

Figure 5.7 Flow chart of the output control algorithm

Finally, it is important to understand that MCU will be running both algorithms simultaneously, by taking the reading of the two connection points of the system using two different ports. Figure 5.8 shows a complete diagram of how the system would look like.

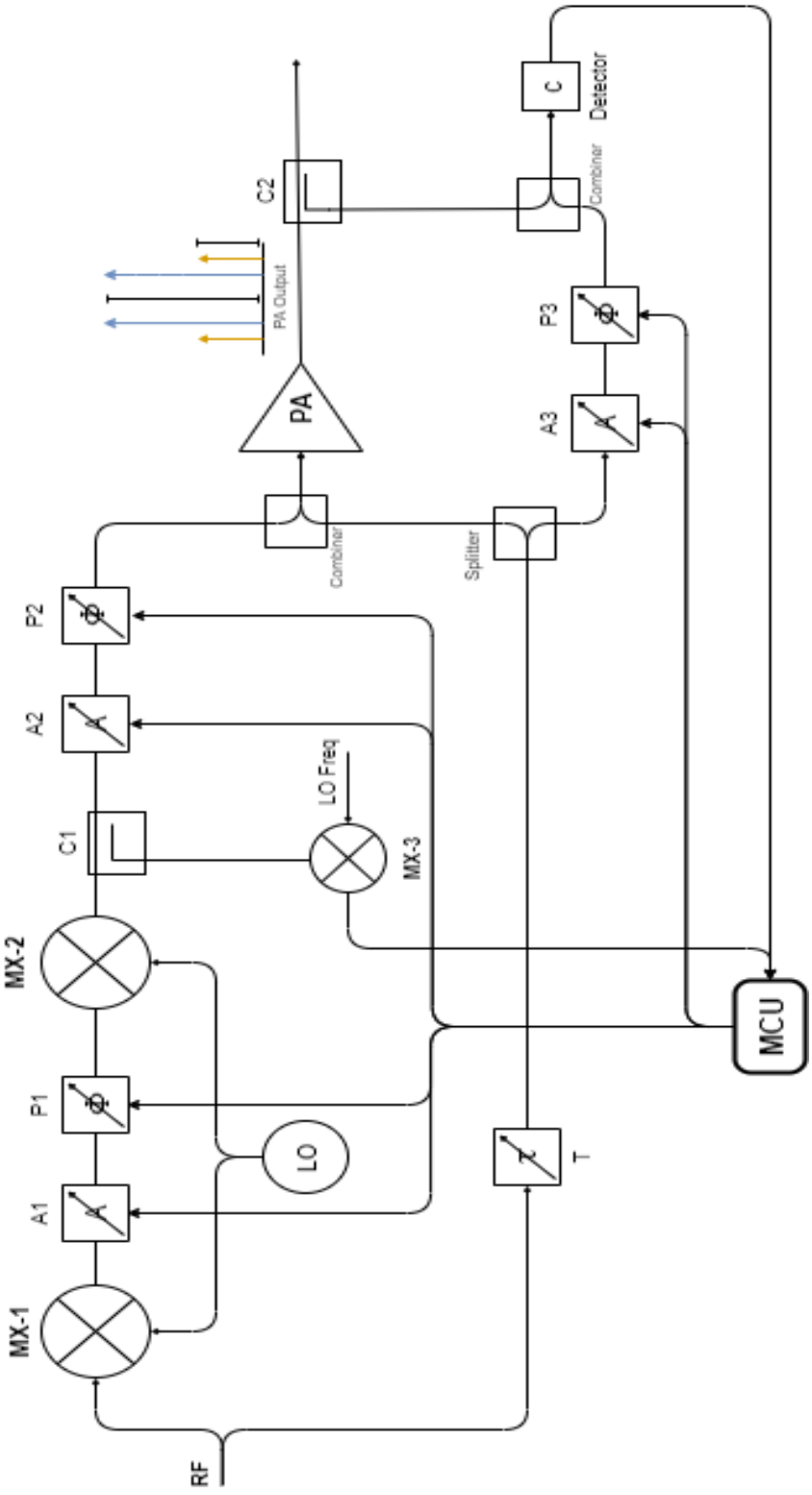

Figure 5.8 A block diagram of the complete system

5.4 Methodology

The methodology behind the proposed adaptive system was a long process of reading previous work, choosing the components appropriate for the task, and finally testing and experimenting. These processes can be explained in the following subsections.

5.4.1 Methodological Approach

The main aim of this work is to introduce an adaptive system that can be integrated into most if not any linearization techniques. To achieve this aim there were a few main concepts that needed to be studied, first, the problem of power amplifiers nonlinearity and efficiency, which is as explained earlier, one of the largest fields of research in the electronics field nowadays, because of its vital role in any technological advances. In order to describe this problem, the power amplifier's input power versus output power is studied and compared with the ideal output power of the amplifier, same process is used to describe the efficiency of the power amplifier.

To be able to solve these problems the data from such studies were investigated to have a better understanding of the problem and its cause. These data, such as in Figure 2.4, Figure 2.5, and Figure 2.6, are the characteristics of power amplifiers and they describe the problem generally for almost all types of power amplifiers. Although these characteristics might change slightly, the general behavior is the same. For this thesis, most of the data required to describe and understand the problem were collected from the literature, as it is described in the previous chapters.

Secondly, the linearization techniques had to be studied and understood properly to decide which technique would be most applicable to implement the adaptive system. By studying the literature and reading more about the different techniques, predistortion linearization was chosen. Thirdly, the work that had been done on adaptive linearization in the literature was studied to build a good background which is the base of moving forward into introducing this work.

The methodological approach, as well as the data needed to build this work, was done by studying the literature and previous studies. Since the field is quite rich with different characterizations of the problem, linearization techniques, and adaptive linearization systems, the need for obtaining primary data that requires experimental work was not necessary. Only while performing simulations, these data were collected specifically for the PA and the linearization technique that was chosen to implement the proposed system.

5.4.2 Data Collection Criteria

For this type of work, the data needed to proceed with simulation and experimenting were information to understand the behavior of the power amplifiers and why they exhibit such behavior. Later on, understanding the linearization techniques and how they are added to the PA. To represent the behavior of PAs some variables needed to be measured, these variables are used to express the linearity of the power amplifier and the effect of the linearization on these variables. 3^{rd} order intermodulation distortion level, 5^{th} order intermodulation distortion level, fundamental signals level, and power efficiency, are the most important parameters that describe the system. Collecting these different variables has been done in different ways, for the simulations Advanced design systems (ADS) software was used since ADS is compatible with the RF range of the PA and the components used in the linearization technique. As for the experimental work a Spectrum Analyzer and an Arduino Mega2560 were used to collect such data.

There are a couple of criteria that were followed to obtain these data. First, the power amplifier is biased properly. Second, the input power of the PA is enough in order to produce the intermodulation distortions that cause the nonlinear behavior.

5.4.3 Data Analysis

As mentioned in the previous subsection, 3^{rd} and 5^{th} order intermodulation distortions, fundamental signal level, and power efficiency are the most important parameters that were considered in this study. In order to prepare the data for analysis a class-AB power amplifier was tested with a 1-tone test to check for the harmonics, note that harmonic distortions are not important in the scale of this work since they can be filtered out easily because they are far away from the fundamentals band, yet the test was done for a better understanding of power amplifiers. Then with a 2-tone signal test to obtain its behavior and to measure the level of 3^{rd} and 5^{th} order IMDs to the fundamentals level. These two different tests were done for the simulation using Advanced Design Systems (ADS) software.

For the experimental work, the analysis was done using Arduino software with Fast Fourier Transform (FFT) algorithm, signal generator as well as Vector Spectrum Analyzer.

5.4.4 Methodology Choices

In this thesis, different choices were made to reach the objective of the thesis starting from the PA to how to achieve adaptability. The power amplifier that was chosen was a class-AB amplifier since it has high efficiency without compromising linearity which was convenient with the desired system. The linearization technique choice is not significant for the adaptive system proposed where it is independent of the linearization technique it is implemented on. Lastly, the adaptive system choice, which is choosing to use a microprocessor to achieve adaptability, is the contribution achieved in this thesis. This choice is to introduce a smart adaptable digital system that doesn't require the human factor to operate it, it makes all measurements and decisions according to how it is programmed, which will open the way for more improvement in future works to be more dependant on digital smart systems that can make decisions. On the other hand, most of the adaptable systems available in the

literature were either using analog components to achieve adaptability which is not applicable for the objective of this thesis at all, since these systems have to be operated manually and the decision-making process is done according to manual observations and measurements unlike what this work proposes. The other type of adaptive systems, which was using a digital approach, was dependent on having a precalculated data that is saved into a table, and accordingly, the decisions are made. The issue with this approach is that the decisions are limited by the values or the options available in that table, which in some cases may not be the optimal option, since some of the changes that might happen to the system can be other than the change in the signal power or the signal itself, it can be caused by aging or even temperature in which cases the characteristics of the amplifier itself changes, hence, the data in the table is no longer the same for that amplifier to achieve the required linearity. Table 5.1 shows a comparison between the different adaptive techniques and this work.

The only limitation that can be noticed by choosing our approach is the capabilities of the microprocessor. Which are the analog to digital conversion (ADC) capabilities or the processing capabilities that might require some time to process a large set of data. But considering the strengths that such approach provides, such as it can be implemented on any linearization technique, the ability to make decisions and differentiate between desired and undesired signals. Those limitations can be out weighted by the strengths. And also noting that these limitations are very easy to fix by choosing a high-end microprocessor. Unfortunately, the microprocessor at hand that was used for this work (Atmega2560) was not one of the capable processing units, but it is enough to prove the concept.

The main reasons for choosing Arduino Mega for this work were the price, the easy access, and the user-friendly workspace, Since the price of this Arduino is low and it can be found almost anywhere. To prove the concept, a low frequency was used as an input to the MCU, and the Arduino was able to sample it and analyze it which indicates that with a more advanced MCU with higher ADC capabilities and sampling rate, this approach is valid.

Table 5.1 Comparison between different adaptive techniques [43]-[62]

Adaptive Type	Cost	Complexty	Advantage	Disadvantage/Limitations
Digital Adaptive linearization	High	High	• Automatic operation • Decision making	• Cost • Complex • Large memory is required for the saved tables • Limited by the data saved
Analog Adaptive Linearization	Low	High	• Cost	• Complex
Proposed System	High	Low	• Simplicity • No memory required/ no data saved • Fast	• Cost • MCU sampling capability

5.5 The Proposed System's Design

The design of the proposed system was done according to three main criterions to meet.

1. The ability of the system to be self-operated once it is set.
2. A system that can be used potentially for any application.
3. A system that is easy to implement, hence easy to be understood.

The first two criterions can be met by the addition of the MCU since it can be programmed to be self-operated, as well as, theoretically, it can be added to any system with the right components choices. Simplicity can be achieved by making all the analysis done via programming rather than the inclusion of an analog component before the MCU.

The first step of designing the system is done by choosing the addition of the MCU. The second step was to determine how it can be connected to a linearization technique and be able to read the signals required for the analysis. This led to two ways that can achieve this task.

1- Reading the signal directly.
2- Reading the signal's power.

In order to be able to read a signal directly by the MCU, that signal must be at a frequency that is compatible with the ADC of the MCU. In the RF domain, the signals are at GHz which is quite high for any ADC, hence a mixer is added to downconvert the signal to the level of the ADC of the MCU. The second way is to read the signal's power which can be easily achieved using an RF power detector. Finally, making sure that all the measurements can be done without disturbing the flow of the linearization technique. For that aim, couplers can be used to sample the signal from the connection points.

At this point the external design of the system was done, meaning that the main components that would achieve the criterions and the signal reading were decided. Moving on to the internal design, which is programming the MCU. After making sure that the MCU had read the signal required for analysis, that signal needed to be analyzed in a way that would allow the MCU to easily differentiate between the wanted and unwanted signal. There are two approaches that were considered in this work.

1- Using Fast Fourier Transform algorithm.
2- Using signal cancellation.

5.5.1 Fast Fourier Transform

The FFT algorithm used in this work is provided in Appendix I, the algorithm is based on the work done by JW Cooley and John Tukey in 1995 [67], in their work the FFT was derived from the Discrete Fourier Transform (DFT) by realizing the symmetries of the algorithm and dividing it so that the execution time would be much lower.

$$X_k = \sum_{n=0}^{N-1} x_n . e^{-j\frac{2\pi kn}{N}} \qquad \text{Eq. 5-1}$$

Eq. 5-1 shows the DFT of a signal. What Cooley and Tukey showed is that the above equation of DFT can be divided into two smaller parts, as shown below.

$$X_k = \sum_{m=0}^{\frac{N}{2-1}} x_{2m} . e^{-j\frac{2\pi k(2m)}{N}} + \sum_{m=0}^{\frac{N}{2-1}} x_{2m+1} . e^{-j\frac{2\pi k(2m+1)}{N}} \qquad \text{Eq. 5-2}$$

$$X_k = \sum_{m=0}^{\frac{N}{2-1}} x_{2m} . e^{-j\frac{2\pi km}{N/2}} + \sum_{m=0}^{\frac{N}{2-1}} x_{2m+1} . e^{-j\frac{2\pi k(m+1)}{N/2}} \qquad \text{Eq. 5-3}$$

Eq. 5-2 and Eq. 5-3, show the division that was done to the main DFT formula. It is seen that now there are two terms for the odd-numbered values and the even-numbered values. The strategy now is not to stop at this point but to realize the symmetries available in each of these terms and dividing them into two smaller parts and so on. With the range of k is $0 \leq k \leq N$, while the range of n is $0 \leq n \leq M \equiv N/2$ it can be seen with the symmetry properties in Eq. 5-3 that only half of the computations need to be executed for each sub-problem [67]. This reduces the computational time from originally being $\mathrm{O}[N^2]$at Eq. 5-1, to $\mathrm{O}[M^2], M = N/2$. To finally, as long as the smaller terms have even-valued *M*, this approach leads to a final computational time of $\mathrm{O}[N\ \mathrm{Log}\ N]$.

Although FFT is one of the most important algorithms in many fields, like Digital Signal Processing (DSP), it has its disadvantages such as the need to apply window function on a waveform to help minimize the oscillations of a function which gives a more desired output. Spectral leakage is a disadvantage that is associated with the windowing method and it happens when windowing a sinusoid, even if the window covers an integer number of cycles. Figure 5.9 shows an example of spectral leakage caused by windowing. [68]

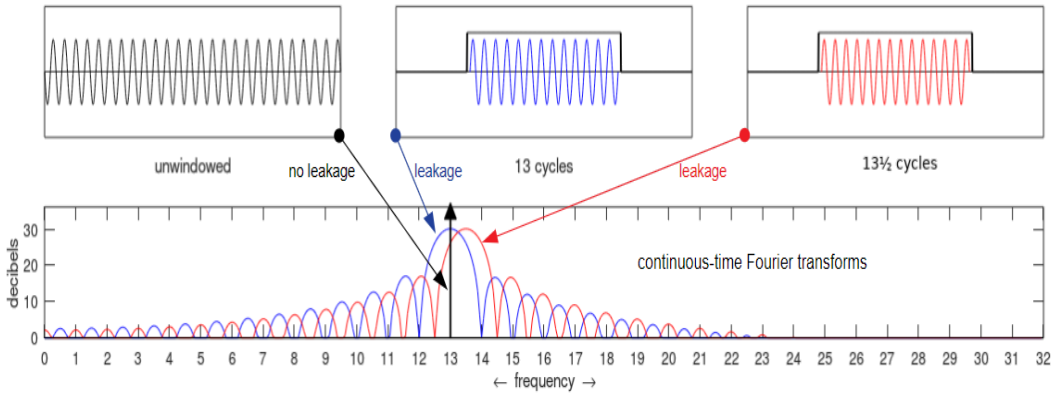

Figure 5.9 Spectral leakage caused by windowing

In order to fix spectral leakage, the sampling frequency has to be increased, which generates longer discrete-time sequences that reduce spectral leakage but don't eliminate the problem.

Choosing a window to be used in the FFT is completely dependent on the application or the processed signal. Different types of windows can be applied, such as Hann, Hamming, Flat Top, Blackman, and Kaiser-Bessel. The difference between these windows is the shape of the window and accordingly its response as well. For instance, a Flat Top window would be a good choice in an application where the amplitude accuracy is important since it has the best amplitude accuracy compared to other windowing functions [69]. Figure 5.10 shows the different shapes of some of the known windowing functions.

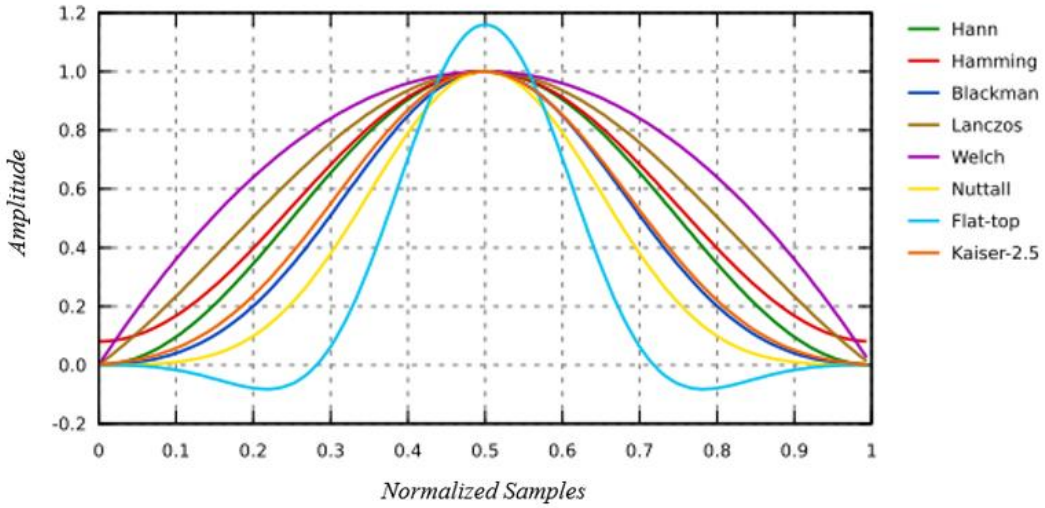

Figure 5.10 Windowing functions

Windowing functions reduce the leakage but do not eliminate the problem. Each type of window has its advantage and disadvantage, some windows are more effective to detect the exact location of the peak (frequency resolution), some others are more effective to detect the amplitude of the peak (amplitude accuracy) [69]. Hence, the error percentage of the windowing function is a result of the window function used and the application it is used with, together. Table 5.2 shows the comparison between different windowing functions [69].

Table 5.2 A comparison between the different windowing functions

Window	Frequency Resolution	Spectral Leakage	Amplitude Accuracy
Barlett	Good	Fair	Fair
Blackman	Poor	Best	Good
Flat Top	Poor	Good	Best
Hanning	Good	Good	Fair
Hamming	Good	Fair	Fair
Kaiser-Bessel	Fair	Good	Good
None (rectangular)	Best	Poor	Poor
Tukey	Good	Poor	Poor
Welch	Good	Good	Fair

As mentioned earlier the windowing functions do not eliminate the leakage problem, in reality, it changes the shape of the leakage in the spectrum. The spectrum of the response of different windowing functions can be seen in Figure 5.11, the response shows the shape of the response of the window functions as well as how the spectral leakage associated with each of the functions would look like.

The effect of the window choice on the proposed method's efficiency and accuracy is very important. In the proposed method the amplitude of the IMD3 and the fundamental signals are to be measured and the measurements have to be accurate, since the error signal control is dependent on the accuracy of the amplitude measurement of these signals. In order to have an accurate measurement, the best choice for the proposed method would be to use the Flat Top windowing function, since it has the best amplitude accuracy compared to other windowing functions [69]. The efficiency of the proposed method is dependent on how accurate the windowing function is, for instance, if the windowing function is accurately detecting the amplitude of the processed signals, then the efficiency of the control mechanism is good. Otherwise, the control mechanism would be poor since it is controlling the

system depending on inaccurate measurements, which in turn would lead to inaccurate generation of the error signal.

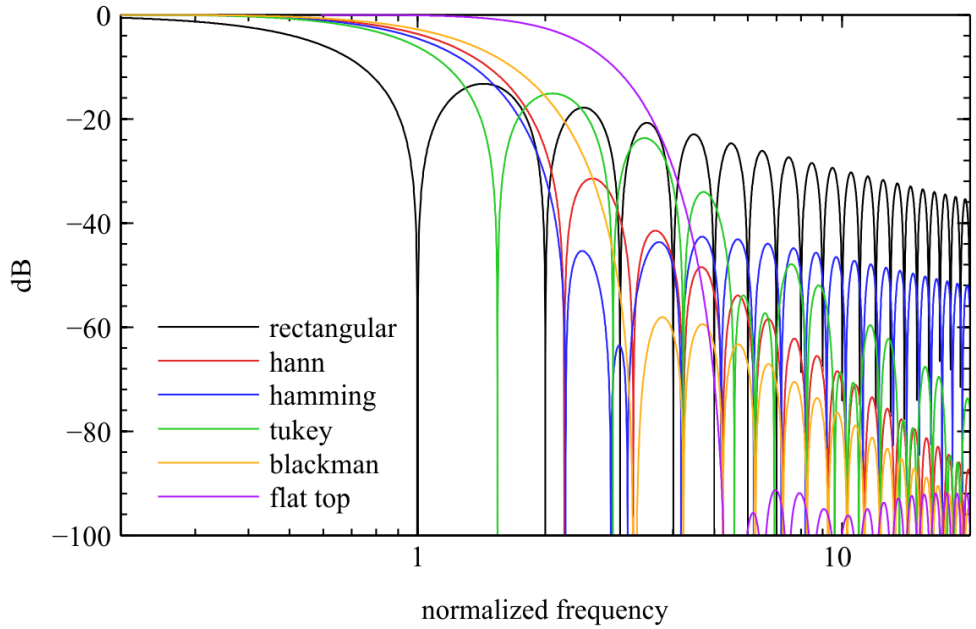

Figure 5.11 Windowing functions in the frequency domain [70]

Another disadvantage that might be faced with the FFT is the Gibbs phenomenon, which occurs due to the periodic discontinuities between the waveform and its sinusoidal representation in the time domain. There are two conventional ways to treat the Gibbs phenomenon, first, to introduce a transition between the passband and the stopband, second, is to apply a window on the waveform between the discontinuities [71]-[73].

5.5.2 Signal Cancellation

Signal cancellation is an easy-to-fathom concept. As the name implies, by using phase and amplitude adjustment on a specific signal and then adding it to another to cancel out the unwanted portions of that signal. In this work, the signal cancellation concept is used with the second reading point in 5.3, which is reading the signal's

power, to cancel out the fundamental signal by using the input signal's fundamentals and remain with the power of the IMD3.

5.5.3 The Control Mechanism

Unlike many control systems, the control mechanism in this work is purely digital, which means that the control is done via the MCU executing a program according to the measurements done. As discussed earlier in this section, there are two measurement approaches considered in this work. The control mechanism is dependent on the measurement approach. Take for example the FFT measurement approach, the result of the FFT algorithm is a spectrum of impulse functions at each frequency component of the input signal, Figure 5.12, shows an example output of an FFT algorithm with an input signal of 4 frequencies 7, 9, 11 and 13 kHz. Depending on what kind of signal this spectrum represents the control mechanism can be done using mathematical optimization (Minimization and Maximization). If the signal represents an error signal, then the optimization should achieve minimization of the fundamental signals.

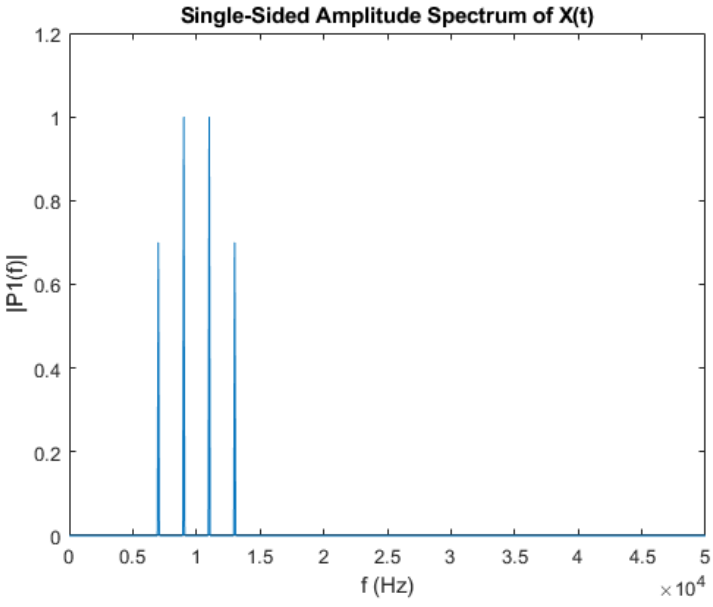

Figure 5.12 Example of FFT spectrum

Assume the fundamentals are given by

$$V(t) = k\,(\cos(\omega_1 t) + \cos\,(\omega_2 t)) \qquad \text{Eq. 5-4}$$

Hence the FT of the signal would be represented with

$$V(\omega) = k(f_1 + f_2) \qquad \text{Eq. 5-5}$$

The aim here is to minimize the fundamentals or minimize *k.* The amplitude of the fundamentals is controlled by two other variables *A*, attenuation and *P*, phase shift. Since both variables have a control voltage that is $0 \leq V_c \leq V_m$, where V_c is the control voltage and V_m is the max value of the control voltage. To achieve the minimum, another variable should be defined, *Min*, which it's usage will be explained later.

Now, the fundamentals are a function of *A* and *P* which are a function of V_c. To find the minimum value available in the spectrum of the control voltage the superposition principle is used till the function converges to a minimum. The superposition principle also known as superposition property, states that in a linear system the overall response caused by the excitation of two or more variables is the sum of the responses that would have been caused by exciting each variable individually. So that if an input *X* results in a response *Y* and an input *Z* results in a response *T* then input (*X*+Y) produces a response (*Z*+*T*) [74]. Superposition property can also be defined by two identities, Additivity Eq. 5-7, Homogeneity Eq. 5-8.

$$F(x_1 + x_2) = F(x_1) + F(x_2) \qquad \text{Eq. 5-6}$$

$$F(ax) = aF(x) \qquad \text{Eq. 5-7}$$

Where *a* is a scalar.

Now, by giving a constant control voltage value to *A*, and change control voltage of *P* from 0 to V_m and then increase the control voltage of *A* by 1 and then do the same with *P*. This process is done for the full spectrum of V_c available for *A*. In programing this can be done using nested loops which are as follows:

Set *Min* = 999999; (A very large value so that the first value measured would be considered as well)

for (Vc(A)=0, Vc(A)<Vm , Vc(A)+1)

{ do for (Vc(P)=0, Vc(P) < Vm, Vc(P)+1)

{do

Out Vc(A)

Out Vc(p)

Measure $V(\omega)$ and save it to X

If X < Min

Then Min = X

Save values of Vc(P) and Vc(A)

return

}

return

}

This use of the superposition concept allows the search for the min value to be done over the complete spectrum of both variables *A* and *P*.

Moving on to the second reading approach and the algorithm associated with it, Appendix II. The algorithm is based on the same two concepts described earlier, superposition and optimization. Since this approach depends on reading the signal's power, hence it is also dependent on canceling the wanted or the unwanted signal so that the power read by the MCU would be associated with only one of those. Signal cancellation in this work is canceling out the components of the fundamental signal in the output of the PA using the input signal.

Assume $S_{in}(t)$ is the input 2-tone signal to a PA, Eq. 5-9. Then the output of the PA would be $S_o(t)$, Eq. 5-10.

$$S_{in}(t) = A\,(\cos(\omega_1 t) + \cos(\omega_2 t)) \quad \text{Eq. 5-8}$$

$$S_o(t) = a_1 S_{in}(t) + a_2 S_{in}^2(t) + a_3 S_{in}^3(t) \quad \text{Eq. 5-9}$$

Which contains the second-order harmonics represented by $a_2 S_{in}^2(t)$, and the third-order harmonics represented by $a_3 S_{in}^3(t)$, where a_1, a_2 and a_3 are scalars for the PA's gain. By adjusting the amplitude and phase of $S_{in}(t)$ and then adding it to $S_o(t)$, the fundamentals would cancel out which leaves the power of the harmonics only, present in the signal. The algorithm is using the same program explained above, but on two levels. The first level is to achieve signal cancellation while holding the phase and attenuation of the linearity unchanged. Then after finding the point at which the best cancellation occurs, the phase and attenuation responsible for signal cancellation are on hold and the adjustment is done on the variables for linearity.

These control mechanisms can be related to the conventional control theories. The control mechanism is close to a traditional P-control mechanism (Proportional control). That is, the correction applied to the controlled variable is proportional to the difference between the desired value and the measured value. P-control systems can be represented mathematically by:

$$P_{out} = G_p e(t) + P_0 \quad \text{Eq. 5-11}$$

Where, P_{out} is the output of the controller, G_p is the gain of the controller, $e(t)$ is the instantaneous process error at time t and P_0 is the output of the controller with zero error [75]. The difference between the control mechanism of this work and the traditional P-control system is that there is no error signal or variable since the control mechanism in this work searches through the entire control spectrum of the controlled variable to find the best result possible (desired output).

5.6 Simulations

In this work, the simulations were mostly done using Advanced Design systems software (ADS). Unfortunately, ADS doesn't include any MCU units to include in the simulations since it is mainly to simulate RF circuits, which are the rest of the system's components. Hence, the simulations started with the two main components of the system, the power amplifier, and the mixer.

Starting with the power amplifier, as mentioned before a class AB PA was used for this work's simulation, Figure 5.13. As expected the PA is built using two switches and in this case, they are MOSFETs.

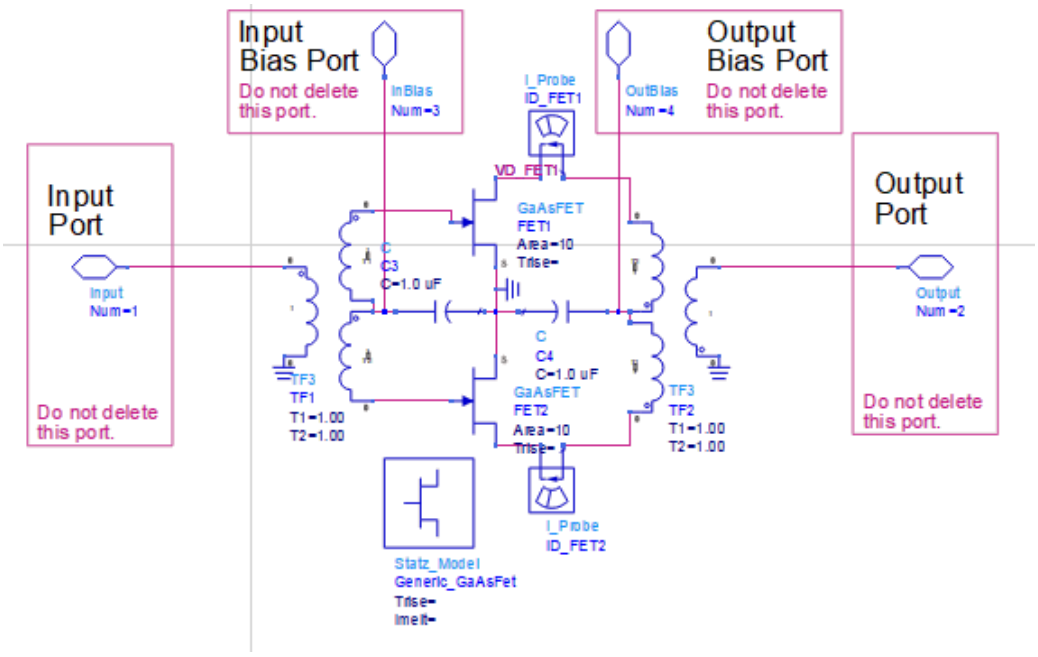

Figure 5.13 Class AB power amplifier

The PA includes 4 ports, input, and output ports, and two ports for biasing. The biasing point of the PA was decided to be enough for the signal's input and outputs swing, since depending on the biasing point or the Q-point of the PA its characteristics change. In this work the interest is to understand the PA's IMDs characteristics and how it behaves with different input powers, then the Q-point must be chosen to allow the signal variation without any clipping of the signal.

Figure 5.14 shows the PA's input vs output characteristics, the graph is obtained by sweeping the input power of the amplifier between 0-30 dBm. As it can be seen from the figure, the amplifier saturation starts at an input power of 18 dBm. Between 20-30 dBm input power the amplifier is operating in the nonlinear region or saturation region.

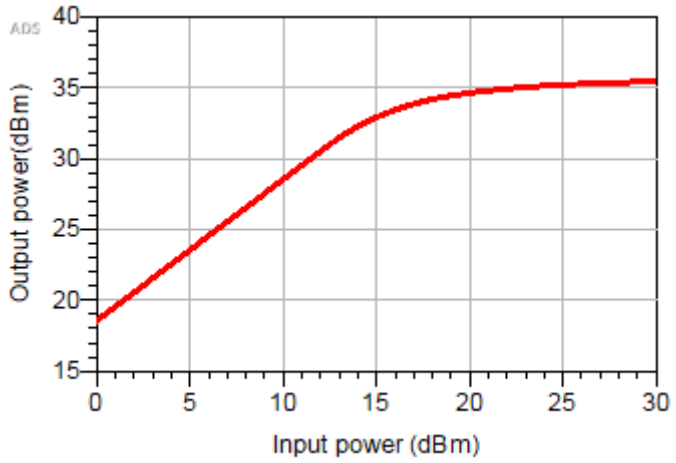

Figure 5.14 Class AB PA input vs output characteristics

The input power vs IMD3 level characteristics can be seen in Figure 5.15. These characteristics were obtained by following the same procedure followed in obtaining Figure 5.14. The input power swept between 0-30 dBm to observe the IMD3 behavior of the PA. The behavior shows that between 0-13 dBm input power the IMD3 level is increasing linearly, at 19 dBm input power the IMD3 level has a dip in its level. With increasing the input power after 19 dBm the IMD3 level increases again till it reaches its maximum value at 30 dBm.

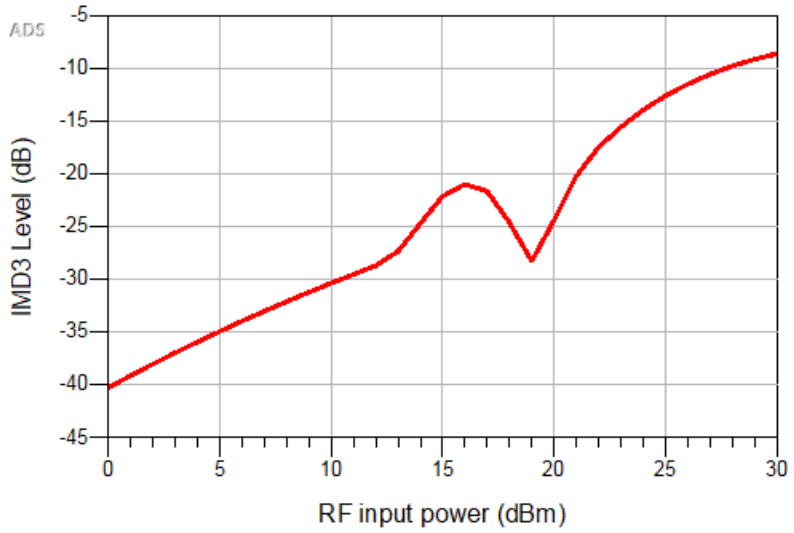

Figure 5.15 PA's input power vs IMD3 characteristics

Figure 5.16 shows the fundamental level to the IMD3 level behavior of the PA, it illustrates the output signal which is composed of a 2-tones ratio to IMD3.

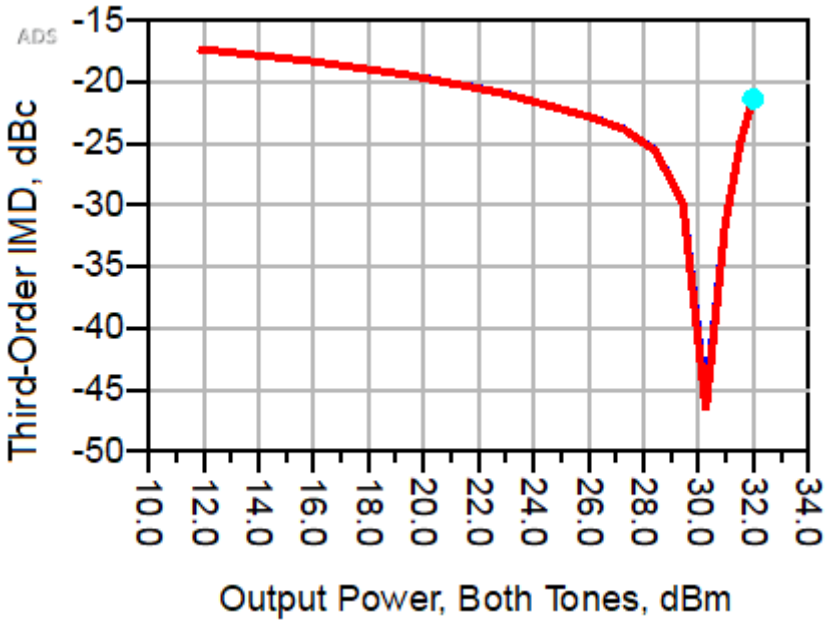

Figure 5.16 PA’s IMD3 to the fundamental ratio

The IMD3 level compared to output signals power level is decreasing with the increase in the output signals power. The importance of this graph representation is that it gives the information needed to know or to expect the IMD3 level by knowing the input signal's level and the gain of the PA. For instance, the graph shows the output power for both tones' input signal on the x-axis, and on the y-axis, it shows the power level of the IMD3 relative to the output 2-tone signal's power. Take for example an output power of 21 dBm which corresponds to -20 dBc of IMD3.

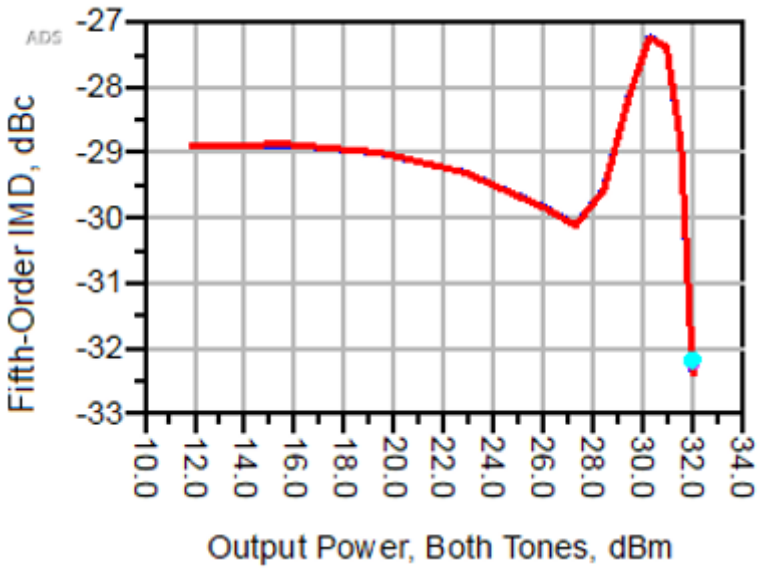

Figure 5.17 PA's IMD5 characteristics

Figure 5.17 shows the PA's IMD5 characteristics, for this work the IMD5 is not the focus but having such simulation would help to understand some of the resultant signals. Also, as the maximum level of the IMD5 is around -27 dBc it does not have as great of an effect on the PA's linearity as does the IMD3.

Moving on to the second main component of the system, which is the mixer. Mixers are essential in this work since they are the error signal generators. Figure 5.18 represents the circuitry that was used for carrying out the mixer's simulation. The simulation was done using a Harmonic Balance (HB) control unit that is to be able to simulate and see the intermodulation distortions in the signal. Two tones were

inputs to the mixer, one as the fundamental signal and the second one as the LO frequency, and the output of the mixer was terminated with a matched load and at that port, the output results were measured. Also, a variable unit (VAR) was used to account for the RF frequency LO frequency and both of their powers.

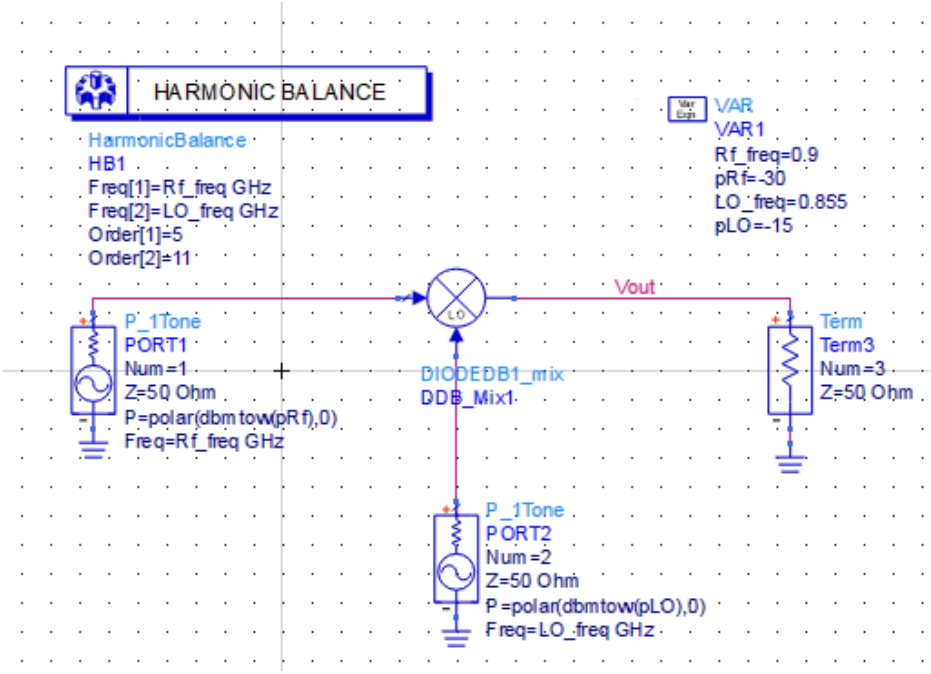

Figure 5.18 Double balanced harmonic mixer simulation circuitry

The first simulation was done by sweeping the input power between 0-30 dBm while keeping the LO's frequency and power constant. Figure 5.19 shows the input vs output characteristics of the DBHM used in the simulations. The output power has a linear increase till 10 dBm input and fluctuates between 10-30 dBm input power.

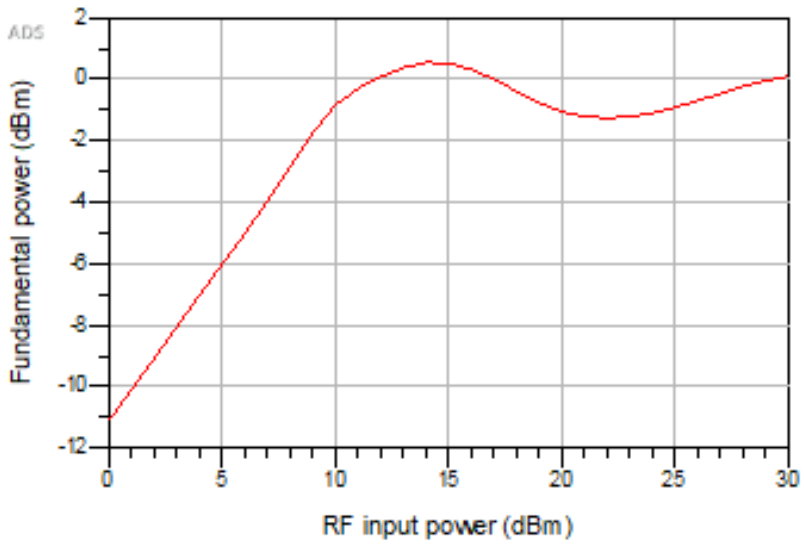

Figure 5.19 DBHM input vs output characteristics

Secondly, the effect of the input power on the DBHM's IMD3 generation. Figure 5.20 illustrates the input power sweep vs the IMD3 level. The figure shows that the input power has an insignificant effect on the DBHM since the highest level of IMD3 is between 0-9 dBm input power, which has a value of -49 dBm.

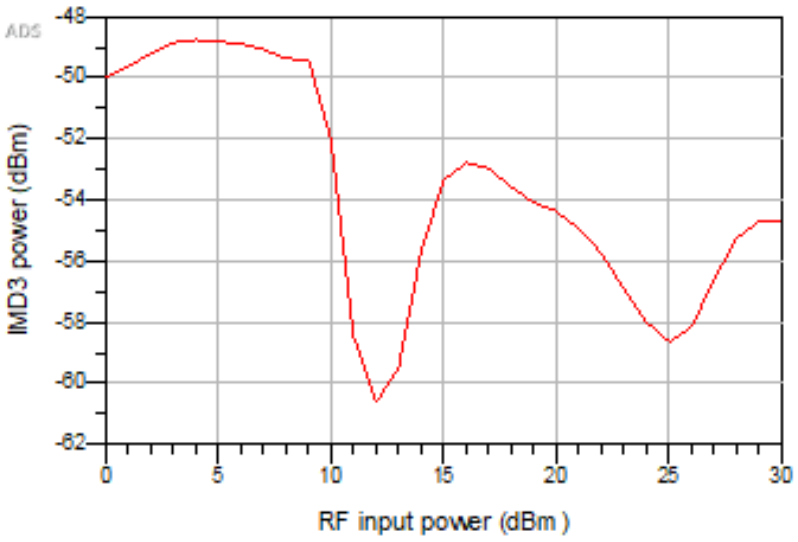

Figure 5.20 Input power vs IMD3 level

Then the simulations continued with sweeping the LO frequency to see the effect on the output signals fundamentals and how much of IMD3 the mixer is going to add to the signal. Figure 5.21 represents the effect of LO frequency over the fundamental signals. Starting from 1 GHz the power of the fundamental signal is dropping with the increase of the LO frequency but notice that after 4 GHz the change in LO frequency does not affect the fundamental signals at all which means it converges.

Choosing the frequency for the mixer's operation point is mainly dependent on the amount of IMD3 required for the system, mainly to choose an optimum point where the frequency is not going to affect the fundamental signal's power level, or at least it would have a minimal effect, and to have a proper level of IMD3 to carry on with the error signal production.

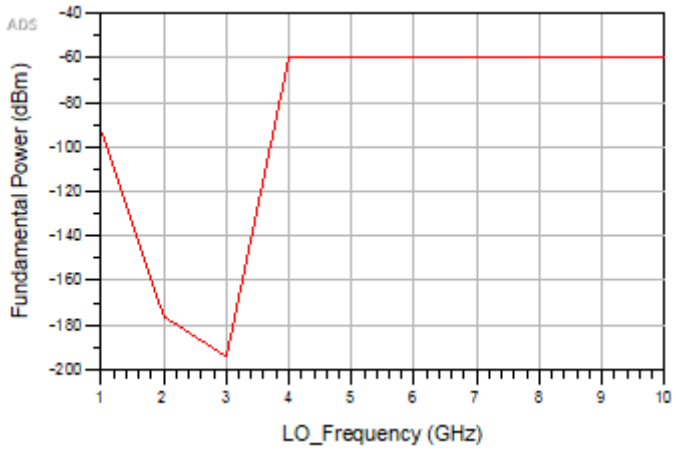

Figure 5.21 Mixer's LO frequency sweep vs fundamental signal's level

Figure 5.22 represents the LO frequency sweep over the production of IMD3. The graph shows that the double-balanced harmonic mixers or DBHM produce the maximum amount of IMD3 at around 2 GHz, at 1 GHz, and from 3 GHz and above the IMD3 power level is very low that it is almost negligible. After 6 GHz the change in the LO frequency doesn't affect the IMD3 level as in the fundamentals case it converges after 6 GHz.

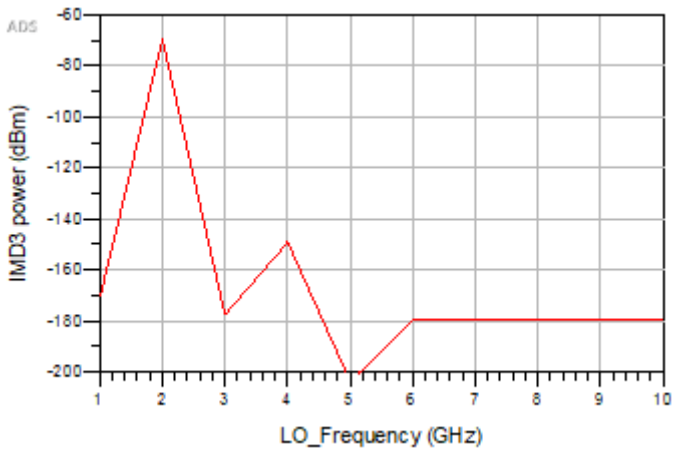

Figure 5.22 Mixer's LO frequency sweep vs IMD3 levels

The second part of simulating the mixer's characteristics was to sweep the power of the LO frequency and notice its effect on the fundamental signals as well as the IMD3 generation.

Figure 5.23 shows the power sweep characteristics of the DBHM. The power swept between -20 to 10 dBm. The effect of the LO power on the IMD3 can be seen on the left-hand side graph, which shows an almost linear increase in the IMD3 production between -20 and 5 dBm, between 5 and 10 dBm the power of the IMD3 increases sharply then decreases again. However, this linear increase in IMD3 is very minimal since it is between -160 and -100 dBm which means zero power.

Which gives the general idea of the behavior of the mixer's characteristic that the IMD3 production is increasing with the increasing LO power.

On the right-hand side graph, the effect of the LO power on the fundamental signals can be seen. Again, it is noticeable that the fundamental signal's power is increasing with the increasing LO power almost linearly between -20 and 5 dBm, unlike the IMD3 production, the increment between 5 and 10 dBm is quite significant which goes from -70 to -40 dBm. The increment between -20 and 5 dBm as in the IMD3 production is negligible. At this point, the simulations required before simulating the

actual system are done. Then the full system was built on ADS and the next phase of simulations started. Figure 5.24 shows the full system implemented on ADS.

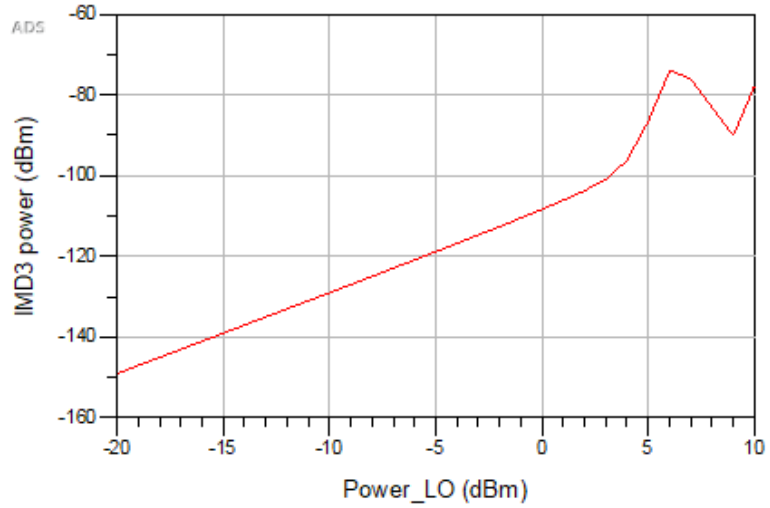

(a)

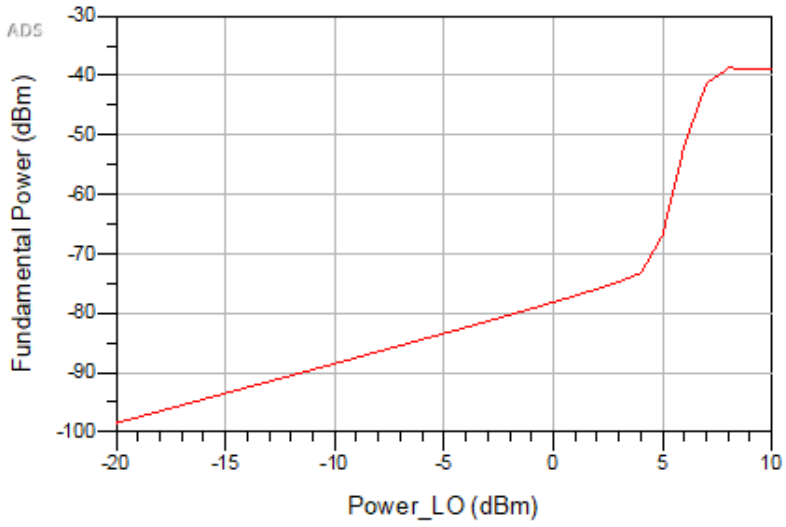

(b)

Figure 5.23 Mixer's LO power sweep characteristics (a) LO power sweep vs IMD3 (b) LO power sweep vs fundamentals

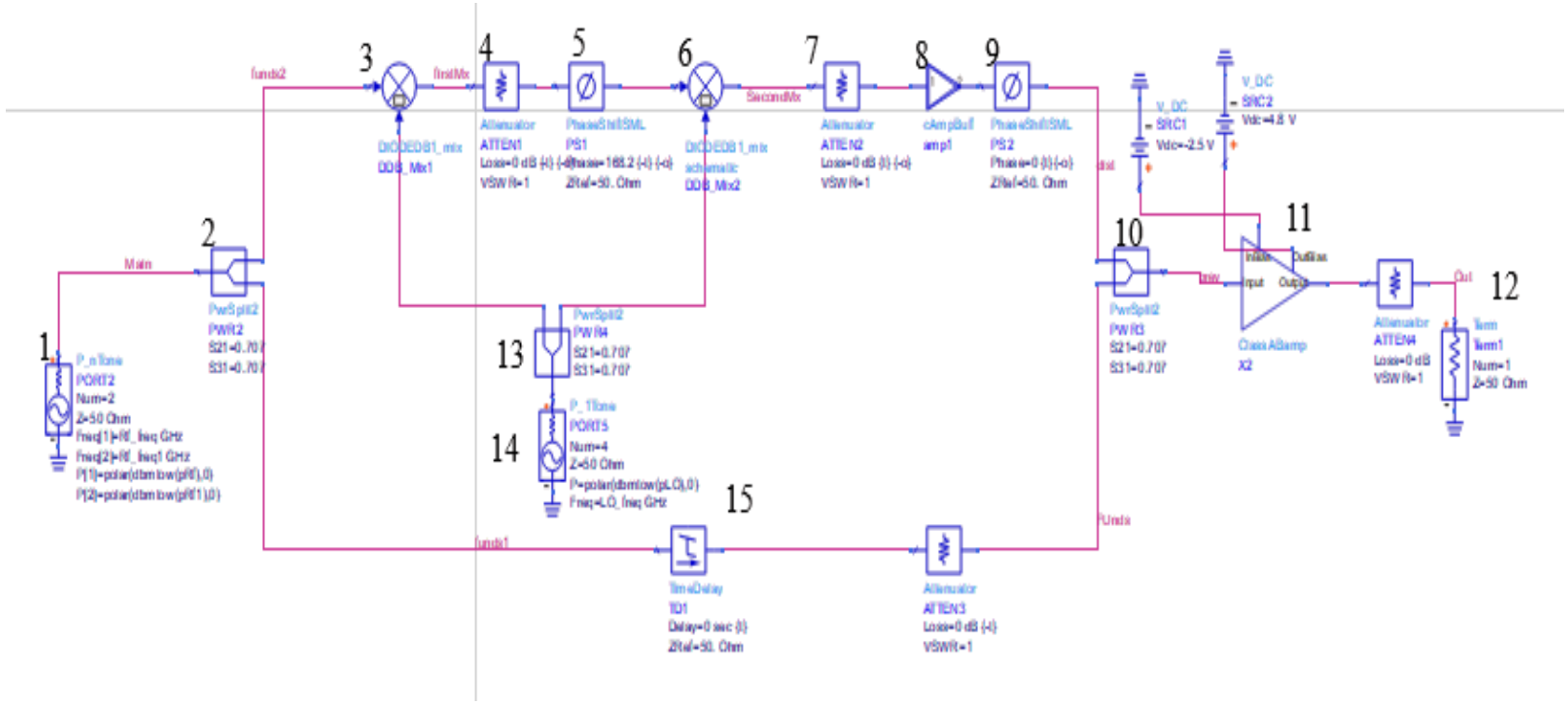

Figure 5.24 Full system Implementation

1- 2-Tone input signal

2,10,13- Power splitters/combiners

3,6- DBHM

4,7- Variable attenuators

5,9- Variable phase shifters

8- Buffer amplifier

11- Main PA

12- Matched load

14- LO frequency

15- Time Delay

Since ADS does not support MCUs, and to simulate the role of the MCU, the optimization function of ADS was used. The optimization allows a goal to be set and accordingly the optimization is being carried out. Unlike the MCU, optimization goals cannot be set to find the best fundamental suppression when simulating the error signal generation, for example, hence, an upper limit is set for the fundamentals. Which means that the fundamentals must be below that limit.

The system was simulated with a 2-tone RF signal at 2.35 and 2.45 GHz with a 25 dBm power for both tones. The LO frequency was set to be 1.2 GHz with a 10 dBm power. As for the previous simulations, Harmonic Balance (HB) function was used and was configured to consider up to the 5th order harmonics of the fundamentals and assuming no harmonics for the LO signal.

So firstly, the error signal generation was simulated. Figure 5.25 shows the part of circuitry used for error signal generation and also the error signal before any optimization.

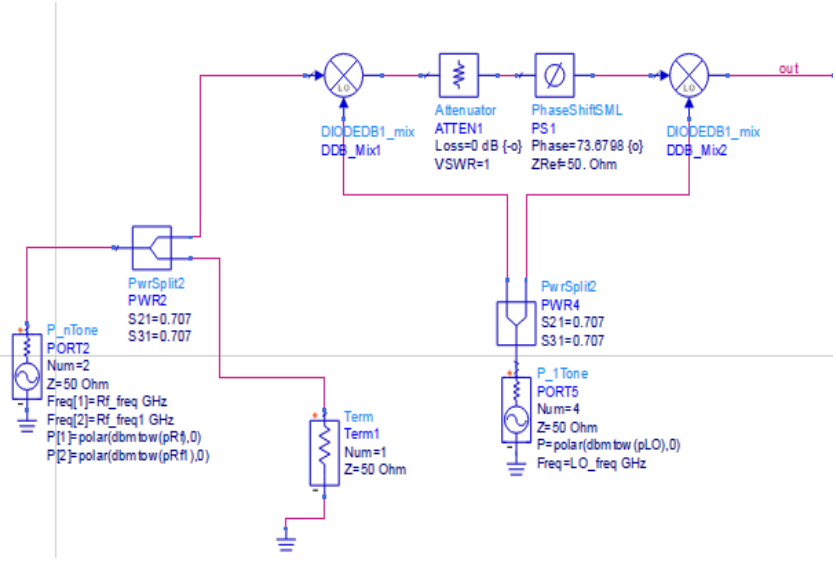

(a)

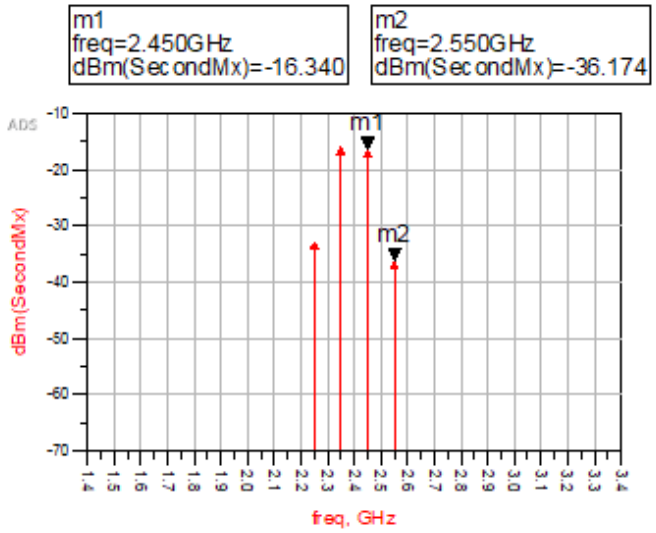

(b)

Figure 5.25 (a)Error signal circuitry (b) The signal before optimization

As it can be seen from the figure, the fundamental signals are at -16 dBm power level and the IMD3 at -36 dBm. The decrease in fundamental signal power is, firstly, because of the power splitter then the insertion loss of each of the components the signal passes through. Now adding the optimization goal and start the optimization process, Figure 5.26 shows the optimization goal and the resultant signal after the optimization is over.

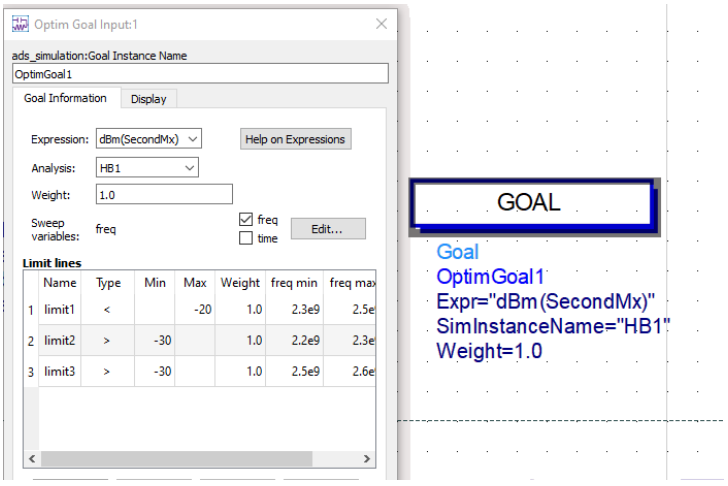

(a)

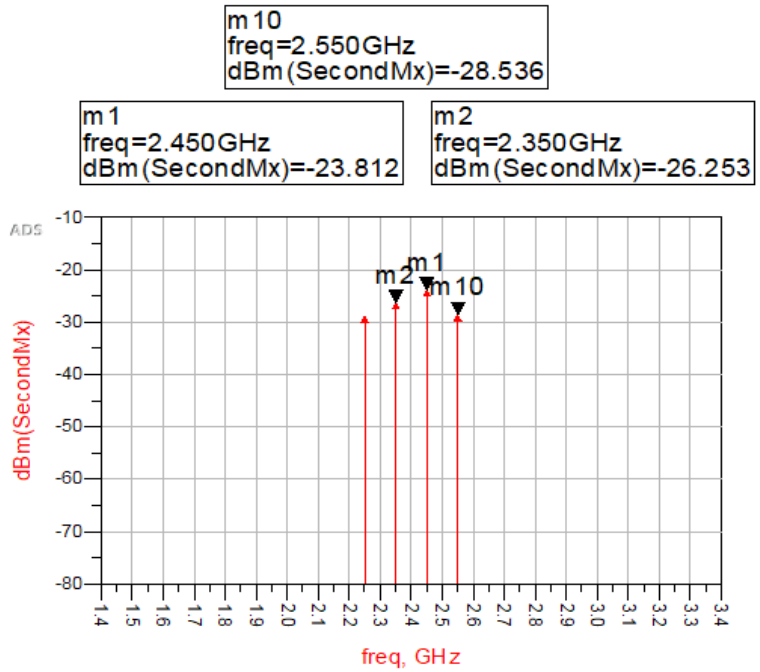

(b)

Figure 5.26 (a) Optimization goal (b) Error signal after optimization

The goal here was targeting the signal's power level, the first limit was set for the fundamentals to have a power level that is less than -20 dBm. The second and third limits were set to ensure that the IMD3 levels remain high or increase as much as possible. An 8-10 dBm suppression in the fundamentals level can be seen and an 8 dB increase in the IMD3 was achieved. The next step was to simulate the change in the output of the PA with the change of the second attenuator and phase shifter. Figure 5.27 shows the output of the PA before and after optimization.

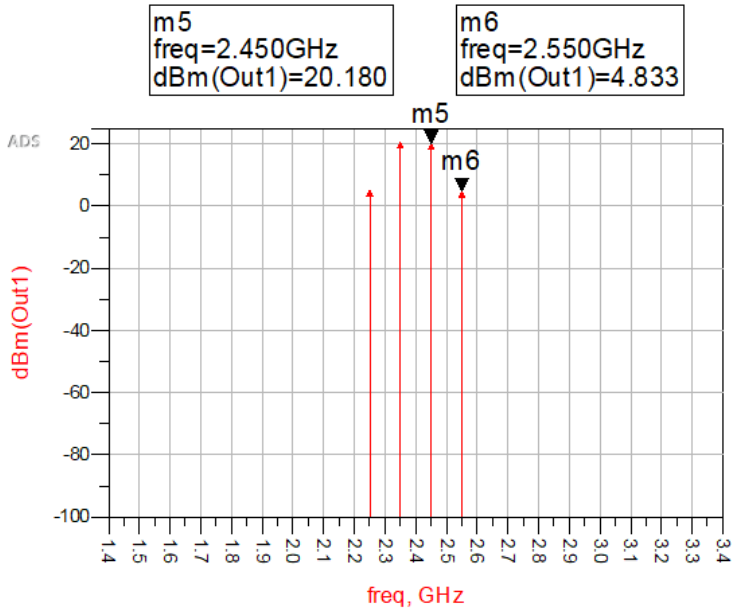

(a)

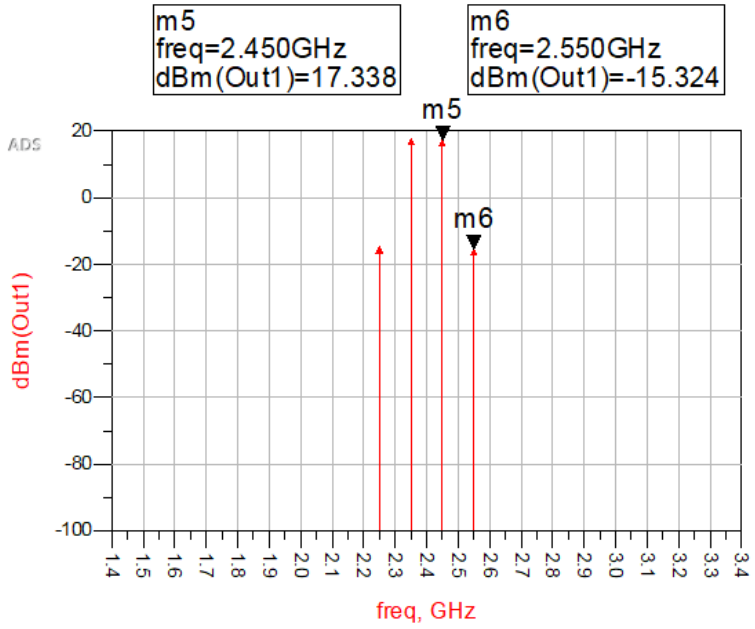

(b)

Figure 5.27 The output signal of the PA (a) before linearization and (b)after

Degradation of 3 dB in the fundamental signals can be seen, which means that the linearization process has affected the PA to back-off the fundamentals by 3 dB. A 3 dB suppression in the fundamentals corresponds to a 9 dB suppression in the IMD3 level. a suppression of nearly 20 dB in the IMD3 is achieved. In which, 9 dB are suppressed because of the suppression of the fundamental, hence, a total of 11 dB suppression in the IMD3 is achieved by the linearization. After simulating the second set of variables (A2 and P2) and their effect on the PA output, the last set of variables (A3 and P3 and coupler C2) were added to the system Figure 5.28, to simulate and validate the second approach to take the reading to the MCU using a crystal diode detector which was explained in 5.3.1.

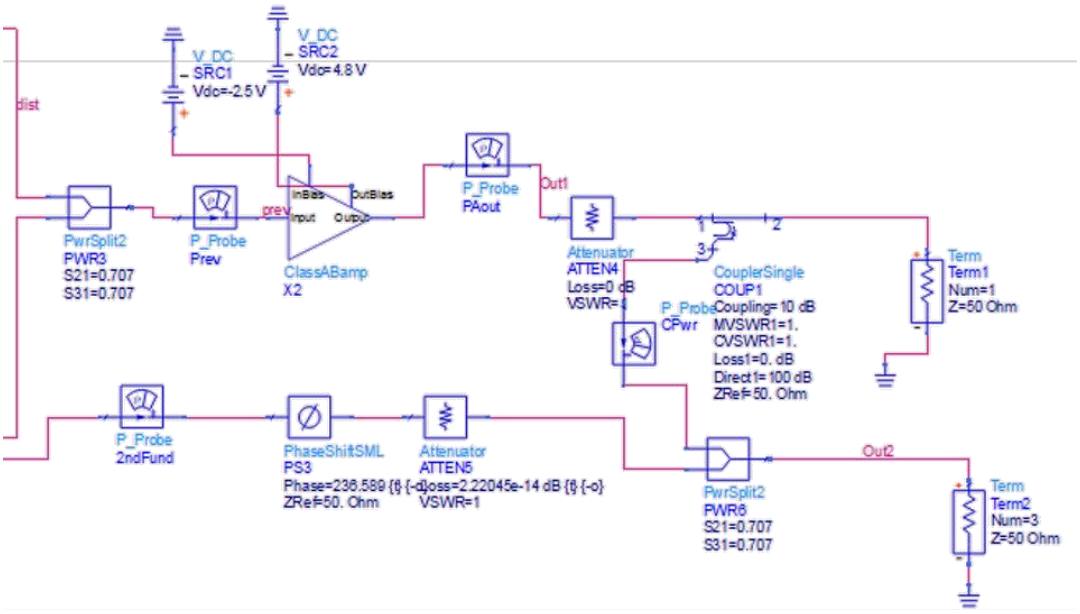

Figure 5.28 Circuitry for simulating the second reading approach

The optimization was achieved by setting a goal for the fundamentals level and simulate the results after changing the variables A3 and P3. Figure 5.29 shows the coupled signal which is then combined with the modified fundamentals resulting in the signal going to the MCU with suppressed fundamentals.

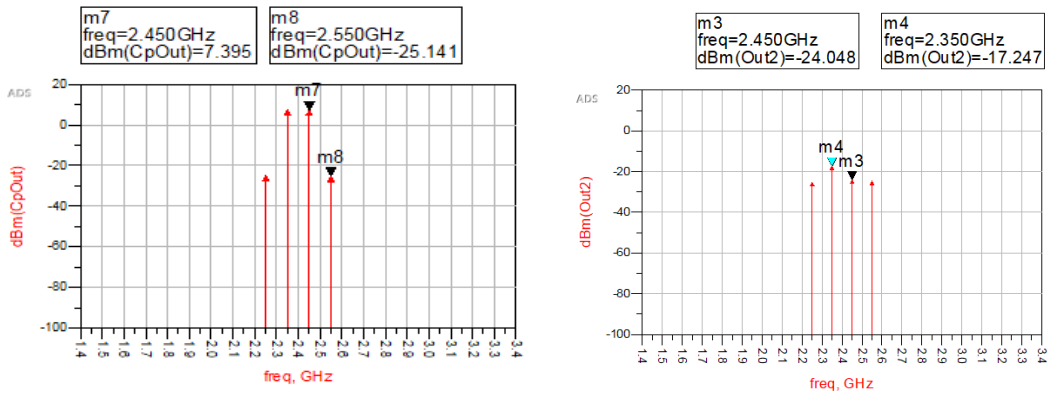

Figure 5.29 Output of the second approach before and after optimization

As it can be seen the fundamental signals were suppressed by 24-30 dB while the IMD3 levels remain unchanged at around 25 dBm. This proves and validates the second approach of reading and analyzing, that the signal's power read by the MCU will be dominantly the IMD3 power. Finally, the simulation for the first approach is down-converting the error signal to a level that can be read by the MCU. The third mixer was added with the same center frequency as the fundamentals, 2.4 GHz, as well as a coupler, Figure 5.30.

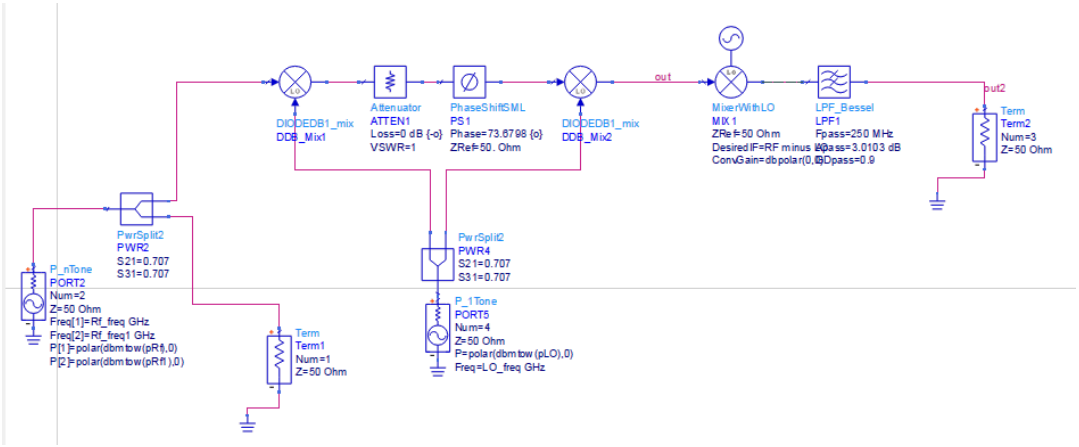

Figure 5.30 Down-conversion circuit

Figure 5.31 shows the spectrum of the down-converted signal which is the upper fundamental signal and the upper IMD3 product. The down-converted signals are to be at 1 and 2 MHz for the fundamental and the IMD3, respectively. The down-

conversion can be with lower frequencies depending on the third mixer's LO frequency and depending on the MCU's capabilities, in this case, the center frequency was chosen to be the same as the input signal just for simulation.

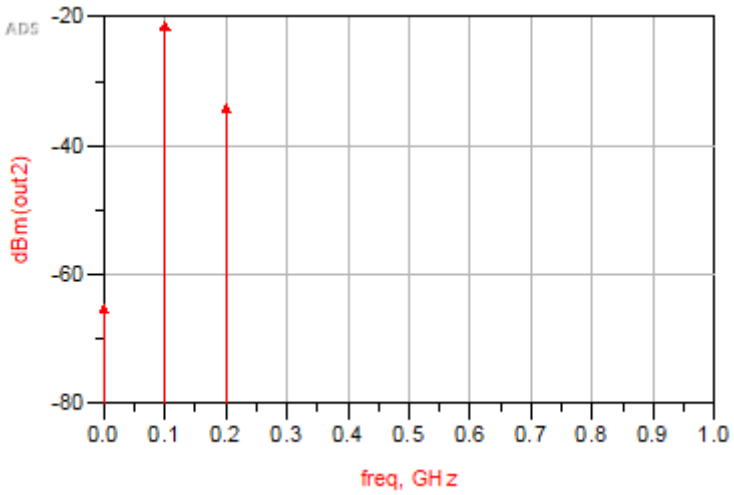

Figure 5.31 Down-converted distortion signal

5.7 Summary

This chapter summarizes the theory behind this work. Starting from the linearization technique that was used to implement the adaptive system, the methodology that was followed in this work, and finally, the simulations are done.

The simulations are carried out by using ADS software which allows the simulation of all RF circuit components but unfortunately does not support MCU. Which lead to the use of the optimization option available in ADS that is to simulate the behavior of the MCU. The simulations achieved the expected results to validate the theory behind it.

CHAPTER 6

EXPERIMENTAL RESULTS AND DISCUSSION

6.1 Introduction

In this study achieving the simultaneous adaptive control of a linearization technique is the main aim. Designing the adaptive system then simulating it to prove its validity is an essential part of any scientific work. However, more important is to validate the simulations by building a prototype that can function as suggested in the study or as it is expected to function. Which is a proof of concept.

The experiments carried out were first designed according to the simulation results, the design of the experiment includes the choice of the components and measuring devices to quantify the results. After the design step, the building of the experiment circuitry was done accordingly, and finally, the measurements were taken from the measurement devices.

In this chapter, the design and building and results of the experiments will be discussed. Two main experiments were carried out to prove the proposed system. Firstly, the error signal generation control and reliability of the Fast Fourier Transform (FFT) algorithm and its accuracy compared to the actual results, and then the control depending on FFT results. Secondly, the MCU's control of the linearity of the PA depending on the output of the PA which is the measured power from the diode detector.

6.2 The Error Signal Generation

As explained earlier in section 5.3.1, the MCU is taking measurements from the system at two points. The first point is as can be seen in Figure 5.4, and it is depending on that measurement that the MCU controls the attenuator A1 and phase shifter P1 to obtain the desired error signal. That desired error signal should have high levels of IMDs and low levels of fundamental signals, to achieve this aim, the differentiation between both signals, IMDs, and fundamentals, is very critical hence the solution of using FFT

to be able to see clearly what frequencies are present in the signal.

The experiment carried out to prove this concept was done using an Arduino Mega2560 chip which has an Atmega2560 MCU on it. Unfortunately, the ADC on the chip has a big time delay per conversion and a very low sampling frequency which are not compatible with the RF frequencies used in the linearization technique. Therefore, to prove the concept the experiment was done on a much lower frequency.

The experiment was done on three different input samples, a 1 kHz signal, a 1.2 kHz signal, and the sum of 600 Hz and 1.2 kHz signal. For all of those signals, a 20 MHz Function Waveform Generator (Agilent 33220A) was used, Figure 6.1 Signal generator at 1 kHz. Firstly, with the 1 kHz, a magnitude of 200 mV peak-to-peak signal was directly input to the MCU's port. The values read were sampled into 256 samples that are saved in an array that is used to perform the FFT on. It is important to note that these values were chosen according to Nyquist criteria, since the Arduino has a sampling frequency of ~8 kHz, and this frequency must be at least two times bigger than the sampled frequency.

Figure 6.1 Signal generator at 1 kHz

The FFT algorithm outputs the spectrum of the signal as well as the top frequency in that signal,

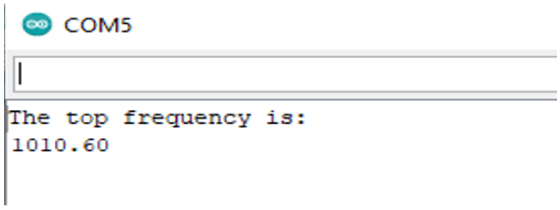

Figure 6.2 shows the top frequency output of the FFT algorithm which is very close almost the same as the 1 kHz input.

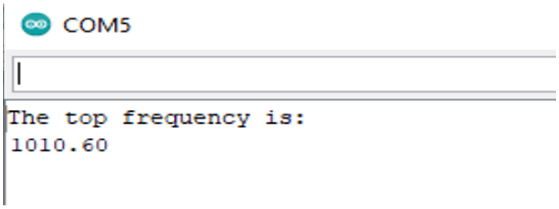

Figure 6.2 FFT output result

For the FFT algorithm experiments, the results were taken from three different readings and three different samples array to be able to ensure the consistency of the algorithm. Figure 6.3 shows the resultant spectrum of the signal from the FFT algorithm for three different measurements, the different measurements were taken for the express purpose of the consistency and reliability of the code. As it is shown, the peak is at 1 kHz as expected and it is very consistent at the three different

readings. It can be directly noticed that two comparably small peaks are not supposed to be there, the reasoning to be is that the circuit picked up another signal that intervened with the 1 kHz input signal. It is also a good measure of how accurate and consistent the algorithm is, that even such small peaks were picked and showed in the result.

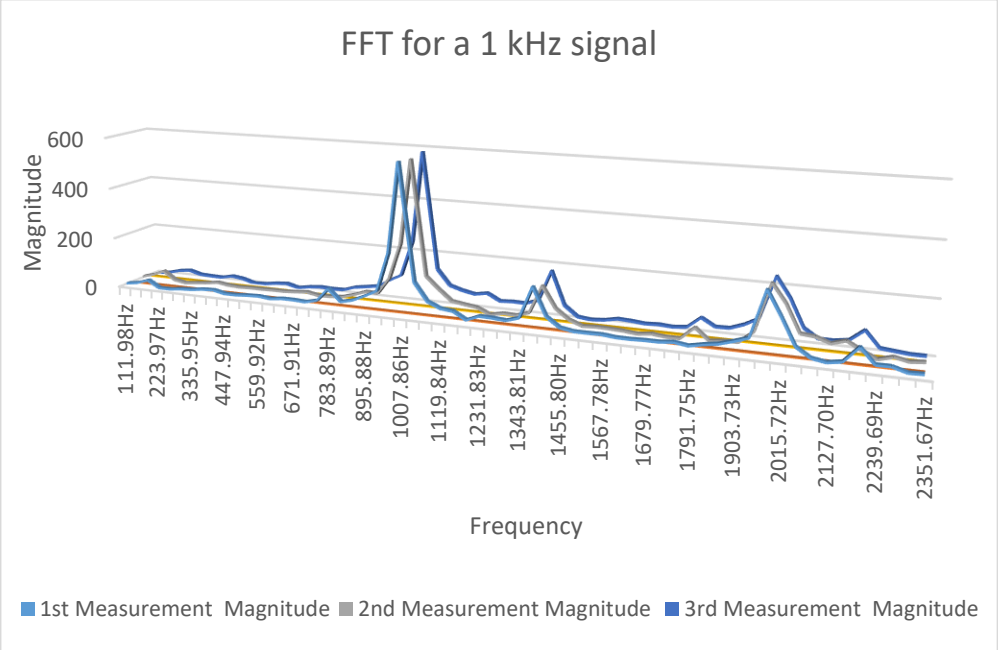

(a)

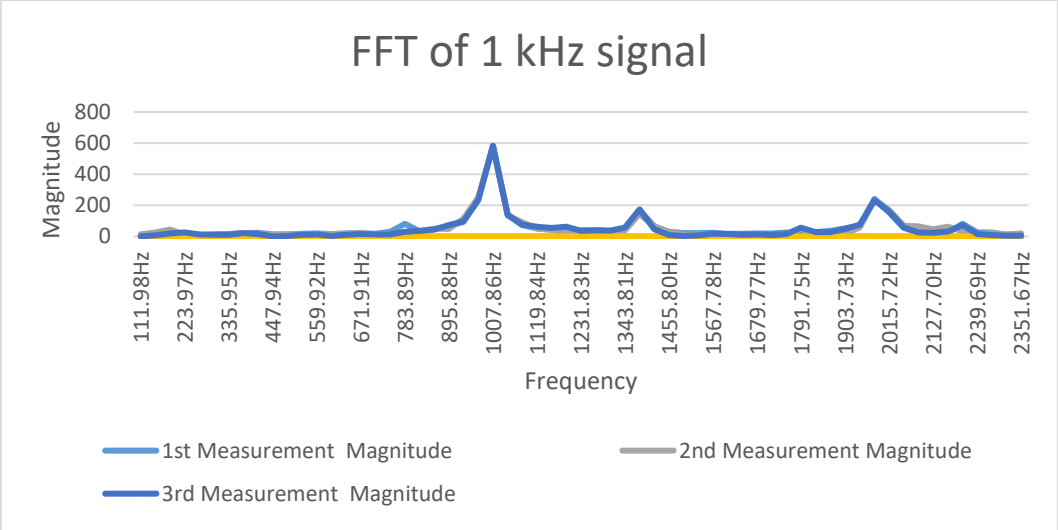

(b)

Figure 6.3 FFT results for the spectrum of the signal (a) side view (b) front view

The second experiment that was done with a 1.2 kHz signal was done in the same manner and the results were not different. The results were very accurate and consistent.

```
The top frequency is:
1198.50
```

(a)

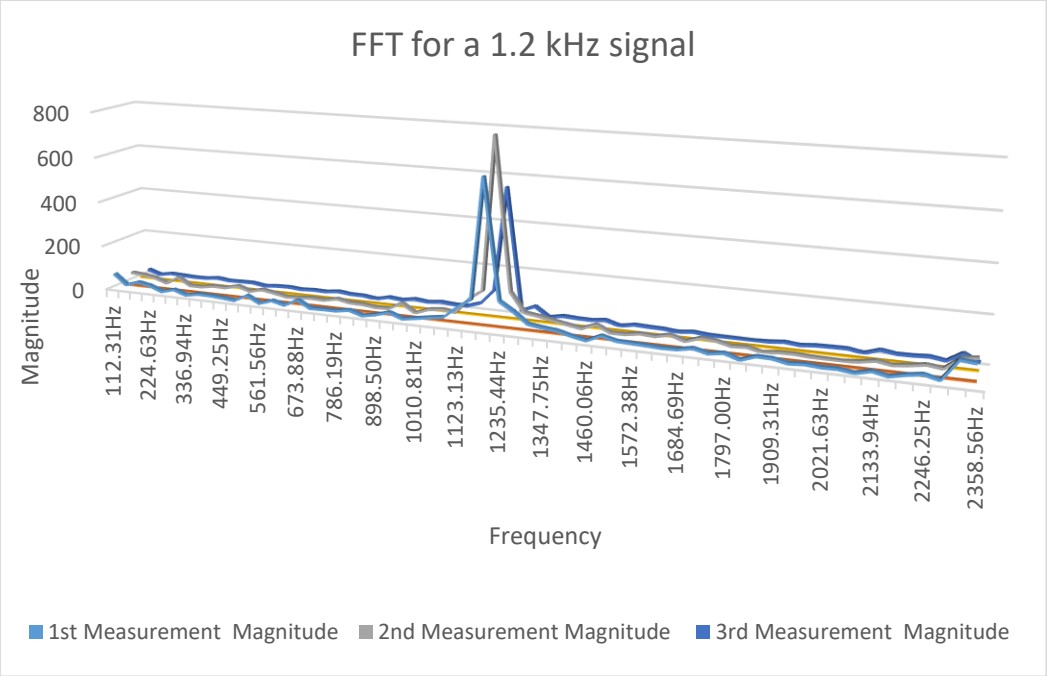

(b)

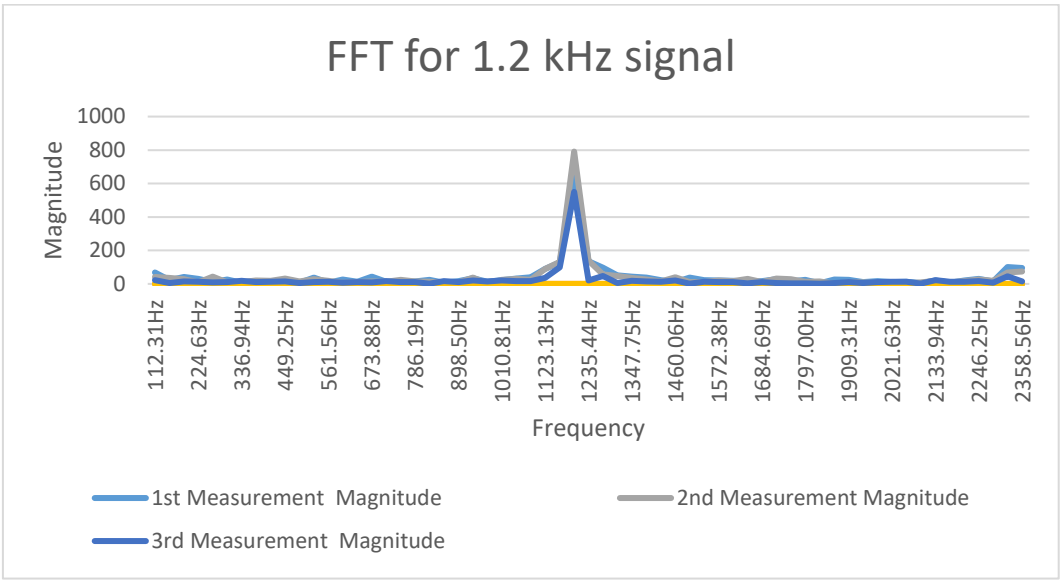

(c)

Figure 6.4 FFT results for a 1.2 kHz signal (a) top frequency (b) spectrum of the signal side view (c)front view

Figure 6.4 shows (a) the top frequency resulted from the FFT and (b) the full spectrum of the signal. It can be seen that the peaks of the spectrum are at 1.2 kHz and there are no other peaks which means there are no errors in the FFT results. It can be noticed that the amplitude of the peaks is not at the same level, and that is since all three measurements were done with three different sample arrays that were measured separately.

Lastly, the experiment was done with a signal that simulates the 2-tone signal in the RF range. This signal contains two main frequencies 600 Hz and 1.2 kHz, a simple OpAmp circuitry, Figure 6.5, was used to add both signals.

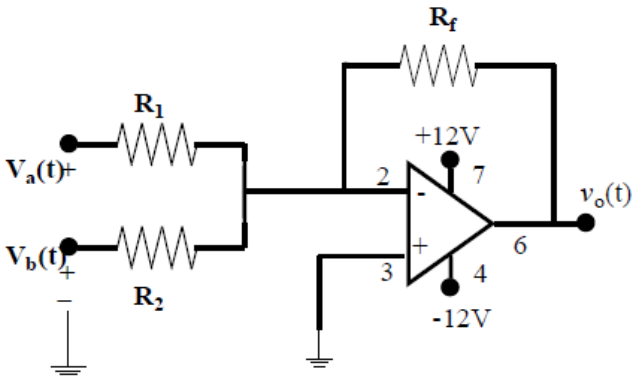

Figure 6.5 A summer OpAmp circuit

As before the output was connected directly to the ADC port of the Arduino, Figure 6.6 shows the setup that was used to perform this experiment.

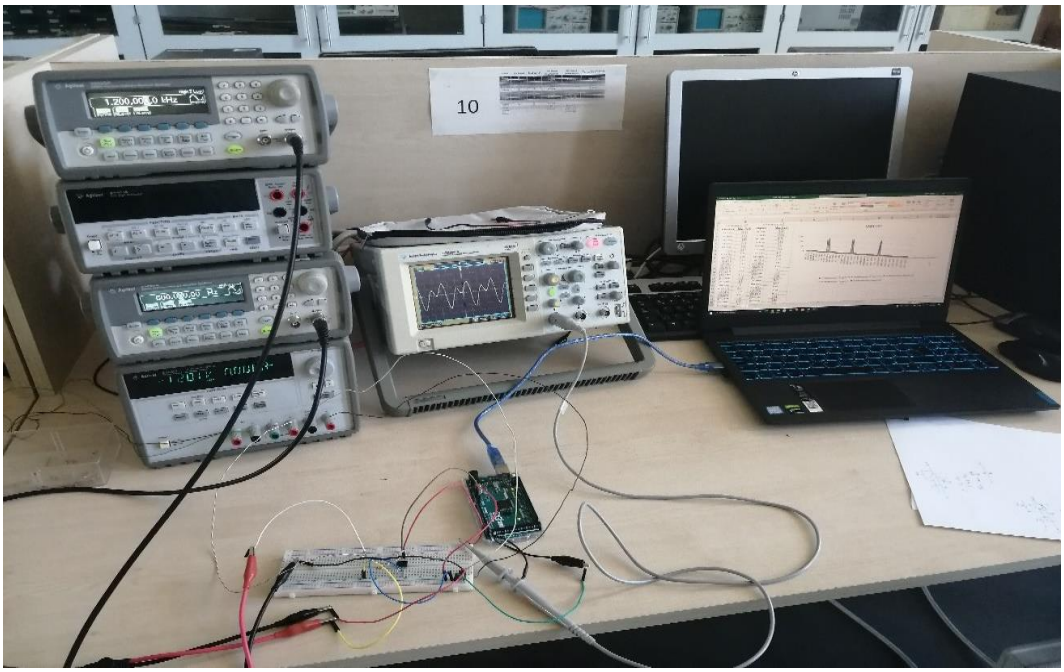

Figure 6.6 The 2-tone signal experiment setup

The results were as expected, where the top frequency obtained by the FFT algorithm was almost perfectly accurate. Figure 6.7 shows the top two frequencies resulted from the FFT and the spectrum of the signal.

The spectrum shows the two signals peaks that are expected which are at 600 Hz and 1.2 kHz, but it also shows a third peak which is almost as high as the main two frequencies, this frequency as it can be seen from the graph is at 1.8 kHz which is also expected since the signals were added together using an OpAmp. It is worth noting that (b) shows the side view of the spectrum to be able to see the three different measurements taken, as (c) shows only the front view where the three measurements are stacked behind each other's, hence only the first measurement can be clearly seen.

```
The top frequencies are:
599.25
1198.50
```

(a)

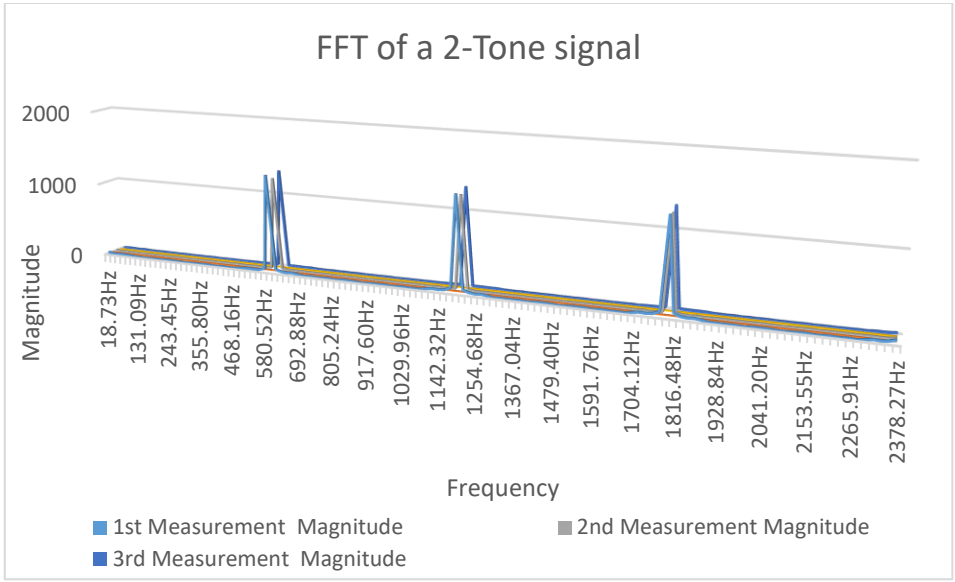

(b)

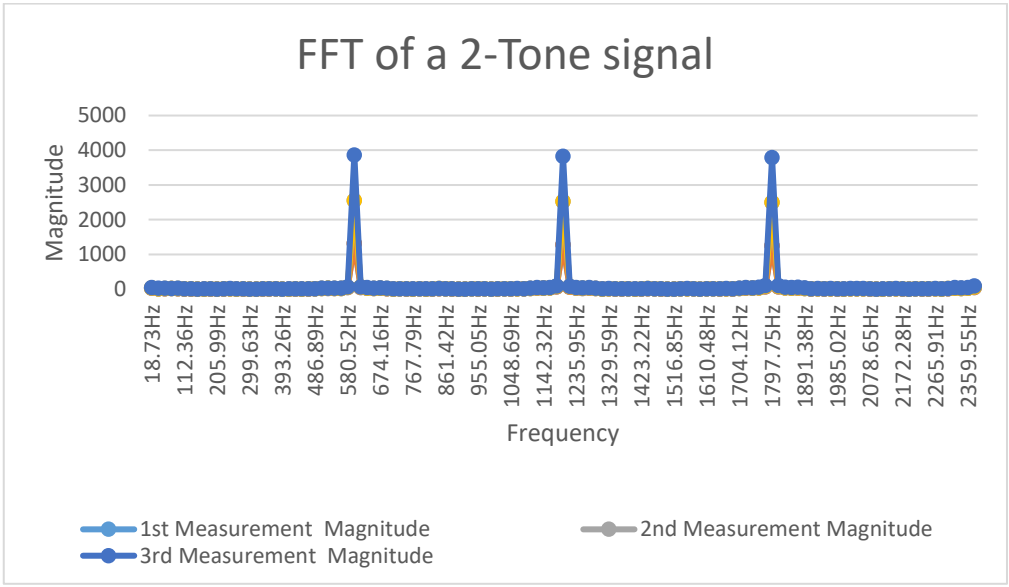

(c)

Figure 6.7 FFT Results of a 2-tone signal (a) top frequencies (b) signal's spectrum side view (c) signal's spectrum front view

6.3 PA's Linearity Adaptive Control

As mentioned before, the MCU is connected to the linearization system at two points, the first point is to control the error signal and the second point is to control the linearity of the amplifier. In this section, the second connection point experiment and results will be discussed.

To conduct this experiment the linearization technique that was chosen before, which was done in [32], had been built and the components required for the adaptive control had been added. Figure 6.8 shows the system.

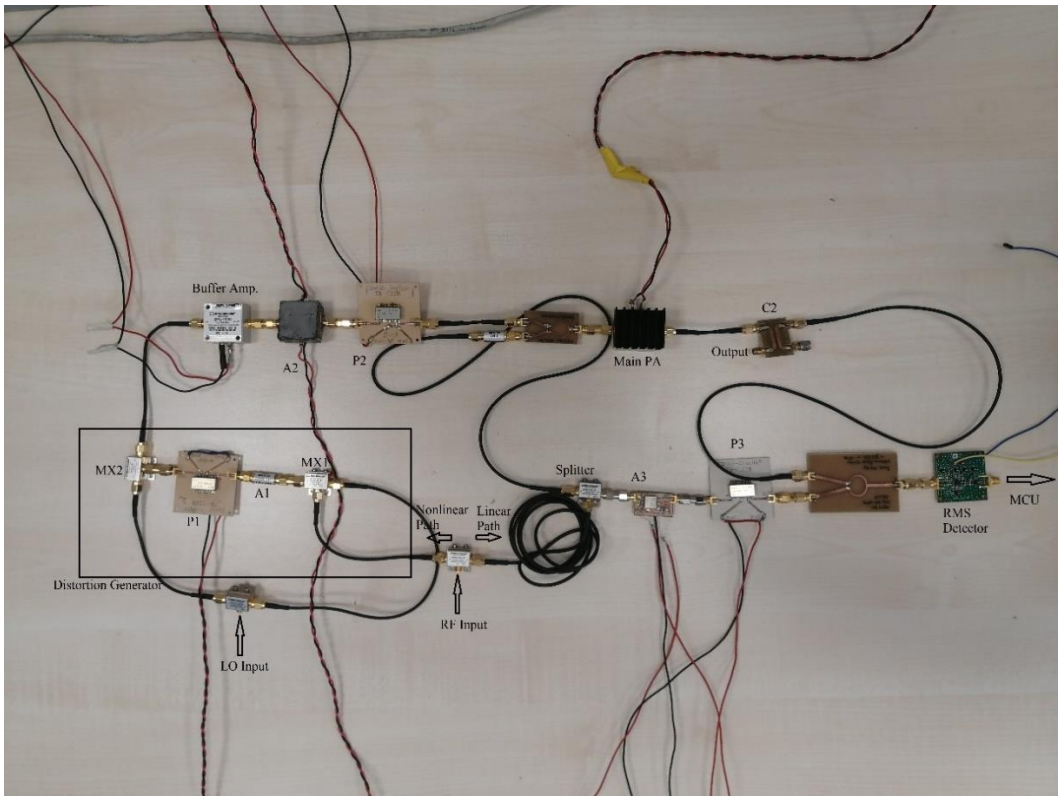

Figure 6.8 The linearization technique with the adaptive control components

Due to the lack of components, and since in this part the focus was on achieving adaptive linearity experimentally. The attenuator A1 was replaced with a fixed attenuator. The value of that attenuator was measured to be 3 dB which was one of the few values available, and after performing some measurements it was found to

be the attenuation value that produces a better error signal. The control voltage value of the phase shifter P1 was also set to be 5 V to achieve that error signal.

After building the linearization technique circuitry, the MCU was connected to the output of the RMS detector and the control voltages of A2, P2, A3, and P3 were connected to the corresponding ports of the MCU. Since the MCU's maximum voltage output is 5 V and the control voltages of the components are 8 V for the attenuators and 15 V for the phase shifters. a simple OpAmp circuitries with a gain of 1.6 and 3 were added to the control ports of the MCU. Figure 6.9 shows the MCU with the OpAmp circuitries added to it.

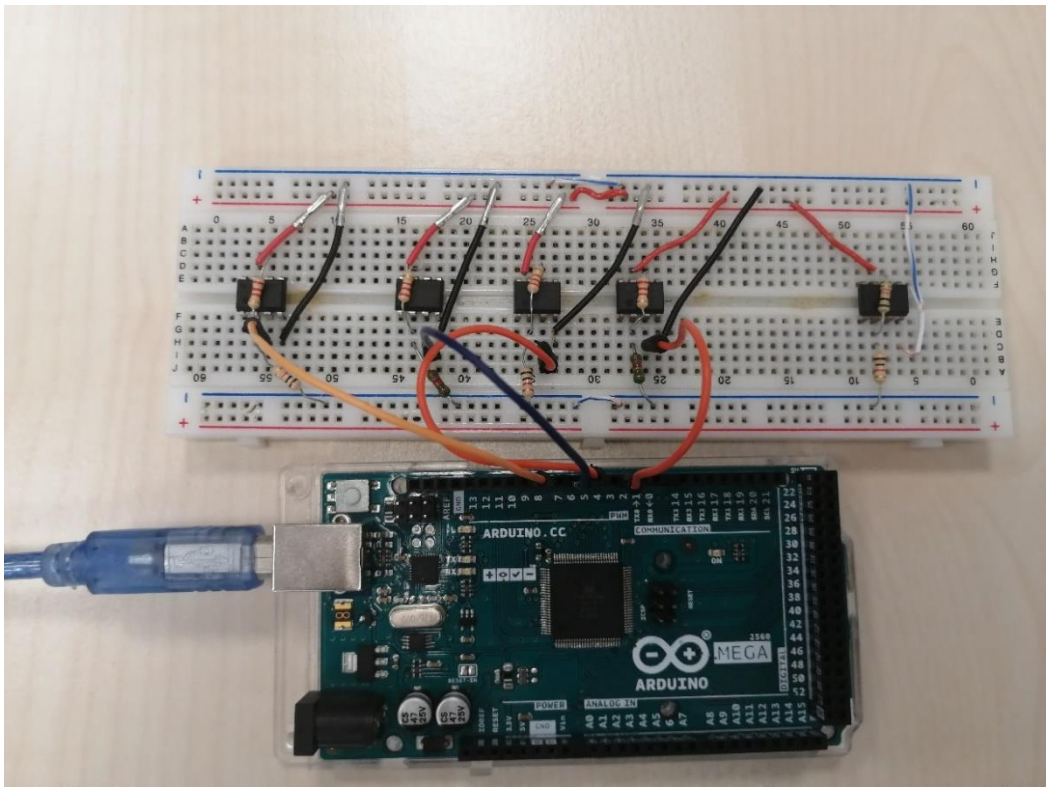

Figure 6.9 The MCU with the OpAmp circuitries

The MCU was then connected to the linearization system and the inputs for the RF and LO were connected as well. Figure 6.10 shows the full system connected for the experiment.

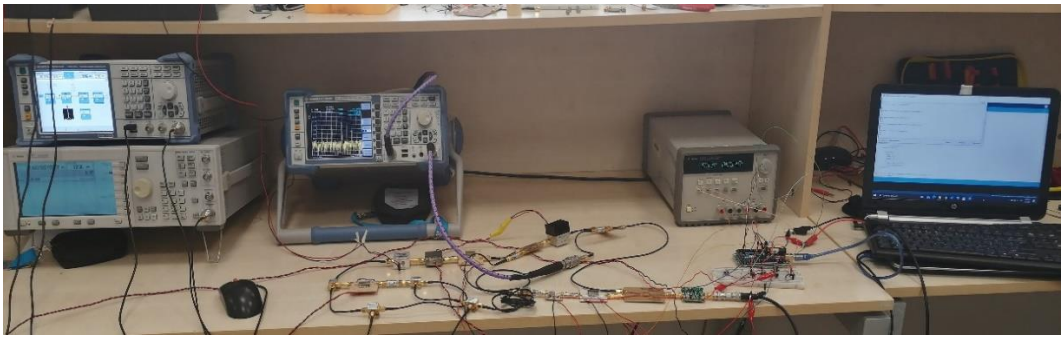

Figure 6.10 The full system test bench

The experiment started by setting the RF input with a 1.7 GHz carrier frequency (CF) with 2-tone frequencies with 1 MHz separation, the RF input was supplied using a vector signal generator. The LO frequency was set to 1.6 GHz.

The experiment was carried out as follows, first, the system was set but the linearization technique was disabled and the output of the PA was measured, then the linearization technique was activated and then the measurements of the output were taken, finally the adaptive control system was activated and then the output was measured. The measurement was done using the spectrum analyzer. Figure 6.11 shows the output of the PA without linearization and adaptive control. Note that the marker M1 is showing the fundamental level signal and the marker D2 is showing the level difference between the fundamentals and the IMD3.

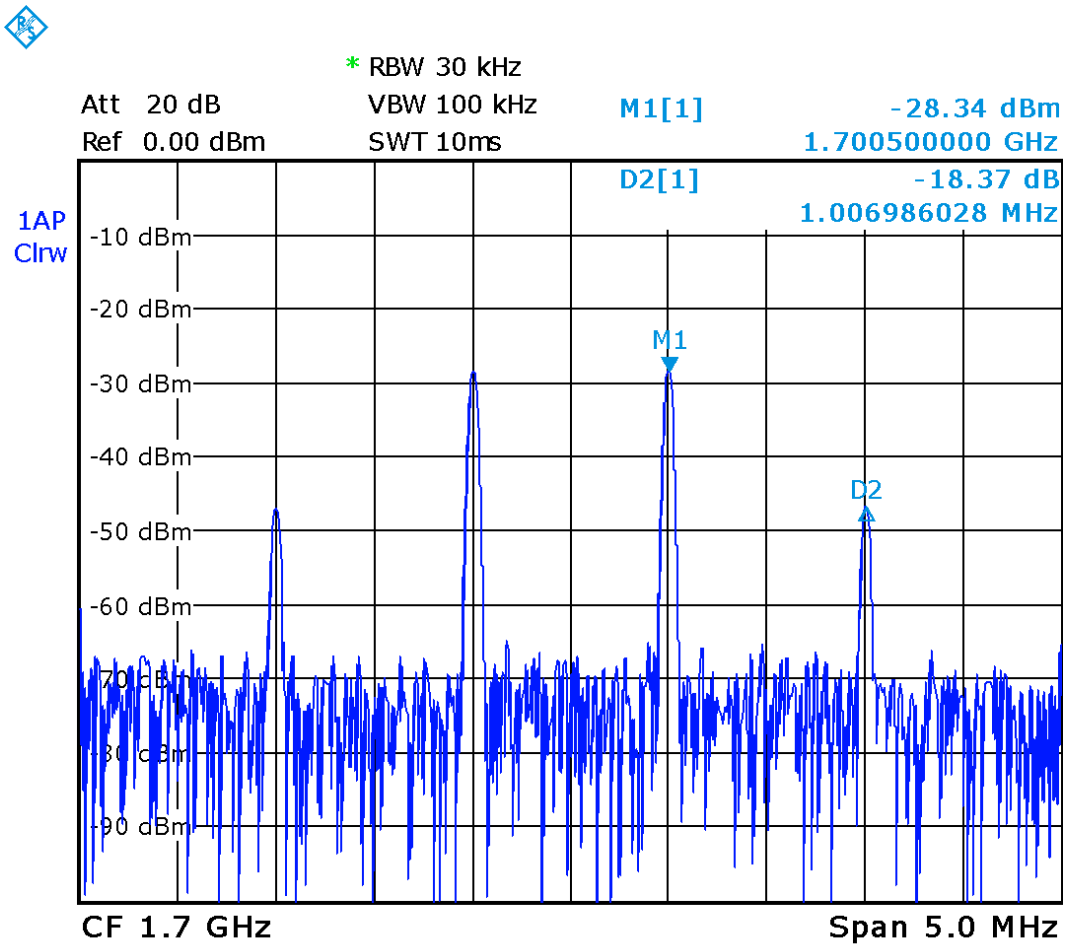

Figure 6.11 The PA's output with no linearization

After this measurement was taken, the linearization technique was enabled but not the adaptive control. The results of the linearization can be seen in Figure 6.12.

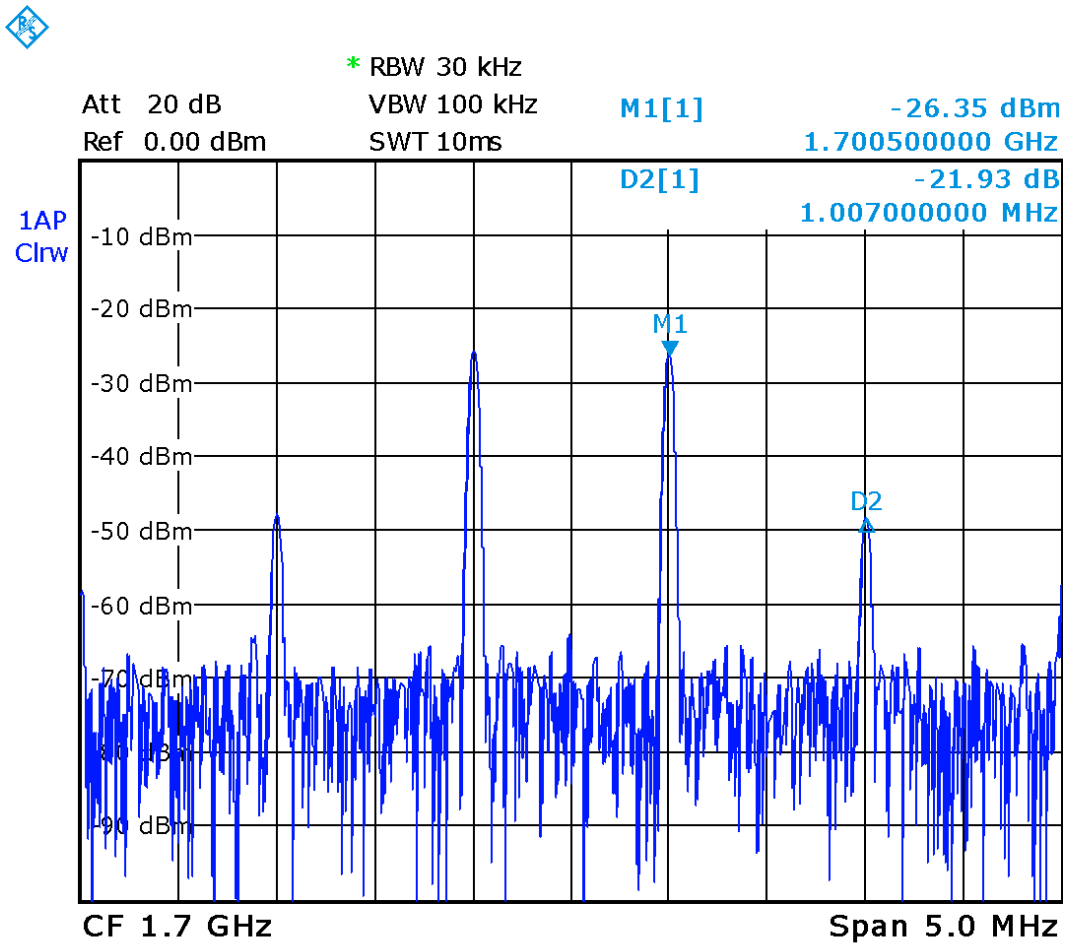

Figure 6.12 The output of the PA with the linearization technique enabled

Enabling the linearization technique has achieved ~4 dB suppression in the IMD3, as well as a 2 dB increment in the fundamentals level. But as mentioned before the measurement shown above for the IMD3 is relative to the fundamentals hence the 4 dB suppression is the overall correction. Keep in mind that this result is not optimal since the distortion generator was tuned manually, and the attenuator value was chosen according to the availability of the components. It is important to understand that the attenuator and phase shifter A2 and P2 are connected to the MCU at this point with an initial value of 0 V control. Which means that A2 provides full attenuation while P2 provides no phase shift.

The next step in the experiment was to enable the adaptive control system and observe the resultant spectrum.

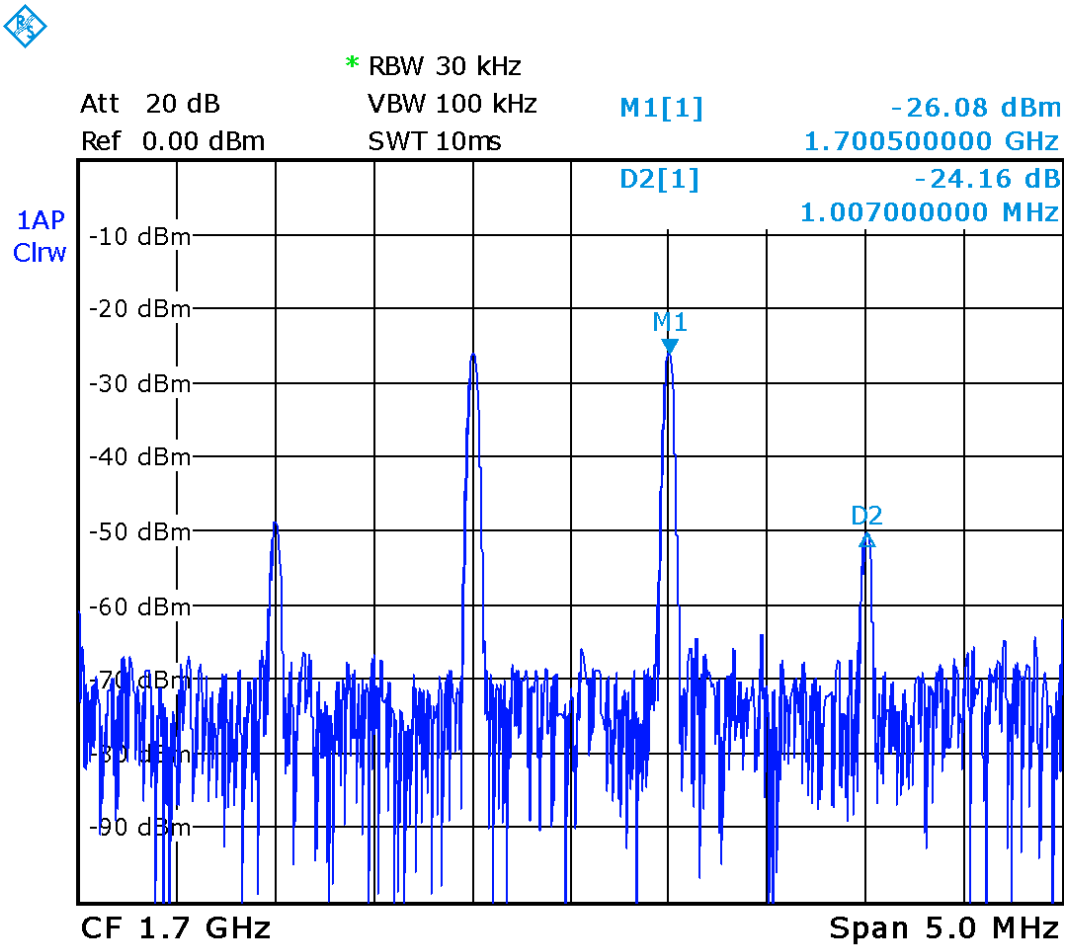

Figure 6.13 The output of the PA with the adaptive control

Figure 6.13 shows the output of the PA with the adaptive control enabled, another ~2 dB suppression of the IMD3 was achieved due to the adaptive control. Resulting in a total of ~6 dB suppression of the IMD3 level. To ensure the working of the adaptive control, the power level of the RF input signal was changed to 20 dBm and 17 dBm to observe how the system will adapt to the change.

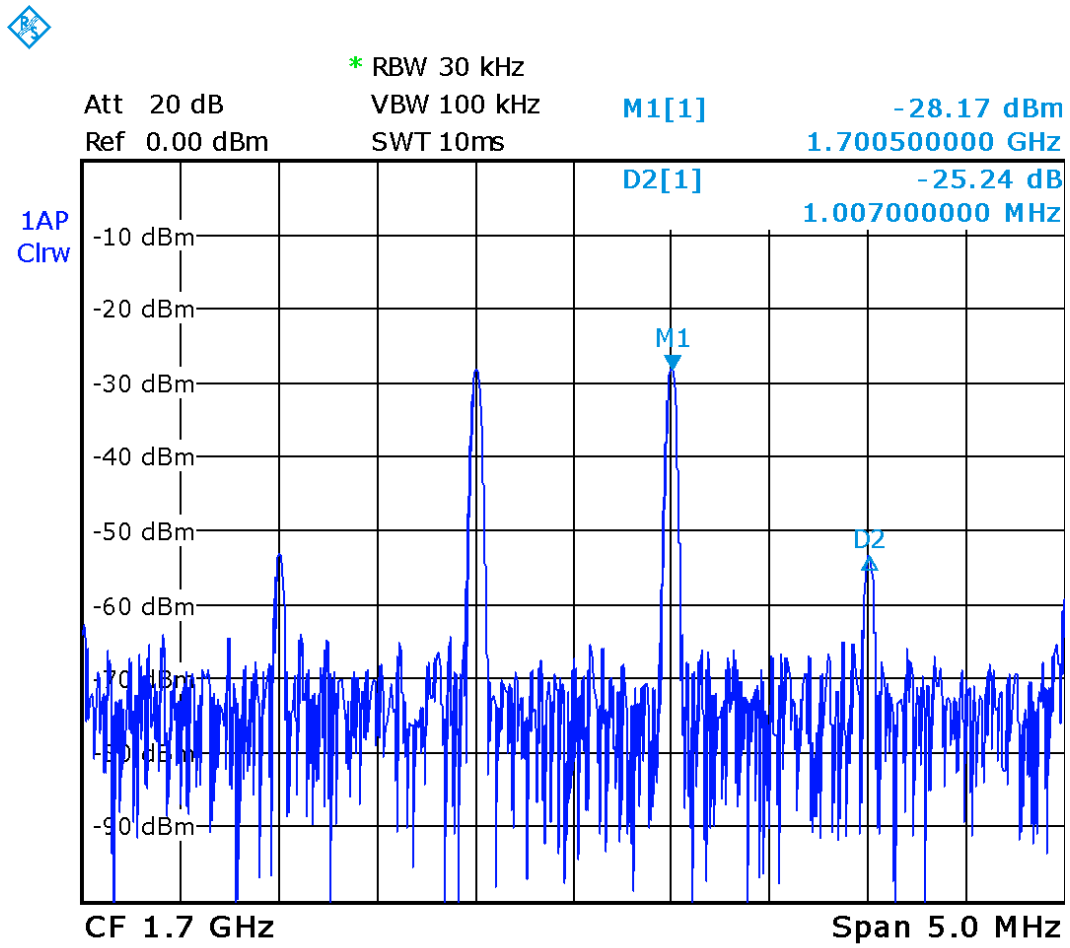

Figure 6.14 The output of the PA with a 20 dBm input

Figure 6.14 shows the spectrum of the PA's output signal after changing the input signal's power level to 20 dBm. A 2 dB suppression in the fundamentals level can be seen, more importantly, the IMD3 level which was around 24 dB is now around 25 dB relative to the fundamentals. This shows that the system adapted to the change and managed to maintain a low IMD3 level. Finally, suppling a 17 dBm input signal and observing the results.

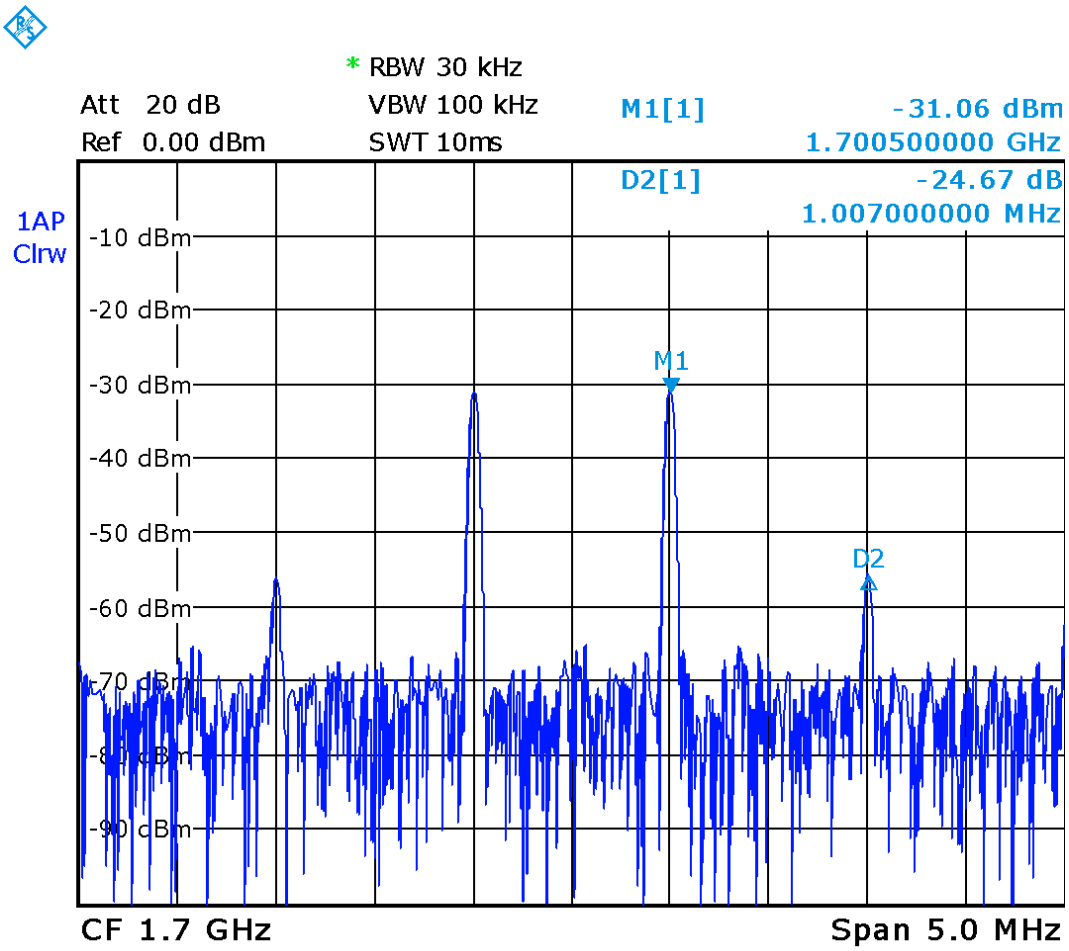

Figure 6.15 The output of the PA with a 17 dBm input

Figure 6.15 shows the spectrum of the output signal with a 17 dBm input. As the IMD3 level is at 24.67 dB, almost 25 dB lower than the fundamentals level. Which is almost the same as in the previous cases of inputs, 20 and 23 dBm. Therefore, the adaptation technique could achieve 6-7 dB suppression in the IMD products and maintain the suppression with the variations in the input signal's power. Which proves that the system has been able to detect the change and adapt the linearization technique to it.

6.3.1 The Control System Analysis

In this work the MCU represents the control system, as explained in 5.3.1. While measuring the results was done using the spectrum analyzer, the MCU is displaying the control voltages values that were used at the point of achieving adaptability. As shown earlier in Figure 5.7, the MCU is achieving linearity by going through the span of the control voltage of the variables.

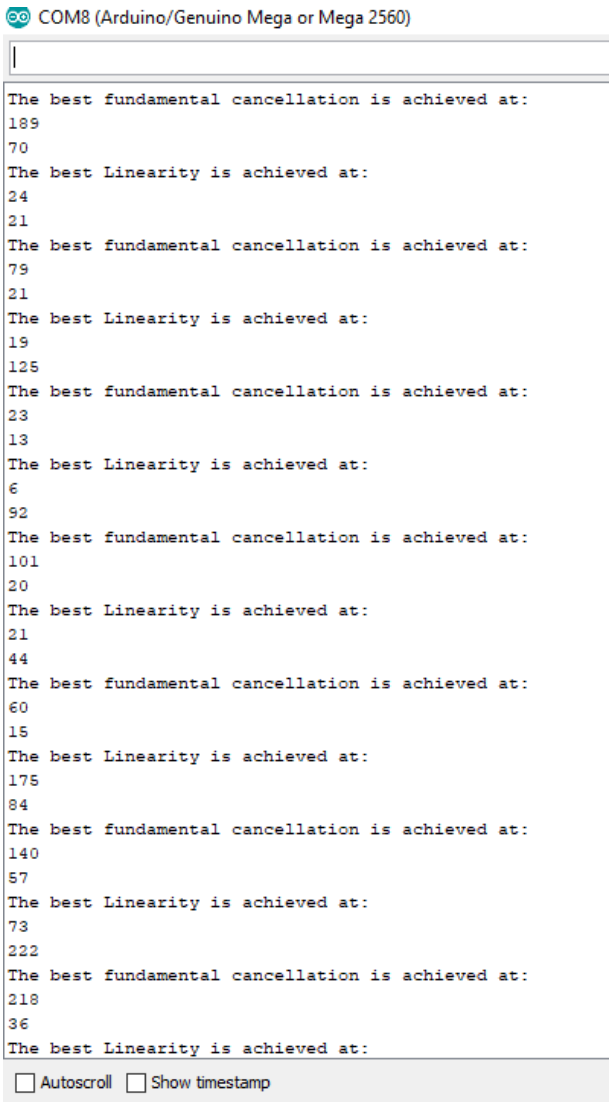

Figure 6.16 The values of the control voltages displayed by the MCU before convergence

Figure 6.16, shows the values displayed by the MCU. There are two values displayed for fundamental cancelation and two values for linearity. The earlier values are for the A3 and P3 values respectively. The later values are for the A2 and P2 respectively. As shown in the figure the values are changing with each iteration, since this figure is showing the values when the adaptive system was first enabled, i.e., before convergence. The MCU outputs the 5 V DC by dividing it into 256 bits, hence the output voltage is measured by the following formula:

$$Vout = n \times \frac{5}{256} \qquad \text{Eq. 6-1}$$

Where n = number of bits. To make sure that the output of the MCU matches the value displayed a multimeter was used to measure the output voltage of the MCU of a displayed value of one iteration. Figure 6.17 shows the number of bits displayed by the MCU vs the actual output voltage. According to Eq. 6-1 above, the theoretical calculations of the values would be:

$$102 \times \frac{5}{256} = 1.989\ V$$

$$211 \times \frac{5}{256} = 4.1145\ V$$

The theoretical values are almost the same as the actual output voltages as expected.

Figure 6.17 The output voltage vs the displayed number of bits

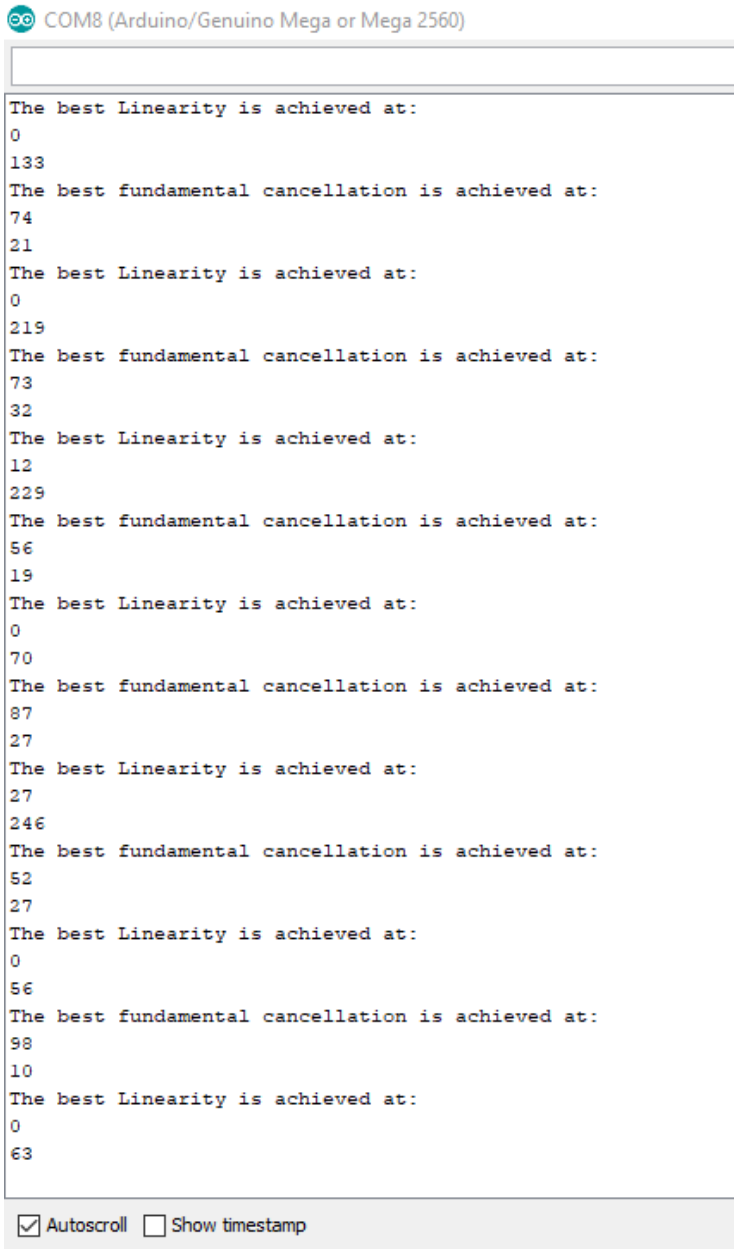

Figure 6.18 The values displayed by the MCU after convergence

Figure 6.18, shows the values achieved after the system converged. The values of the control voltage of A2 and P2 which are responsible for linearity are barely changing, while for A3 and P3 the values have a bigger change than that of A2&P2, yet the change is not significant. Figure 6.19 shows the number of iteration vs the output of the MCU control voltage. The attenuator A2 reaches convergence after the

5th iteration, Figure 6.19. Then a small change in the control voltage can be noticed. As for the phase shifter P2, it is continuously changing, the reasoning here is that the error signal is not constant since it passes through many components and a buffer amplifier before A2 & P2, Figure 6.8, which can add a phase difference.

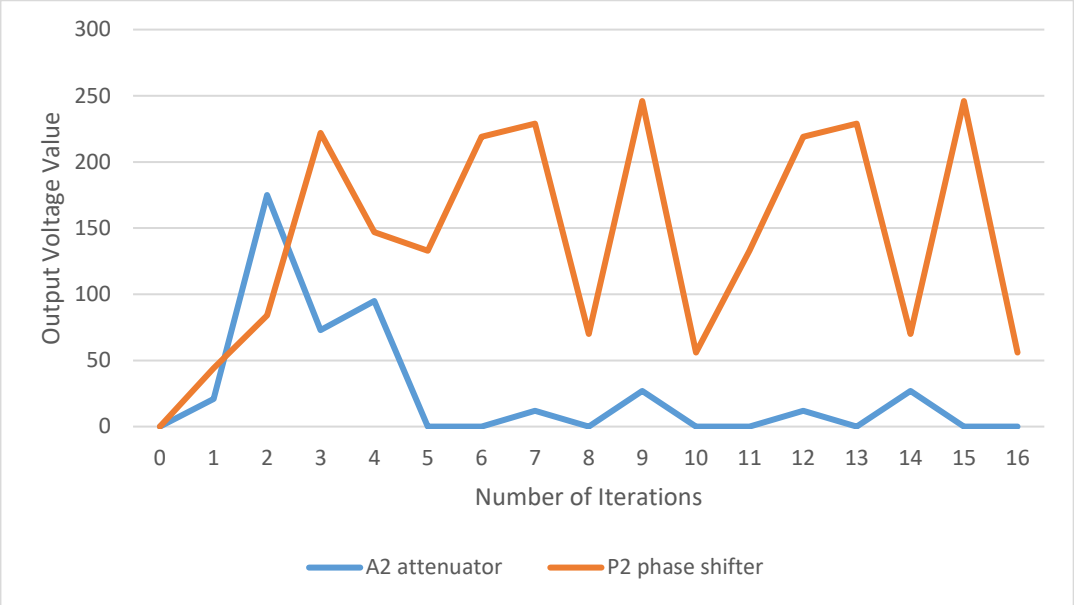

Figure 6.19 The number of iteration vs output

The time required for one iteration for the linearity adaptive control algorithm, Appendix II, was calculated using the built-in command in the Arduino "micros()" which calculates the number of microseconds since the program started running. The number of microseconds for one iteration was 16,912,248 µs or 16.9 s. Note that, the time for one iteration includes the signal cancellation and linearity iteration times. Hence, for instance, the total time required for 10 iterations would be 169 s or 2.8 minutes.

The control system's response time can be found by adding the response time of all the components involved in the system, i.e., the MCU, attenuators, phase shifters, and power detectors. In the system, there are two phase shifters and two attenuators as well as the MCU and a power detector. The response time of the MCU can be estimated by the time required for the ADC/DAC to be completed, that is 100 µs per

one ADC/DAC. As for the attenuators it can be found by the switching time which is 40 μs [75]. The phase shifters have no data on their response time or switching time, so it won't be included. The power detector has a very fast response time with a rise/fall time of 0.2/10 μs [76]. Ergo, the total response time of the system is:

$$(2 \times 100) + (2 \times 40) + 10 = 290\ \mu s$$

Then according to the response time of the closed-loop system and to obtain the natural frequency of the system, the iteration time must be added to the response time of the components. Which results in a total time of 16,912,538 μs or 16.9 s. then the natural frequency at which the system operates is $\frac{1}{16.9} \approx 0.6$ Hz.

As mentioned earlier, the system converges after the 5th iteration, hence the damping delay of the system is 1.4 min. Figure 6.20, shows the A2 attenuator reaching stability. From the graph, the closed-loop system can be described as an underdamped system, since the system reaches equilibrium quickly, but remains oscillating around the equilibrium.

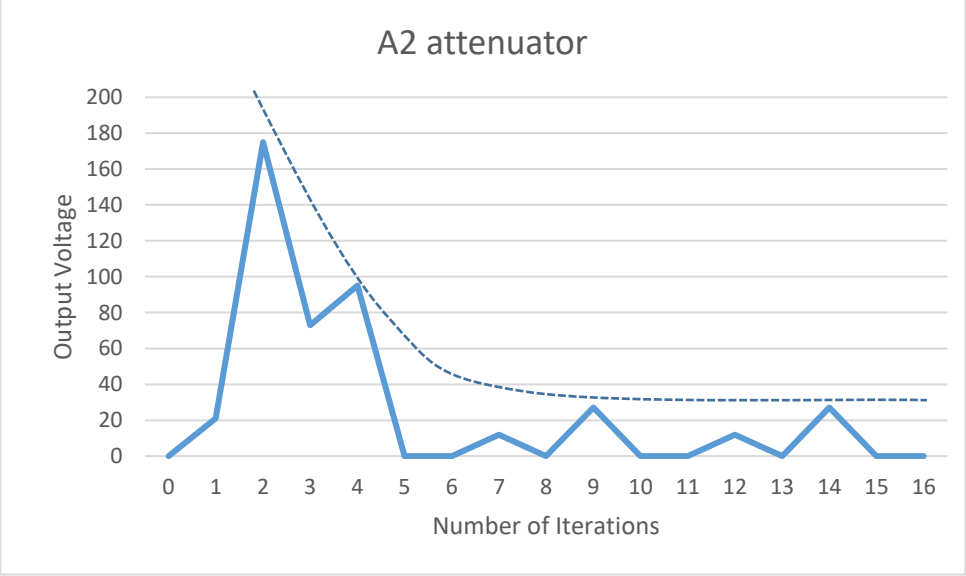

Figure 6.20 The system reaching steady-state

The previous calculations of the timings of the working system show that there is a delay before the system can output a result. For instance, the system converges in 1.4 min. which affects the results of the linearization technique, since the detection of the IMD3 in the error signal generation is solely dependent on the FFT results. This affects the applicability of the adaptive method proposed to some applications. If the proposed adaptive method is used in a system that requires a faster response than the convergence time, then that would create a problem and the proposed method would not be the best choice for this application. On the other hand, the proposed method would be applicable for an application that doesn't require a fast response time.

The closed-loop control system can be modeled as two 2^{nd} order control systems. That claim rests entirely on the fact that the control system has 4 variables (2 attenuators and 2 phase shifters), each pair are operating at the same time under the control of the voltage of the MCU. While the other pair of variables are on hold. The accurate closed-loop modeling would require mathematical modeling for each of the components used in the system, the PA, attenuators, the MCU, and phase shifters. Then obtaining the overall transfer function, which is then will give the exact order of the control system. However, modeling the components requires difficult mathematical operations and on its own would require a dedicated study.

6.3.2 Discussion

In this section, some of the results as well as some of the comparisons will be discussed. To start with, Table 6.1 shows a comparison between the results achieved in simulations and in the experiment, including the parameters that were used to perform both simulations and experiments.

Table 6.1 Simulation vs experiment parameters and results

System \ Parameter	INPUT					OUTPUT			Correction achieved
	Frequency		Power	Number of Tones	Tones Spacing (MHz)	Power			
	LO (GHz)	CF (GHz)	Tones (dBm)			Tones (dBm)	IMD3 (dBc)		
							Before	After	
Simulations	1.6	2.4	25	2	1	17	-15.2	-32	9 (dB)
Adaptive Control Linearization (Experiments)	1.6	1.7	23	2	1	-26	-18	-24.2	6-7 (dB)

As the table shows, there are a few differences between the parameters used in simulations and the ones used in experiments, for instance, the CF is changed from 2.4 GHz to 1.7 GHz between simulation and experiment, respectively. The change that happened in the experimental work was to match with the available components to try to achieve the optimal results. It is also worth noting that as mentioned before, the PA in the simulation was backed off by 3 dB hence the overall correction is 9 dB.

Moving on to the parameters used in experiments and the details of the results. Table 6.2 provides all the parameters for the closed-loop system where it shows all the input and output signals delivered and obtained in the experiments carried out to prove the adaptive control system.

Table 6.2 System's experimental inputs and outputs

	INPUT						OUTPUT	
Parameter / System	Frequency		Power		Number of Tones	Tones Spacing (MHz)	Power	
	LO (GHz)	CF (GHz)	Tones (dBm)	IMD3 (dBm)			Tones (dBm)	IMD3 (dBc)
With No Linearization	1.6	1.7	23	-	2	1	-28	-18
Linearization Enabled	1.6	1.7	23	-	2	1	-26	-22
Adaptive Control Enabled	1.6	1.7	23	-	2	1	-26	-24.2
			20	-	2	1	-28	-25
			17	-	2	1	-31	-24.7

Table 6.3 Comparison between prior work and the proposed work [43]-[62]

	Prior art		Proposed system
	Analog	Digital	
Control Mechanism	• The control mechanism is achieved in analog adaptive linearization by controlling the input signal of the PA using analog components. I.e., filters, couplers, attenuators, and phase shifters.	• The control mechanism is achieved in digital adaptive linearization by controlling the input signal of the PA by a comparison done between a measured sample signal and a model and then accordingly control the analog components to adjust the input signal.	• The control mechanism is achieved in this work is done by DSP a sampled signal and accordingly controls the voltage control of the variables in the linearization technique that are responsible for producing the error signal, linearity.

Analysis Criterion	• The continuous comparison between the output signal and the input signal.	• The analysis is done by modeling the PA behavior, or some specific characteristic of its behavior and saving this model to be compared with the actual output. • There are different models for the PA, such as: ➢ Thermal model of the transistors junction temperature. ➢ The ideal linear behavior of the PA. • The model is saved into a look-up table. • There are many different methods to obtain the model saved in the LUT, such as: ➢ Cartesian LUT. ➢ Crest Factor. ➢ Least Mean Squares.	• The analysis in the proposed work is done via two main approaches. ➢ Using the FFT algorithm to be able to identify the wanted and unwanted signals. ➢ Using the direct power reading with signal cancellation to achieve minimization/maximization depending on what is the signal that is being processed.
Results	• 20-40 dB reduction in the IMD3 level	• 15-40 dB reduction in the IMD level • 5-10 % increase in the efficiency	• 6-7 dB reduction in the IMD3 level

The table shows the differences between what has been done before and what the proposed system suggests, it also shows that the prior artworks had different approaches than the proposed system which suggests an original different approach as far as the author's knowledge goes regarding the previous artworks.

At this point, it is important to realize that, for a closed-loop system there might be some errors that can affect the behavior of the system. Such as the reduction of the overall gain of the system, the creation of oscillations in the system, and the steady-state error. The earlier two errors can be reduced but not totally avoided by the careful design of the closed-loop control system and by making the control system as simple as possible to reduce oscillations. As for the steady-state error, this error is only applicable when there is a known desired output value since the steady-state error is defined to be the difference between the desired and the actual value as time reaches infinity. However, in the control system proposed the desired output value is not fixed.

Although the results were positive and supportive of the theory, the IMD3 suppression was not as significant. There are a couple of reasons or limitations that were faced during the experiment. First, The MUC's objective in this part is to achieve linearity depending on lowering the sampled power by canceling the fundamentals and then by suppressing the IMD3. After a certain point, the total output power becomes insufficient for the measurements by the MCU. That means the coupled output power is too low for the MCU to detect.

Second, which is as mentioned before, the error signal generator was optimized according to the validity of the components, not to the best fit error generation, which affected the linearity capability of the whole system.

6.4 Summary

In this chapter, the experiments conducted to support the proposed system were discussed. Starting with the error signal generation experiment that was done by using the FFT algorithm to capture and differentiate between the wanted and unwanted signals.

And lastly, with the adaptive control experiment, the chosen system to carry out this experiment was built and tested with the addition of the MCU and detection components. Despite the limitations faced while conducting this experiment, the results were promising.

CONCLUSION

Linear power amplifiers (PAs) are crucial components for nearly all electronic devices in any application. The importance of the PA's linearity has led to making this field of study a major field in the RF domain. With many different linearization techniques available, the adaptability of the linearization technique has become another important branch of studies and research. This study aimed to create a control system that can be added to almost any linearization technique, that will make this technique adaptive, without frequency restrictions. Based on simulations and experiments that were conducted in the duration of this study, it can be concluded that the proposed system is capable of achieving adaptability when added to a linearization technique. The results suggest that the system can operate completely automatically once it is set up.

The approach implemented in this study, which is using an MCU as the brain of the adaptive system, was selected for a variety of reasons. These reasons being, the system's independence from the linearization technique, and frequency, the ability to analyze the signal and identify the wanted signal from the unwanted signal, making decisions based on these analysis, and having continuous monitoring over the linearity level. While studying, researching, and simulating this approach the system was expected to achieve an adaptive linearization technique that can maintain the best linearity and detecting any inconsistency that might take place in the system simultaneously. This study indicates that the proposed system can meet the expected goal. However, during the experimentation, a few limitations to the system arose that were not anticipated in the simulations, such as the DC output voltage of the MCU that controls the linearization system's variables.

The implementation of the proposed system in this study has led to a few important conclusions. The integration of an MCU to a linearization technique without the need for a demodulator and modulators is one of the important takes from this study. The fast response of the system, as a few numbers of iterations, and the ability to analyze the direct signal that is coming from the system. More importantly, the independence of the PA behavior since the measurements used for analysis are done continuously. Finally, the experiments done showed a positive result of the proposed system, where the system was tested with varying the input power of the system between 17-23 dBm, while the system was able to maintain the IMD3 level below the fundamentals by 6-7 dB.

Based on these findings, a practical implementation of this system should be considered in applications that are sensitive to signal distortions or applications that are costly or hard to be controlled by operators or engineers. For instance, a signal that is required to travel long distances is needed to have significant power, this power drops while the signal is traveling, hence a power station is normally built to enhance the signal's power. These stations might be located in very far uninhabited areas, which would be hard and costly to reach. Which having a fully automatic system in such a place will come in handy.

This study represents a different approach to achieve adaptable linearization techniques, which are originally built for a specific application with frequency limitations. The proposed system suggests a possibility for completely adaptable digitally controlled PA linearization techniques that can be used in most applications. The components required for adding the MCU to a linearization technique might differ, however, the control mechanism and the reading approaches remain the same.

REFERENCES

[1] Pozar, D. M. (2011). Microwave engineering. John wiley & sons.

[2] ETSI, E. 300 440-1 Ver. 1.3. 1,“. Electromagnetic compatibility and radio spectrum matters (ERM), short range devices, radio equipment to be used in the, 1.

[3] Harmonized, E. N. (2006). Final draft ETSI EN 300 328 V1. 7.1 (2006-05).

[4] Wolf, Peter (2008). Innovations in biological cancer therapy, a guide for patients and their relatives. Hannover: Naturasanitas. pp. 31–3.

[5] Mallory M, Gogineni E, Jones GC, Greer L, Simone CB 2nd (August 2015). "Therapeutic hyperthermia: The old, the new, and the upcoming". Crit Rev Oncol Hematol. 97 (15): 30018–4.

[6] Nesimoglu, T. (2009). RF and Microwave Amplifier Linearization for Wireless Communications: Harmonic Injection and Polynomial Predistortion. VDM Verlag.

[7] Yeom, K. W. (2015). Microwave circuit design: a practical approach using ADS. Prentice Hall.

[8] Serhan, A., Lauga-Larroze, E., Bourdel, S., Fournier, J. M., & Corrao, N. (2014, September). Comparison between MOS and bipolar mm-wave power amplifiers in advanced SiGe technologies. In 2014 IEEE Bipolar/BiCMOS Circuits and Technology Meeting (BCTM) (pp. 159-162). IEEE.

[9] Raab, F. H., Asbeck, P., Cripps, S., Kenington, P. B., Popovic, Z. B., Pothecary, N., ... & Sokal, N. O. (2003). RF and microwave power amplifier and transmitter technologies—Part 3. high frequency electronics, 2(3), 22-36.

[10] Kubowicz, R. (2000). Class-E Power Amplifier. MA, Canada. https://www.collectionscanada.gc.ca/obj/s4/f2/dsk1/tape4/PQDD_0017/MQ53437.pdf

[11] Cripps, S. C. (2006). RF Power Amplifiers for Wireless Communications, (Artech House Microwave Library (Hardcover)). Norwood, MA, USA: Artech House, Inc.

[12] Tamjid, F., Ghahremani, A., Richardson, M., & Fathy, A. E. (2017, January). A novel approach to the design of a broadband high efficiency Class-E power amplifier with over 87% bandwidth. In 2017 IEEE Topical Conference on RF/Microwave Power Amplifiers for Radio and Wireless Applications (PAWR) (pp. 25-28). IEEE.

[13] H. Xu, S. Gao, S, Heikman, S. Long, U. Mishra, and R. York, "A high efficiency class-E GaN HEMT power amplifier at 1.9 GHz," Microwave and Wireless Components Letters, IEEE, vol. 16, no.1, pp.22,24, Jan 2006.

[14] M.P. Vander Heijden, M.Acar, and J.S. Vromans,"A compact 12-watt high-efficiency 2.1–2.7 GHz class-E GaN HEMT power amplifier for base stations," in IEEE MTT-S Int. Microw. Symp. Dig., Jun. 2009, pp. 657–660.

[15] K. Chen, P. Peroulid, "Design of Highly Efficient Broadband Class-E Power Amplifier Using Synthesized Low-Pass Matching Networks" IEEE Transcations on Microwave Theory and Technologies, vol. 59, No.12, December 2011

[16] N. Tuffy; Guan Lei, Zhu Anding; T. J. Brazil "A Simplified Broadband Design Methodology for Linearized HighEfficiency Continuous Class- F Power Amplifiers," Microwave Theory and Techniques, IEEE Transactions, vol.60, no.6, pp.1952,1963, June 2012.

[17] B. Merrick, J. King, T. Brazil, "A simplified procedure for the design of Continuous Class-F power amplifiers," Microwave Integrated Circuits Conference, no, pp.508-511, Oct. 2013.

[18] P. Wright, J. Lees, J. Benedikt, P. J. Tasker, and S. C. Cripps, "A methodology for realizing high efficiency ClassJ linear and broadband PA," IEEE Trans. Microw. Theory Tech., vol. 57, no. 12, pp. 3196–3204, Dec. 2009.

[19] Yadav, S. P., & Bera, S. C. (2014, August). Nonlinearity effect of high power amplifiers in communication systems. In 2014 International Conference on Advances in Communication and Computing Technologies (ICACACT 2014) (pp. 1-6). IEEE.

[20] Miehle, K. (2003). A new linearization method for cancellation of third order distortion (Doctoral dissertation, University of North Carolina at Charlotte).

[21] I. Meier and J. B. De Swardt, "Error-feedback for amplifier linearization," *Proceedings of the 1998 South African Symposium on Communications and Signal Processing-COMSIG '98 (Cat. No. 98EX214)*, Rondebosch, South Africa, 1998, pp. 381-386, doi: 10.1109/COMSIG.1998.736987.

[22] BoBo Shi and L. Sundstrom, "Linearization of RF power amplifiers using power feedback," *1999 IEEE 49th Vehicular Technology Conference (Cat. No.99CH36363)*, Houston, TX, USA, 1999, pp. 1520-1524 vol.2, doi: 10.1109/VETEC.1999.780601.

[23] *T. Nesimoglu, C. N. Canagarajah, J. P. McGeehan and R. J. Wilkinson, "A novel wideband active feedback amplifier linearization scheme suitable for handsets," VTC2000-Spring. 2000 IEEE 51st Vehicular Technology Conference Proceedings (Cat. No.00CH37026), Tokyo, Japan, 2000, pp. 1712-1716 vol.3, doi: 10.1109/VETECS.2000.851564.*

[24] J. L. Dawson and T. H. Lee, "Cartesian feedback for RF power amplifier linearization," *Proceedings of the 2004 American Control Conference*, Boston, MA, USA, 2004, pp. 361-366 vol.1, doi: 10.23919/ACC.2004.1383631.

[25] N. Delaunay, N. Deltimple, D. Belot and E. Kerherve, "Linearization of a 65nm CMOS power amplifier with a Cartesian Feedback for W-CDMA standard," *2009 Joint IEEE North-East Workshop on Circuits and Systems and TAISA Conference*, Toulouse, France, 2009, pp. 1-4, doi: 10.1109/NEWCAS.2009.5290427.

[26] Sang-Gee Kang, Il-Kyoo Lee and Ki-Suk Yoo, "Analysis and design of feedforward power amplifier," 1997 IEEE MTT-S International Microwave Symposium Digest, Denver, CO, USA, 1997, pp. 1519-1522 vol.3, doi: 10.1109/MWSYM.1997.596621.

[27] Y. Xiang and G. Wang, "Doherty power amplifier with feedforward linearization," 2009 Asia Pacific Microwave Conference, Singapore, 2009, pp. 1621-1624, doi: 10.1109/APMC.2009.5384357.

[28] A. Ghadam, S. Burglechner, A. H. Gokceoglu, M. Valkama and A. Springer, "Implementation and Performance of DSP-Oriented Feedforward Power Amplifier Linearizer," in *IEEE Transactions on Circuits and Systems I: Regular Papers*, vol. 59, no. 2, pp. 409-425, Feb. 2012, doi: 10.1109/TCSI.2011.2163890.

[29] M. X. Xiao, S. W. Cheung and T. I. Yuk, "A simple and effective RF predistorter for use in the HPAs of base stations in cellular mobile systems," 2008 11th IEEE Singapore International Conference on Communication Systems, Guangzhou, China, 2008, pp. 805-808, doi: 10.1109/ICCS.2008.4737296.

[30] M. X. Xiao, S. W. Cheung and T. I. Yuk, "An intermodulation products generator for predistortion of base station HPAs," 2009 IEEE Radio and Wireless Symposium, San Diego, CA, USA, 2009, pp. 602-605, doi: 10.1109/RWS.2009.4957423.

[31] M. X. Xiao, S. W. Cheung and T. I. Yuk, "An RF predistorter for base station HPAs of NADC system," 2009 IEEE 20th International Symposium on Personal, Indoor and Mobile Radio Communications, Tokyo, Japan, 2009, pp. 1587-1591, doi: 10.1109/PIMRC.2009.5449718.

[32] Nesimoglu, T. (2018). Broadband analogue predistortion using a distortion generator based on two-stage RF mixer topology. International Journal of Electronics, 105(7), 1185-1199.

[33] Abuelma'atti, M. T., Abuelma'atti, A. M., & Yeung, T. K. (2012). A new diode-based curve-fitting predistortion lineariser for GaN power amplifier. International Journal of Electronics, 99(5), 719-734.

[34] S. Rezaei, M. S. Hashmi, B. Dehlaghi and F. M. Ghannouchi, "A systematic methodology to design analog predistortion linearizer for dual inflection power amplifiers," 2011 IEEE MTT-S International Microwave Symposium, Baltimore, MD, USA, 2011, pp. 1-4, doi: 10.1109/MWSYM.2011.5972885.

[35] Bassam, S. A., Chen, W., Helaoui, M., Ghannouchi, F. M., & Feng, Z. (2011). Linearization of concurrent dual-band power amplifier based on 2D-DPD technique. IEEE Microwave and Wireless Components Letters, 21(12), 685-687.

[36] Lee, Y. S., Lee, M. W., & Jeong, Y. H. (2009). A wideband analog predistortion power amplifier with multi-branch nonlinear path for memory-effect compensation. IEEE microwave and wireless components letters, 19(7), 476-478.

[37] Sahan, N., Inal, M. E., Demir, S., & Toker, C. (2008). High-power 20-100-MHz linear and efficient power-amplifier design. IEEE transactions on microwave theory and techniques, 56(9), 2032-2039.

[38] Kaur, R., & Patterh, M. S. (2016). Overview of the linearization techniques to mitigate the nonlinear effects of power amplifier. An International Journal of Engineering Sciences, 17, 479-485.

[39] Singh, H., & Sappal, A. S. (2016). Comparative study of power amplifier linearization techniques. Int. J. Eng. Res. Devel, 12(3).

[40] Miller, S. J. (2017). The method of least squares. In The Probability Lifesaver (pp. 625-635). Princeton University Press.

[41] R. J. Baxley, C. Zhao and G. T. Zhou, "Constrained Clipping for Crest Factor Reduction in OFDM," in IEEE Transactions on Broadcasting, vol. 52, no. 4, pp. 570-575, Dec. 2006, doi: 10.1109/TBC.2006.883301.

[42] R. Sperlich, Y. Park, G. Copeland and J. S. Kenney, "Power amplifier linearization with digital pre-distortion and crest factor reduction," 2004 IEEE MTT-S International Microwave Symposium Digest (IEEE Cat. No.04CH37535), Fort Worth, TX, USA, 2004, pp. 669-672 Vol.2, doi: 10.1109/MWSYM.2004.1336077.

[43] K. J. Muhonen, M. Kavehrad and R. Krishnamoorthy, "Adaptive baseband predistortion techniques for amplifier linearization," Conference Record of the Thirty-Third Asilomar Conference on Signals, Systems, and Computers (Cat. No.CH37020), Pacific Grove, CA, USA, 1999, pp. 888-892 vol.2, doi: 10.1109/ACSSC.1999.831837.

[44] S. J. Grant, J. K. Cavers and P. A. Goud, "A DSP controlled adaptive feedforward amplifier linearizer," Proceedings of ICUPC - 5th International Conference on Universal Personal Communications, Cambridge, MA, USA, 1996, pp. 788-792 vol.2, doi: 10.1109/ICUPC.1996.562683.

[45] G. Zhao, F. M. Ghannouchi, F. Beauregard and A. B. Kouki, "Digital implementations of adaptive feedforward amplifier linearization techniques," 1996 IEEE MTT-S International Microwave Symposium Digest, San Francisco, CA, USA, 1996, pp. 543-546 vol.2, doi: 10.1109/MWSYM.1996.510992.

[46] M. Faulkner and M. Johansson, "Adaptive linearization using predistortion-experimental results," in IEEE Transactions on Vehicular Technology, vol. 43, no. 2, pp. 323-332, May 1994, doi: 10.1109/25.293651.

[47] D. Di Zenobio, G. Santella and F. Mazzenga, "Adaptive linearization of power amplifier in orthogonal multicarrier schemes," IEEE Wireless Communication System Symposium, Long Island, NY, USA, 1995, pp. 225-230, doi: 10.1109/WCSS.1995.588513.

[48] J. A. Sills and R. Sperlich, "Adaptive power amplifier linearization by digital pre-distortion using genetic algorithms," Proceedings RAWCON 2002. 2002 IEEE Radio and Wireless Conference (Cat. No.02EX573), Boston, MA, USA, 2002, pp. 229-232, doi: 10.1109/RAWCON.2002.1030159.

[49] P. Varahram and Z. Atlasbaf, "Adaptive digital predistortion for high power amplifiers with memory effects," 2005 Asia-Pacific Microwave Conference Proceedings, Suzhou, China, 2005, pp. 4 pp.-, doi: 10.1109/APMC.2005.1606627.

[50] Y. Y. Woo et al., "Adaptive Digital Feedback Predistortion Technique for Linearizing Power Amplifiers," in IEEE Transactions on Microwave Theory and Techniques, vol. 55, no. 5, pp. 932-940, May 2007, doi: 10.1109/TMTT.2007.895145.

[51] P. Jardin and G. Baudoin, "Filter Lookup Table Method for Power Amplifier Linearization," in IEEE Transactions on Vehicular Technology, vol. 56, no. 3, pp. 1076-1087, May 2007, doi: 10.1109/TVT.2007.895566.

[52] S. Chung, J. W. Holloway and J. L. Dawson, "Open-Loop Digital Predistortion Using Cartesian Feedback for Adaptive RF Power Amplifier Linearization," 2007 IEEE/MTT-S International Microwave Symposium, Honolulu, HI, USA, 2007, pp. 1449-1452, doi: 10.1109/MWSYM.2007.380506.

[53] H. Li, D. H. Kwon, D. Chen and Y. Chiu, "A Fast Digital Predistortion Algorithm for Radio-Frequency Power Amplifier Linearization With Loop Delay Compensation," in IEEE Journal of Selected Topics in Signal Processing, vol. 3, no. 3, pp. 374-383, June 2009, doi: 10.1109/JSTSP.2009.2020562.

[54] H. Le Duc, B. Feuvrie, M. Pastore and Y. Wang, "An Adaptive Cascaded ILA- and DLA-Based Digital Predistorter for Linearizing an RF Power Amplifier," in IEEE Transactions on Circuits and Systems I: Regular Papers, vol. 66, no. 3, pp. 1031-1041, March 2019, doi: 10.1109/TCSI.2018.2872465.

[55] H. Q. He and M. Faulkner, "Performance of adaptive predistortion temperature in RF power amplifier linearization," ISSPA '99. Proceedings of the Fifth International Symposium on Signal Processing and its Applications (IEEE Cat. No.99EX359), Brisbane, QLD, Australia, 1999, pp. 717-720 vol.2, doi: 10.1109/ISSPA.1999.815772.

[56] H. Qian, S. Yao, H. Huang and W. Feng, "A Low-Complexity Digital Predistortion Algorithm for Power Amplifier Linearization," in IEEE Transactions on Broadcasting, vol. 60, no. 4, pp. 670-678, Dec. 2014, doi: 10.1109/TBC.2014.2352911.

[57] Anding Zhu and T. J. Brazil, "An adaptive Volterra predistorter for the linearization of RF high power amplifiers," 2002 IEEE MTT-S International Microwave Symposium Digest (Cat. No.02CH37278), Seattle, WA, USA, 2002, pp. 461-464 vol.1, doi: 10.1109/MWSYM.2002.1011655.

[58] J. Lu et al., "Machine Learning based Adaptive Predistorter for High Power Amplifier Linearization," 2019 IEEE Cognitive Communications for Aerospace Applications Workshop (CCAAW), Cleveland, OH, USA, 2019, pp. 1-6, doi: 10.1109/CCAAW.2019.8904896.

[59] S. P. Stapleton and F. C. Costescu, "An adaptive predistorter for a power amplifier based on adjacent channel emissions (mobile communications)," in IEEE Transactions on Vehicular Technology, vol. 41, no. 1, pp. 49-56, Feb. 1992, doi: 10.1109/25.120144.

[60] S. Jin, B. Park, K. Moon, M. Kwon and B. Kim, "Linearization of CMOS Cascode Power Amplifiers Through Adaptive Bias Control," in *IEEE Transactions on Microwave Theory and Techniques*, vol. 61, no. 12, pp. 4534-4543, Dec. 2013, doi: 10.1109/TMTT.2013.2288206.

[61] A. K. Talwar, "Reduction of noise and distortion in amplifiers using adaptive cancellation," in *IEEE Transactions on Microwave Theory and Techniques*, vol. 42, no. 6, pp. 1086-1087, June 1994, doi: 10.1109/22.293582.

[62] S. P. Stapleton, "Adaptive FeedForward Linearization For RF Power Amplifiers," 55th ARFTG Conference Digest, Boston, MA, USA, 2000, pp. 1-7, doi: 10.1109/ARFTG.2000.327387.

[63] Rubiola, E. (2006). Tutorial on the double balanced mixer. arXiv preprint physics/0608211.

[64] CURRENT, D. O. I. B. Op Amp Input Bias Current.

[65] Hank Zumbahlen, Basic Linear Design, Analog Devices, 2006, ISBN: 0-915550-28-1. Also available as Linear Circuit Design Handbook, Elsevier-Newnes, 2008, ISBN-10: 0750687037, ISBN-13: 978- 0750687034. Chapter 1.

[66] Walter G. Jung, Op Amp Applications, Analog Devices, 2002, ISBN 0-916550-26-5, Also available as Op Amp Applications Handbook, Elsevier/Newnes, 2005, ISBN 0-7506-7844-5. Chapter 1.

[67] Cooley, J. W., & Tukey, J. W. (1965). An algorithm for the machine calculation of complex Fourier series. Mathematics of computation, 19(90), 297-301.

[68] Harris, F. J. (1978). On the use of windows for harmonic analysis with the discrete Fourier transform. Proceedings of the IEEE, 66(1), 51-83.

[69] Note14, A. Understanding FFT Windows. Application Note 14 LDS Dactron.

[70] Labuda, A. (2012, April 1). Overlayed window functions in the frequency domain [Graph].https://en.wikipedia.org/wiki/File:Window_functions_in_the_frequency_domain.png

[71] Cheh Pan, "Gibbs phenomenon removal and digital filtering directly through the fast Fourier transform," in *IEEE Transactions on Signal Processing*, vol. 49, no. 2, pp. 444-448, Feb. 2001, doi: 10.1109/78.902128.

[72] A. Antoniou, Digital Filters: Analysis and Design. New York: McGraw-Hill, 1979, p. 524.

[73] A. V. Oppenheim and R. W. Schafer, Discrete-Time Signal Processing. Englewood Cliffs, NJ: Prentice-Hall, 1989, p. 879.

[74] The Penguin Dictionary of Physics, ed. Valerie Illingworth, 1991, Penguin Books, London

[75] Bequette, B. Wayne (2003). Process Control: Modeling, Design, and Simulation. Upper Saddle River, New Jersey: Prentice Hall PTR. pp. 165–168. ISBN 978-0-13-353640-9.

[76] Mini-Circuits,"Voltage Variable Attenuator EVA-3000+",REV. D M151108 EVA-3000+ EDR-7165/2 RAV 161211.

[77] Analog Devices," 10 MHz to 10 GHz 67 dB TruPwr Detector ADL5906", ADL5906 (Rev. A),2013.

APPENDICES

A. Appendix I

This appendix includes the Fast Fourier Transform algorithm that was used during this study.

```
//-------------------------------------------------------------------------------//

byte sine_data [91]=

 {

0,

4,   9,   13,  18,  22,  27,  31,  35,  40,  44,

49,  53,  57,  62,  66,  70,  75,  79,  83,  87,

91,  96,  100, 104, 108, 112, 116, 120, 124, 127,

131, 135, 139, 143, 146, 150, 153, 157, 160, 164,

167, 171, 174, 177, 180, 183, 186, 189, 192, 195,

198, 201, 204, 206, 209, 211, 214, 216, 219, 221,

223, 225, 227, 229, 231, 233, 235, 236, 238, 240,

241, 243, 244, 245, 246, 247, 248, 249, 250, 251,

252, 253, 253, 254, 254, 254, 255, 255, 255, 255

  };

float f_peaks[5]; // top 5 frequencies peaks in descending order

//-------------------------------------------------------------------------------//

int data_in[512];
```

```
unsigned long t;
void setup()
        {
        Serial.begin(250000);
        }
void loop() {


t=micros();
// for loop to sample the signal and save it into a sample array
for (int i=0;i<512;i++){
data_in[i]= analogRead(A0);
delayMicroseconds(1); //depending on the application
  }
t=micros()-t;
t=512000000/t;
FFT(data_in,512,t);        // perform FFT
Serial.println("The Top Frequencies are:");
Serial.println(f_peaks[0]);
Serial.println(f_peaks[1]);
delay(10000);  // repeat the program every 10 secs, adjustable
}
```

//----------FFT Function----------//

float FFT(int in[],byte N,float Frequency)

{

/*

sine_data [91]: global variable

1. in[] : Data array,

2. N : Number of sample (recommended sample size 2,4,8,16,32,64,128...)

3. Frequency: sampling frequency required as input (Hz)

If sample size is not in power of 2 it will be clipped to lower side of number.

i.e, for 150 number of samples, code will consider first 128 sample, remaining sample will be omitted.

For Arduino nano, FFT of more than 128 sample not possible due to mamory limitation (64 recomended)

For higher Number of sample may arise Mamory related issue,

Code by ABHILASH

Contact: abhilashpatel121@gmail.com

Documentation:https://www.instructables.com/member/abhilash_patel/instructables/

*/

```
unsigned int data[13]={1,2,4,8,16,32,64,128,256,512,1024,2048};
int a,c1,f,o,x;
a=N;

    for(int i=0;i<12;i++)              //calculating the levels
      { if(data[i]<=a){o=i;} }

int in_ps[data[o]]={};     //input for sequencing
float out_r[data[o]]={};   //real part of transform
float out_im[data[o]]={};  //imaginory part of transform

x=0;
    for(int b=0;b<o;b++)                  // bit reversal
      {
       c1=data[b];
       f=data[o]/(c1+c1);
            for(int j=0;j<c1;j++)
              {
               x=x+1;
               in_ps[x]=in_ps[j]+f;
              }
      }
```

```
 for(int i=0;i<data[o];i++)          // update input array as per bit reverse order
    {
     if(in_ps[i]<a)
     {out_r[i]=in[in_ps[i]];}
     if(in_ps[i]>a)
     {out_r[i]=in[in_ps[i]-a];}
    }
int i10,i11,n1;
float e,c,s,tr,ti;

  for(int i=0;i<o;i++)                          //fft
  {
   i10=data[i];            // overall values of sine/cosine  :
   i11=data[o]/data[i+1];    // loop with similar sine cosine:
   e=360/data[i+1];
   e=0-e;
   n1=0;

      for(int j=0;j<i10;j++)
      {
      c=cosine(e*j);
      s=sine(e*j);
```

```
        n1=j;

            for(int k=0;k<i11;k++)
             {
             tr=c*out_r[i10+n1]-s*out_im[i10+n1];
             ti=s*out_r[i10+n1]+c*out_im[i10+n1];

             out_r[n1+i10]=out_r[n1]-tr;
             out_r[n1]=out_r[n1]+tr;

             out_im[n1+i10]=out_im[n1]-ti;
             out_im[n1]=out_im[n1]+ti;

             n1=n1+i10+i10;
              }
          }
    }

/*
for(int i=0;i<data[o];i++)
{
Serial.print(out_r[i]);
```

```
Serial.print("\t");                         // un comment to print RAW o/p
Serial.print(out_im[i]); Serial.println("i");
}
*/
//---> here onward out_r contains amplitude and our_in conntains frequency (Hz)
   for(int i=0;i<data[o-1];i++)              // getting amplitude from compex number
       {
        out_r[i]=sqrt(out_r[i]*out_r[i]+out_im[i]*out_im[i]); // to  increase the speed delete sqrt
        out_im[i]=i*Frequency/N;

        Serial.print(out_im[i]); Serial.print("Hz");
        Serial.print("\t");                  // un comment to print freuency spectrum vs magnitude of the frequency
        Serial.println(out_r[i]);

       }
x=0;       // peak detection
  for(int i=1;i<data[o-1]-1;i++)
     {
     if(out_r[i]>out_r[i-1] && out_r[i]>out_r[i+1])
     {in_ps[x]=i;    //in_ps array used for storage of peak number
     x=x+1;}
```

```
    }


s=0;
c=0;
   for(int i=0;i<x;i++)            // re arraange as per magnitude
   {
      for(int j=c;j<x;j++)
      {
         if(out_r[in_ps[i]]<out_r[in_ps[j]])
            {s=in_ps[i];
            in_ps[i]=in_ps[j];
            in_ps[j]=s;}
      }
   c=c+1;
   }
   for(int i=0;i<5;i++)     // updating f_peak array (global variable)with descending
order
   {
   f_peaks[i]=out_im[in_ps[i]];
   }
}
```

```
float sine(int i)
{
  int j=i;
  float out;
  while(j<0){j=j+360;}
  while(j>360){j=j-360;}
  if(j>-1   && j<91){out= sine_data[j];}
  else if(j>90  && j<181){out= sine_data[180-j];}
  else if(j>180 && j<271){out= -sine_data[j-180];}
  else if(j>270 && j<361){out= -sine_data[360-j];}
  return (out/255);
}

float cosine(int i)
{
  int j=i;
  float out;
  while(j<0){j=j+360;}
  while(j>360){j=j-360;}
  if(j>-1   && j<91){out= sine_data[90-j];}
```

```
  else if(j>90  && j<181){out= -sine_data[j-90];}
  else if(j>180 && j<271){out= -sine_data[270-j];}
  else if(j>270 && j<361){out= sine_data[j-270];}
  return (out/255);
}
//------------------------------------------------------------------------------//
```

B. Appendix II

This appendix includes the second code that was used to control and check the DC control of the variables that controls the linearity of the PA.

```
void setup() {
Serial.begin(9600);
}
void loop() {
int i;int j;   // Counters for the values of the variables
int TempI; int TempJ; // Temporary variables to save the index of best linearity
float Min = 99999; //
for (i=0; i<256;i++){
  for (j=0; j<256;j++){
    analogWrite(2,i);   // change the values of first set of variables
    analogWrite(4,j);

    int x = analogRead(A1); // read the change on the PA output
        if(x <Min){
          Min= x;
          TempI = i;
          TempJ= j;
         }
```

```
    }
  }
Serial.println("The best fundamental cancellation is at: ");
Serial.println(TempI);
Serial.println(TempJ);

delay(10000); // wait for 10 secs

for (i=0; i<256;i++){
  for (j=0; j<256;j++){
     analogWrite(6,i);
     analogWrite(8,j);

          int x = analogRead(A1);
          if(x <Min){
            Min= x;
            TempI = i;
            TempJ= j;
           }

    }
  }
```

```
Serial.println("The best Linearity is at: ");
Serial.println(TempI);
Serial.println(TempJ);

delay(10000); // The program will run every 20 secs
}
```

TEZ İZİN FORMU / THESIS PERMISSION FORM

PROGRAM / PROGRAM

Sürdürülebilir Çevre ve Enerji Sistemleri / Sustainable Environment and Energy Systems ☐

Siyaset Bilimi ve Uluslararası İlişkiler / Political Science and International Relations ☐

İngilizce Öğretmenliği / English Language Teaching ☐

Elektrik Elektronik Mühendisliği / Electrical and Electronics Engineering ☐

Bilgisayar Mühendisliği / Computer Engineering ☐

Makina Mühendisliği / Mechanical Engineering ☐

YAZARIN / AUTHOR

Soyadı / Surname : .....

Adı / Name : .....

Programı / Program : .....

TEZİN ADI / TITLE OF THE THESIS (**İngilizce** / English) : .....

.....

.....

.....

TEZİN TÜRÜ / DEGREE: **Yüksek Lisans** / Master ☐ **Doktora** / PhD ☐

1. **Tezin tamamı dünya çapında erişime açılacaktır. /** Release the entire work immediately for access worldwide. ☐

2. **Tez iki yıl süreyle erişime kapalı olacaktır.** / Secure the entire work for patent and/or proprietary purposes for a period of **two years. *** ☐

3. **Tez altı ay süreyle erişime kapalı olacaktır.** / Secure the entire work for period of **six months. *** ☐

Yazarın imzası / Author Signature ..... **Tarih** / Date .....

Tez Danışmanı / Thesis Advisor Full Name: .....

Tez Danışmanı İmzası / Thesis Advisor Signature: .....

Eş Danışmanı / Co-Advisor Full Name: .....

Eş Danışmanı İmzası / Co-Advisor Signature: .....

Program Koordinatörü / Program Coordinator Full Name: .....

Program Koordinatörü İmzası / Program Coordinator Signature: .....